

Imaging Macromolecules with X-ray laser pulses

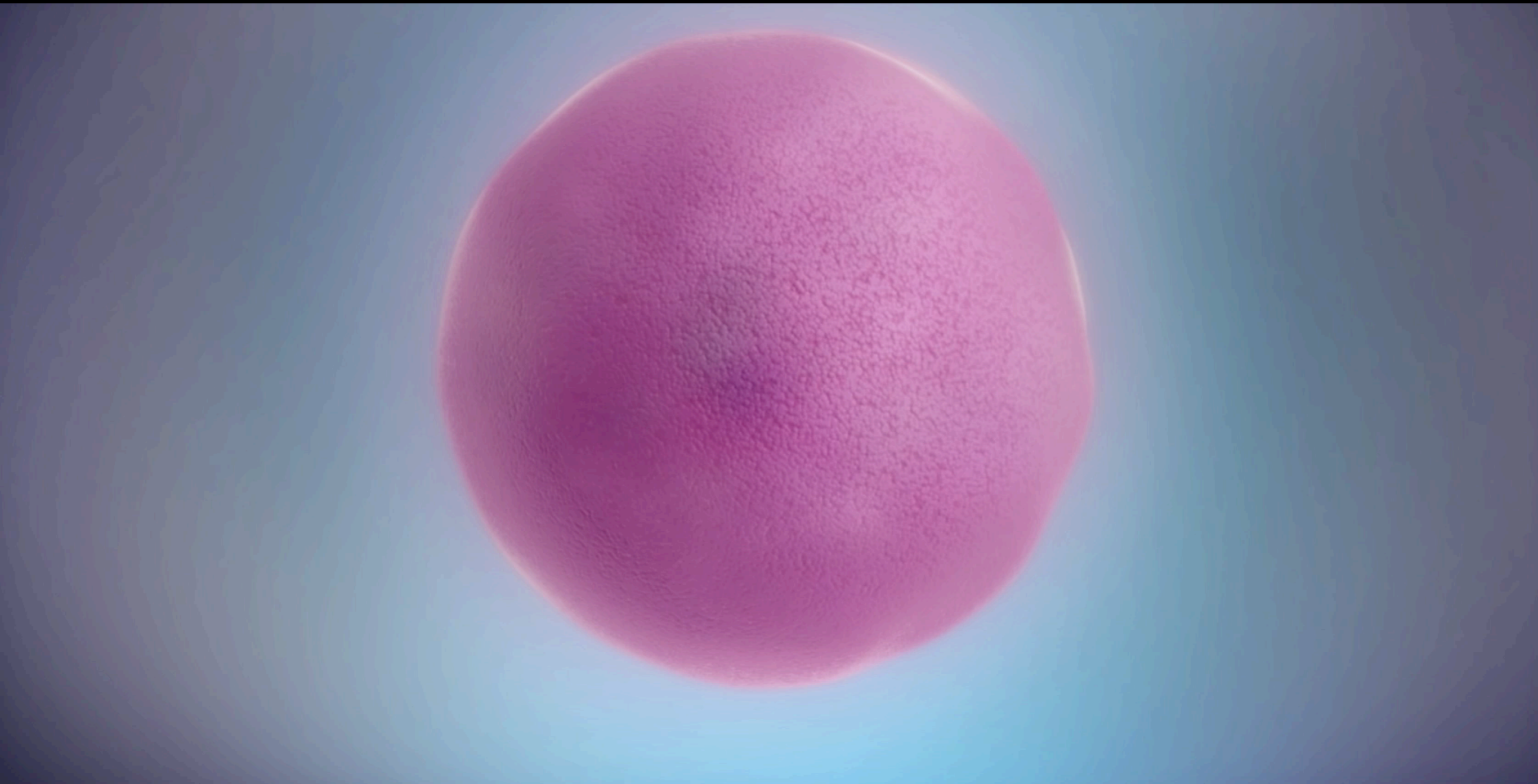
Henry Chapman
*Center for Free-Electron Laser Science
DESY and University of Hamburg*

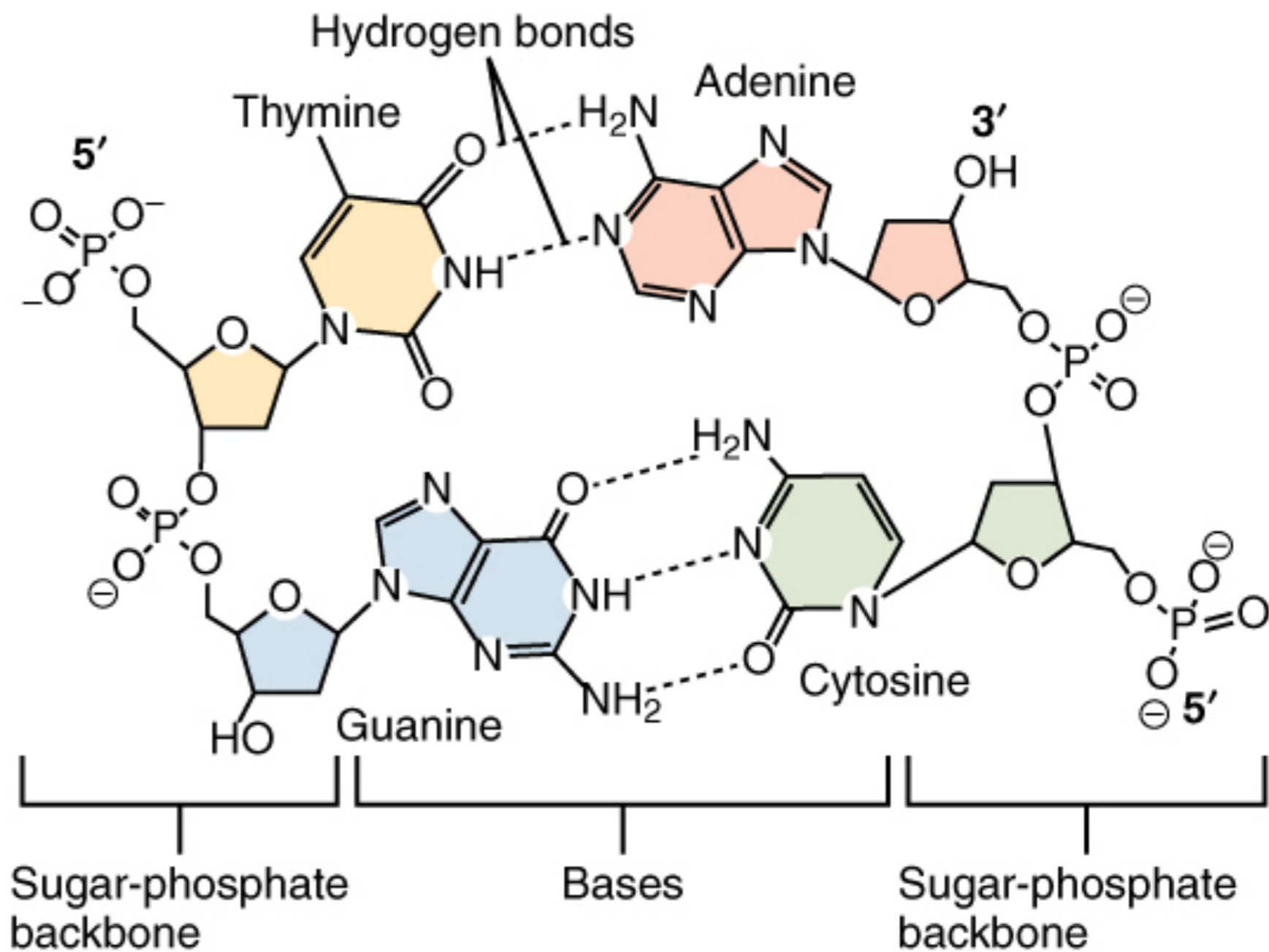
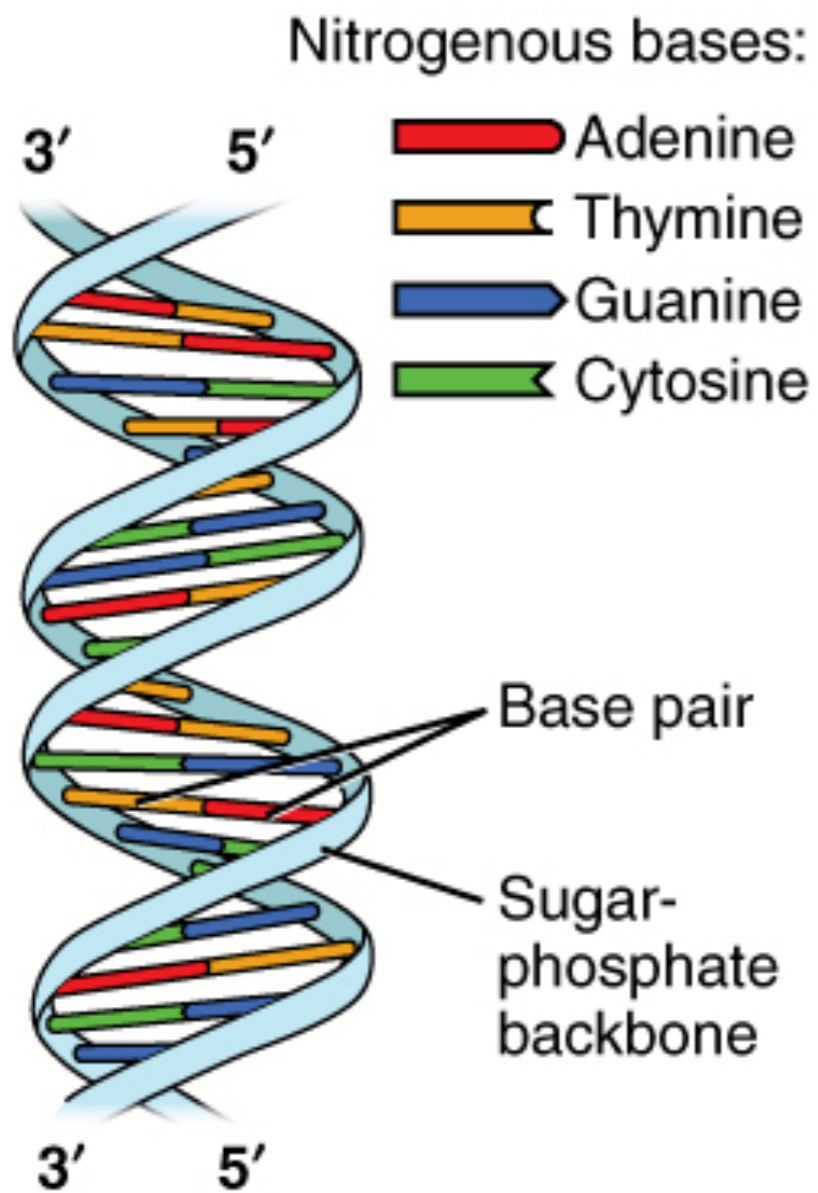
CERN Colloquium - July 2017

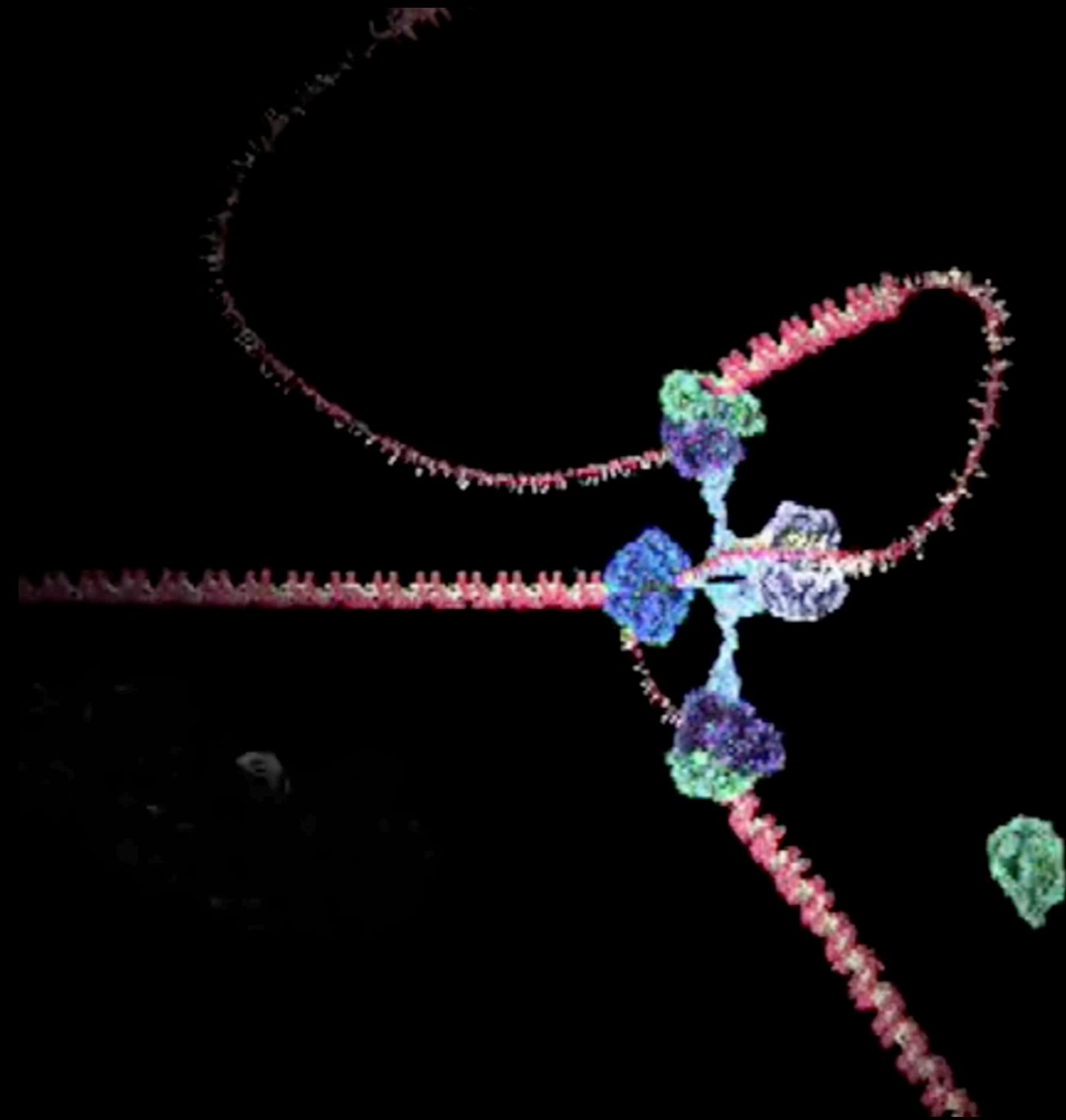


European Research Council
Established by the European Commission



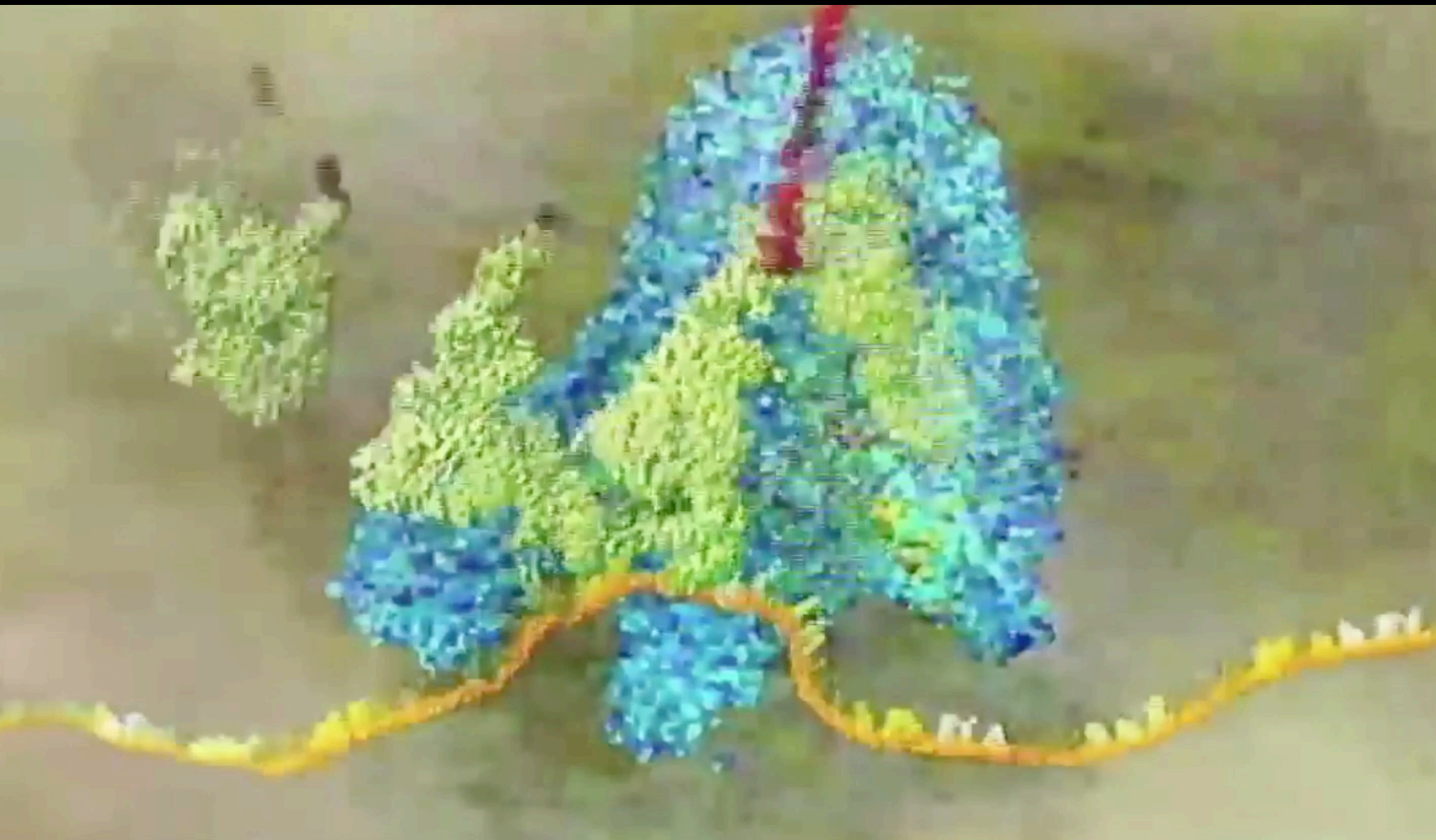






wehi.edu.au

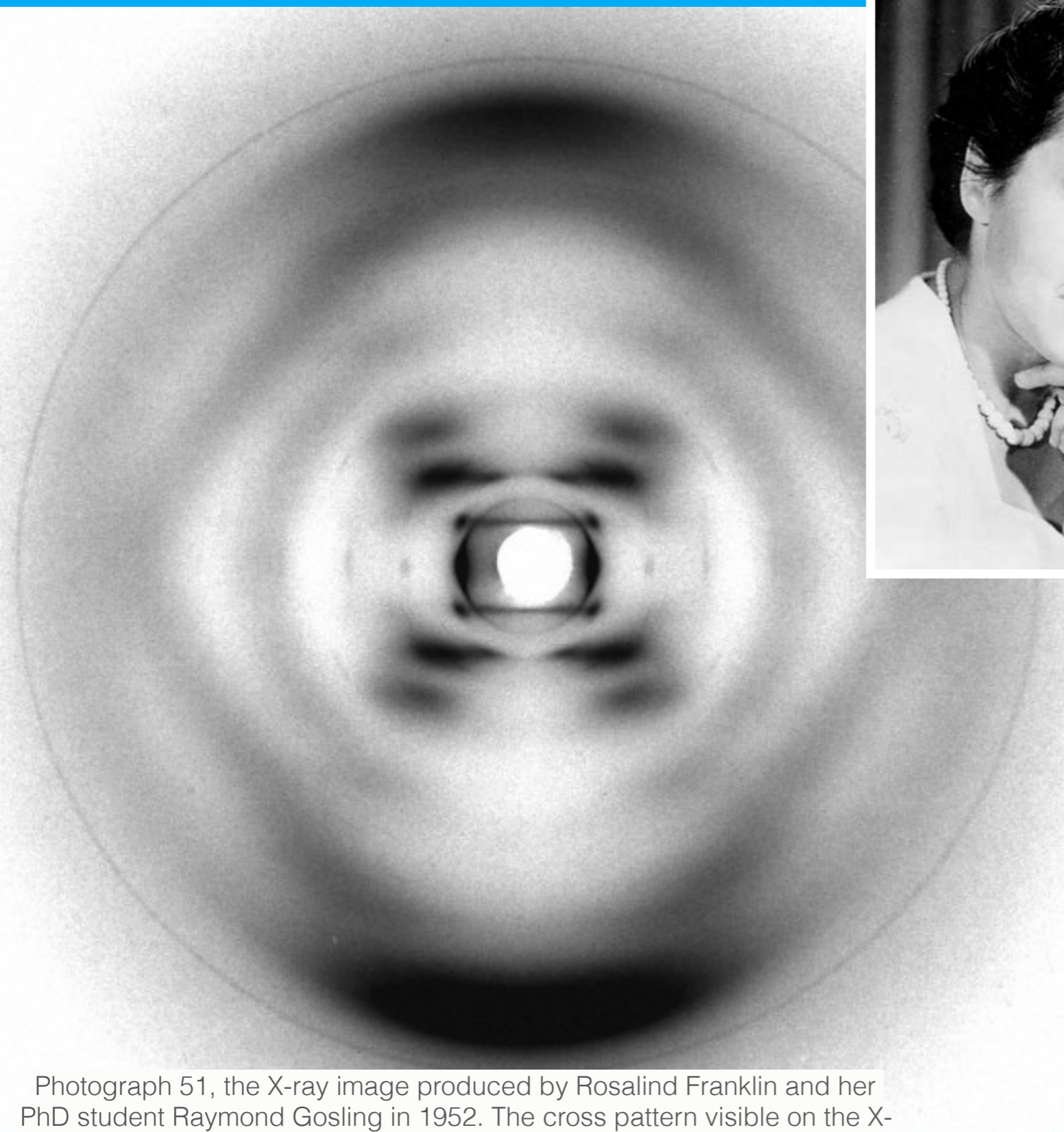




Walter & Eliza Hall Institute

Yonath group, Weizmann Institute & Max Planck group Hamburg

X-ray diffraction led to the discovery of the double helix



Rosalind Franklin

James Watson
& Francis Crick

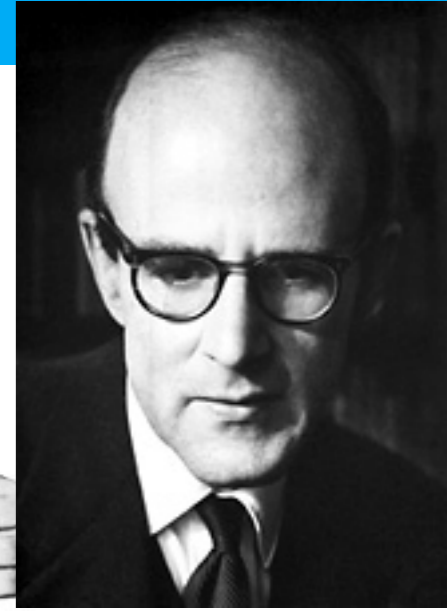


Photograph 51, the X-ray image produced by Rosalind Franklin and her PhD student Raymond Gosling in 1952. The cross pattern visible on the X-ray highlights the helical structure of DNA.

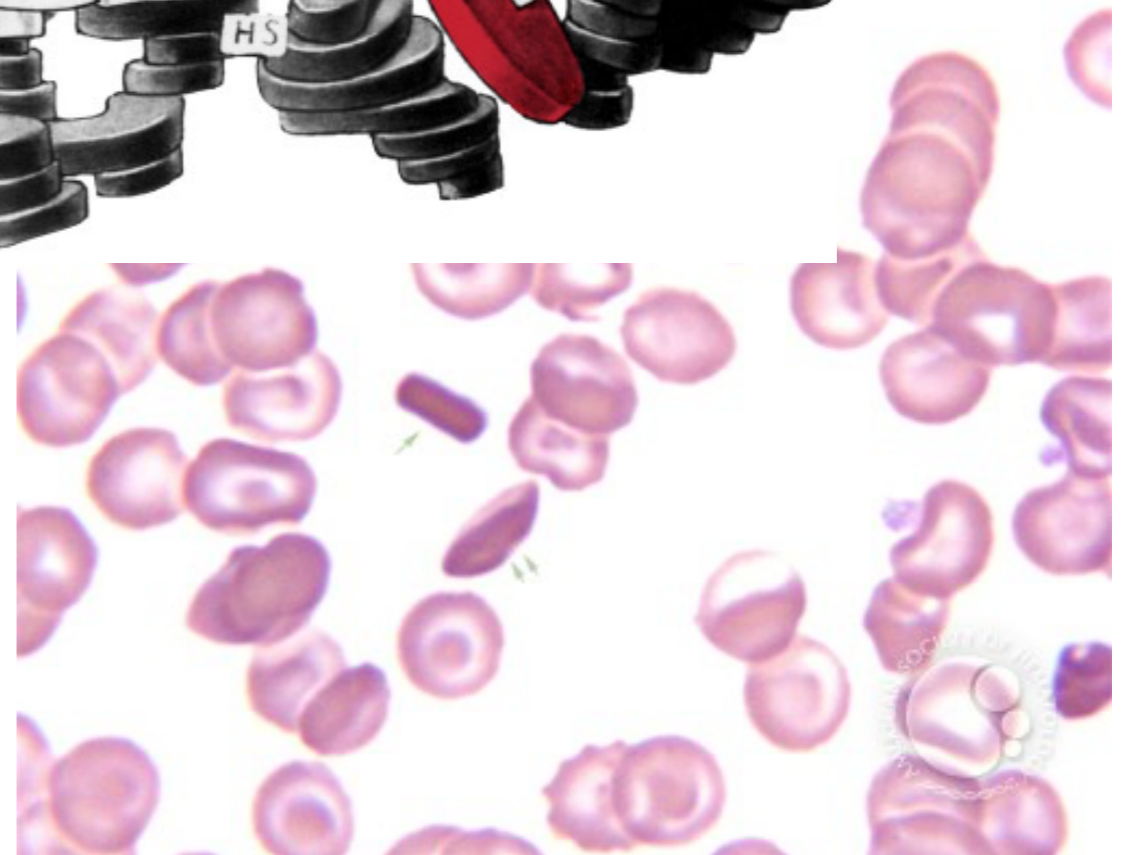
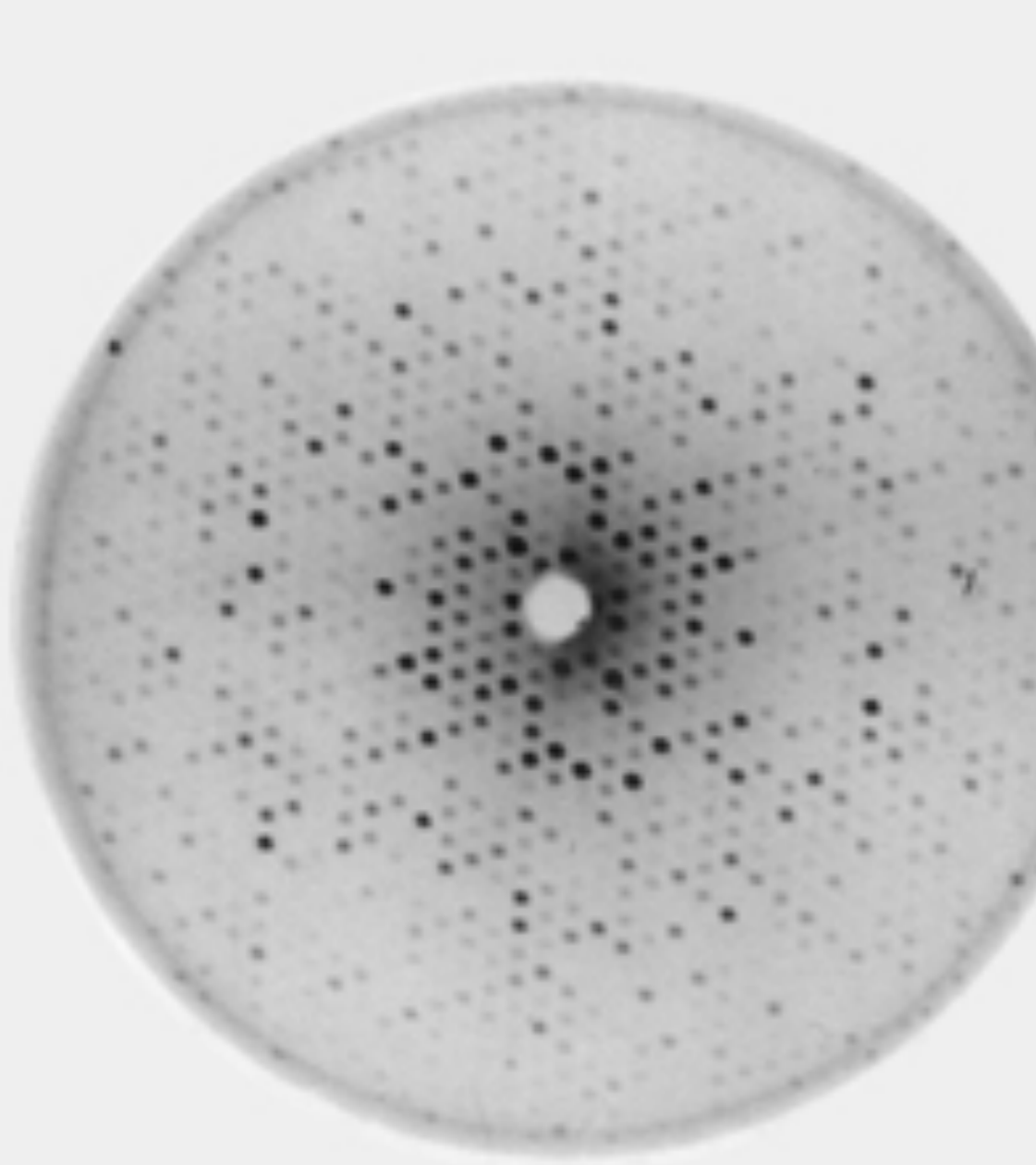
Wellcome Images

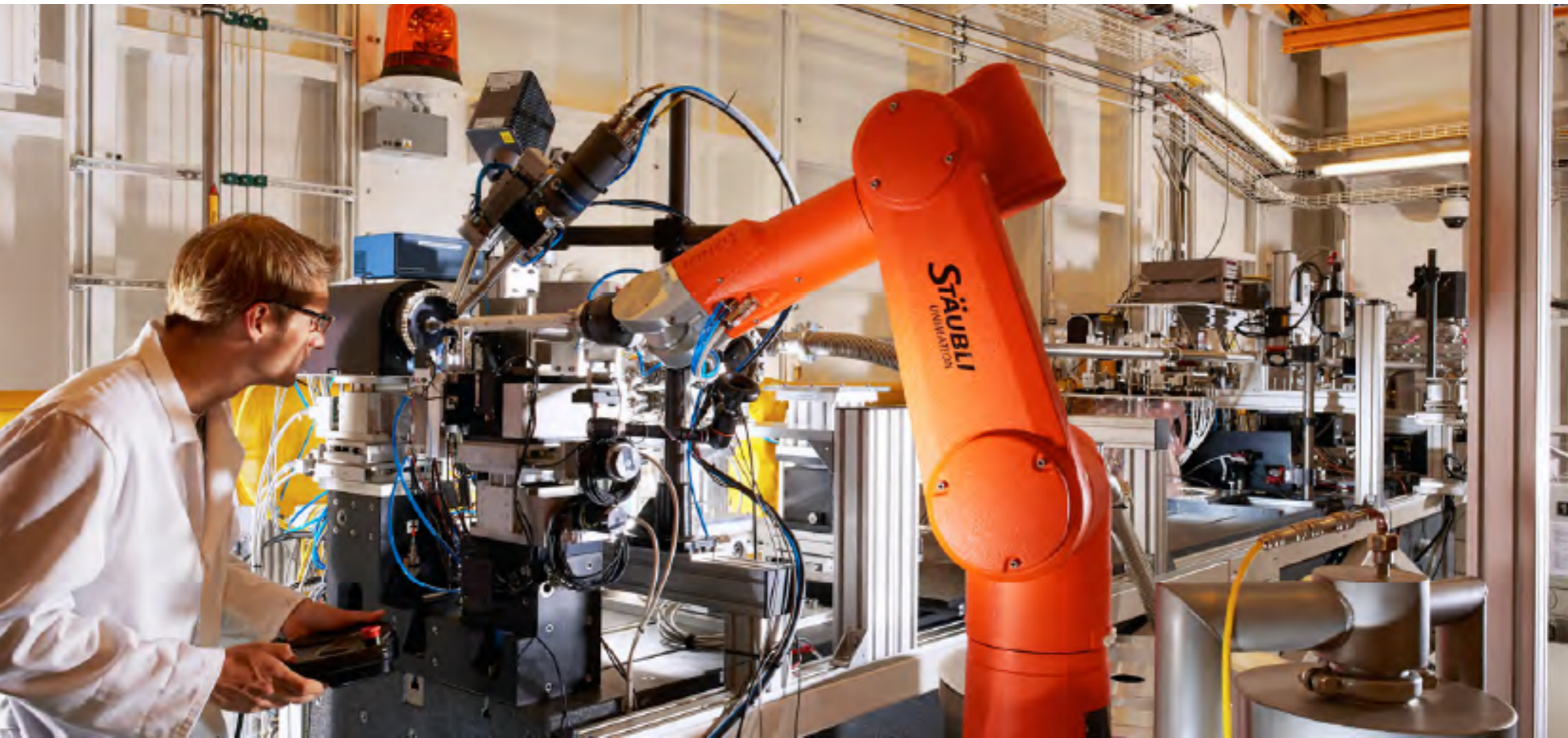
<http://dataphys.org/list/watson-and-cricks-3d-model-of-dna/>

The first protein structure to be determined was haemoglobin, in 1959

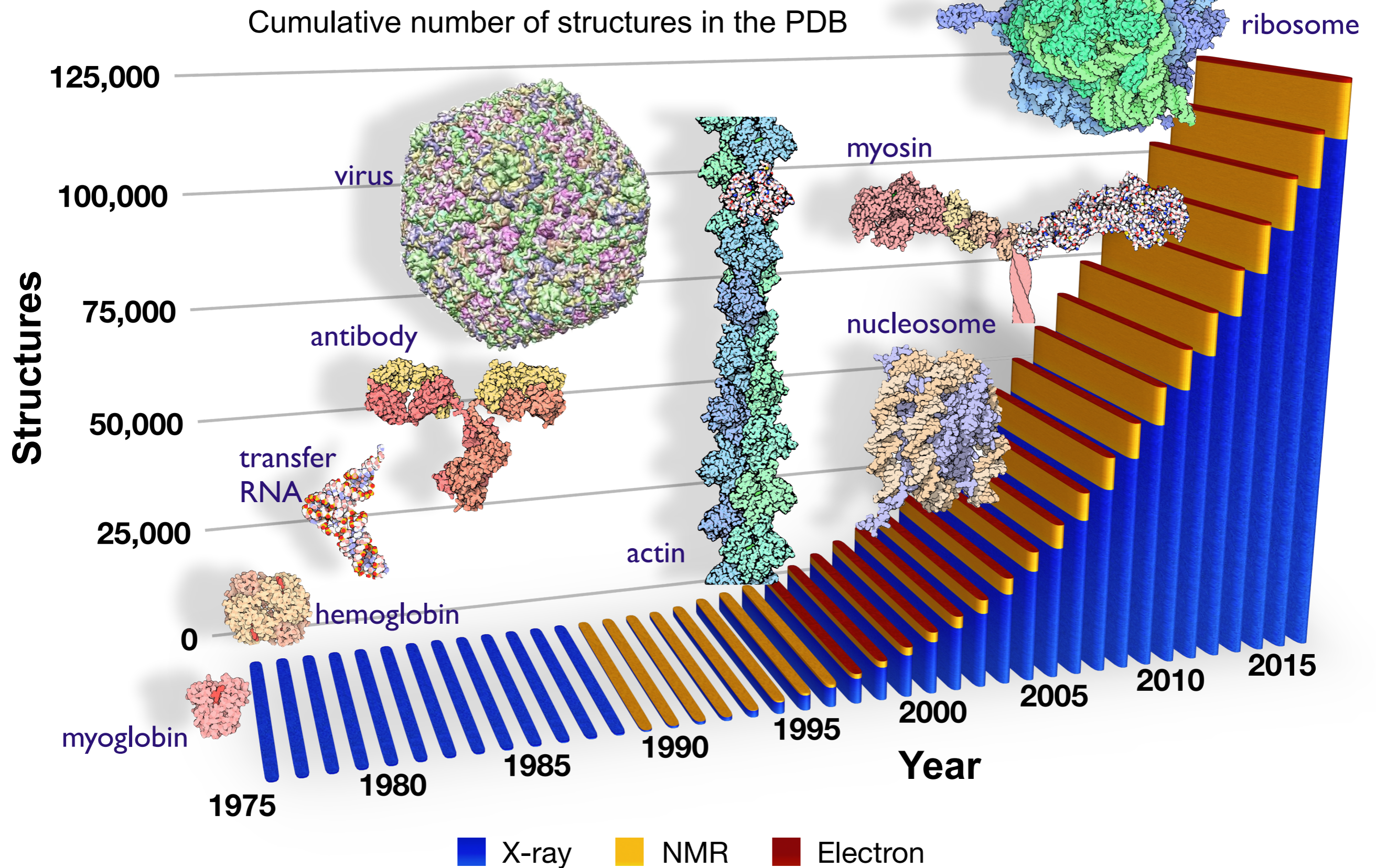


Max Perutz

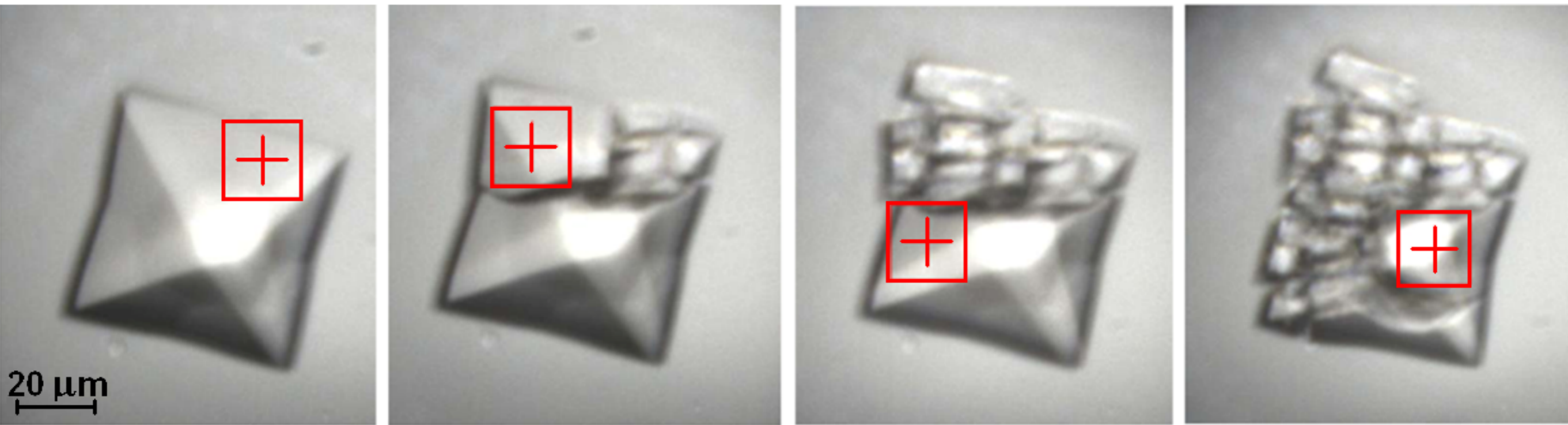




Over 100,000 macromolecular structures have been solved using synchrotron sources



High radiation dose causes changes in molecular structure



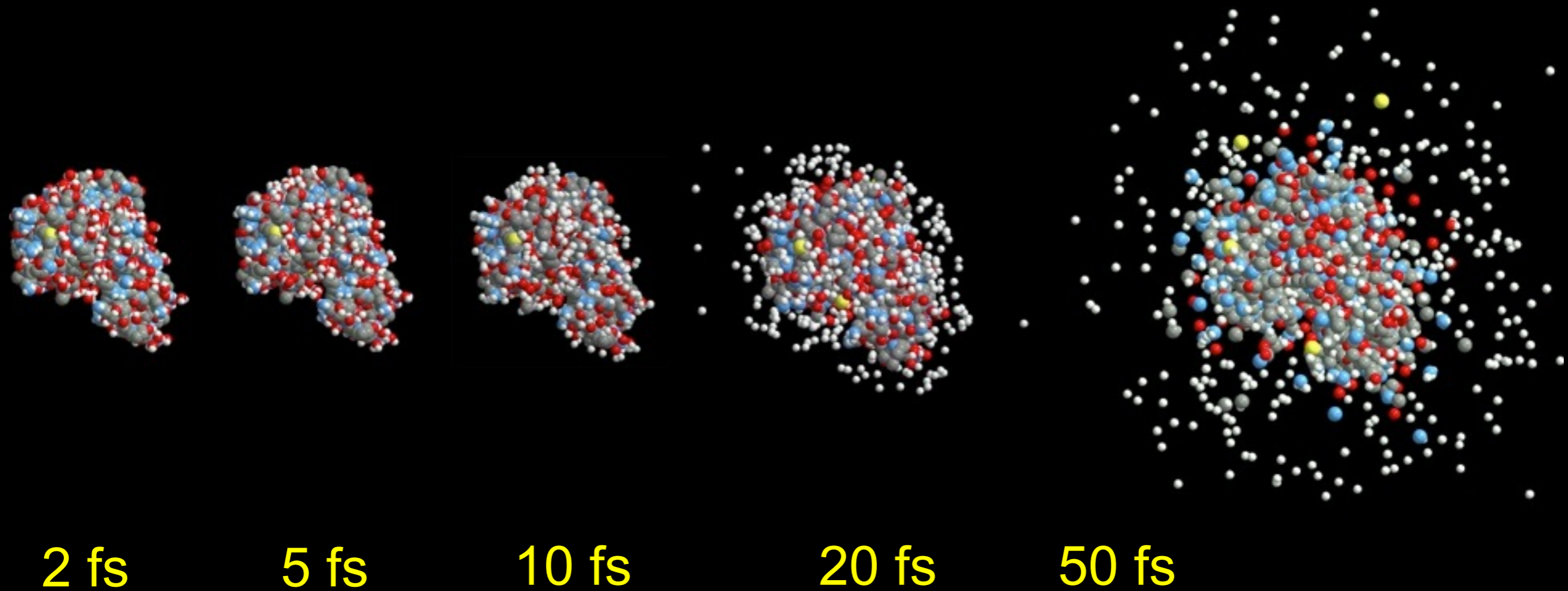
Crystal of Bovine enterovirus 2 (BEV2) after subsequent exposures of 0.5 s, 6×10^8 ph/ μm^2
300 kGy dose
Room temperature

Cryogenic cooling gives 30 MGy tolerance

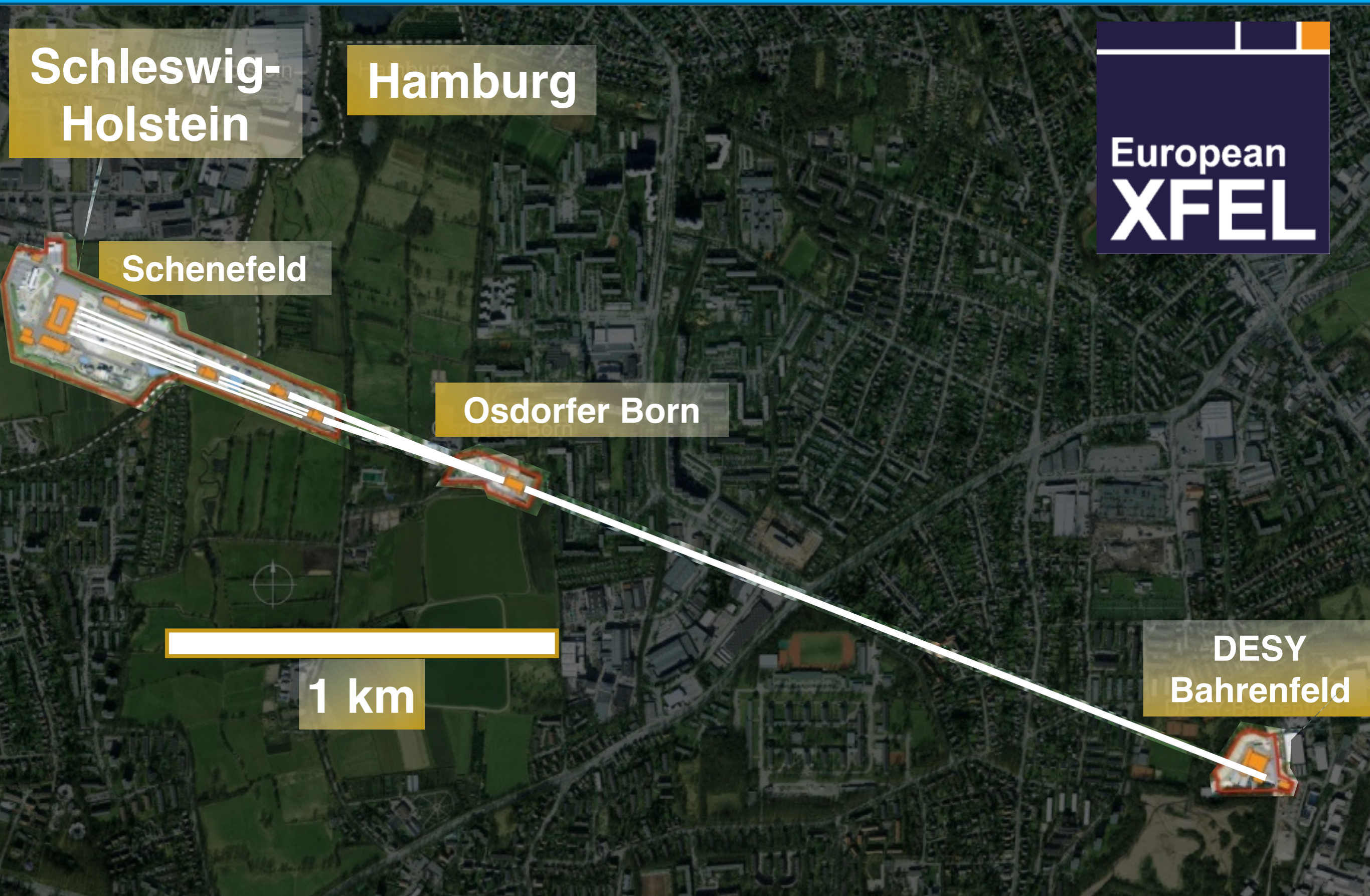


Axford et al. Acta Cryst. D68 592 (2012)
Diamond Light Source (courtesy Robin Owen & Elspeth Garman)

X-ray free-electron lasers may enable atomic-resolution imaging of biological macromolecules



The European XFEL is located in Hamburg



Schleswig-Holstein

Hamburg



Schenefeld

Osdorfer Born

1 km

DESY Bahrenfeld

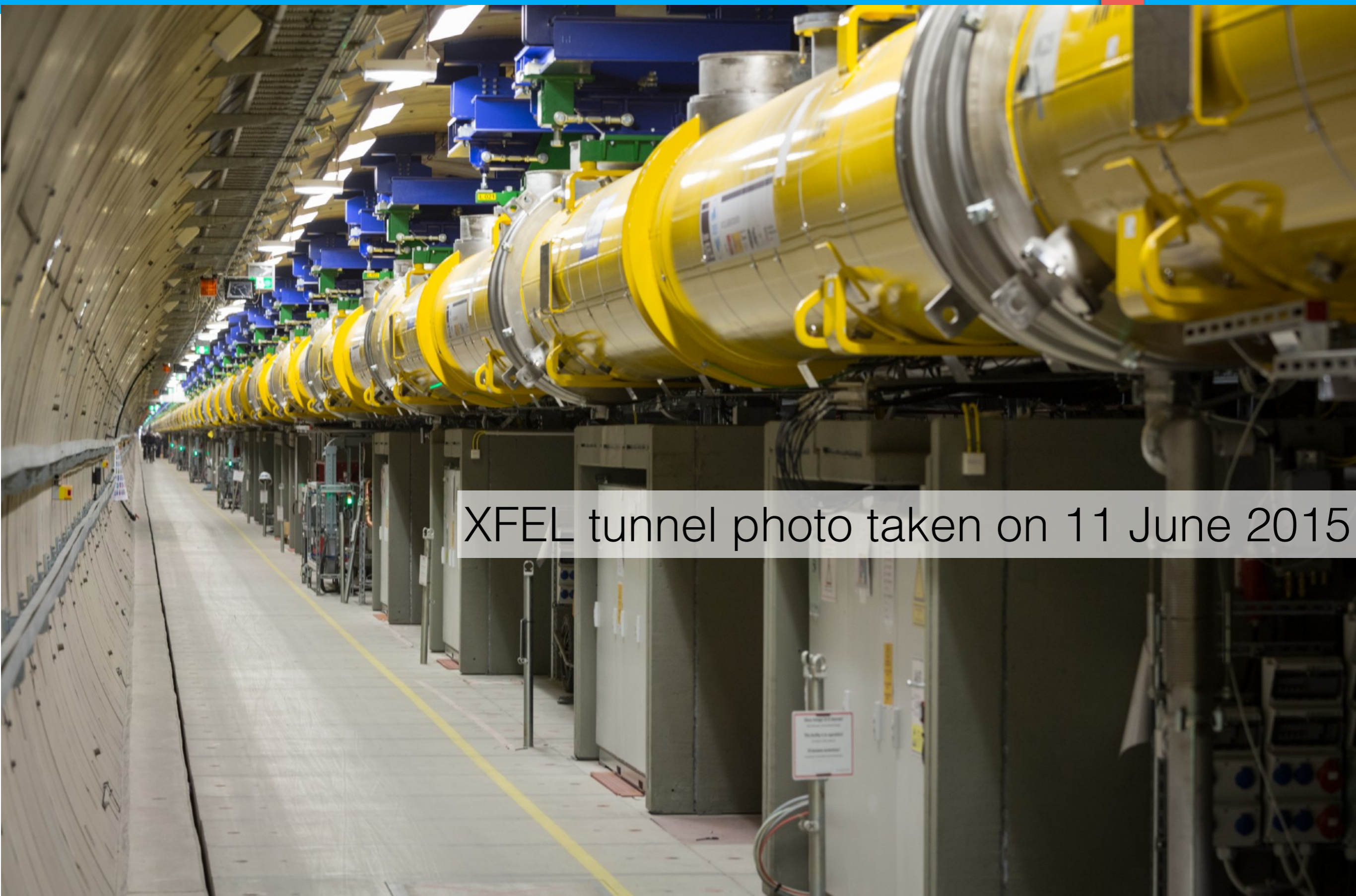
The European XFEL in Hamburg

injector



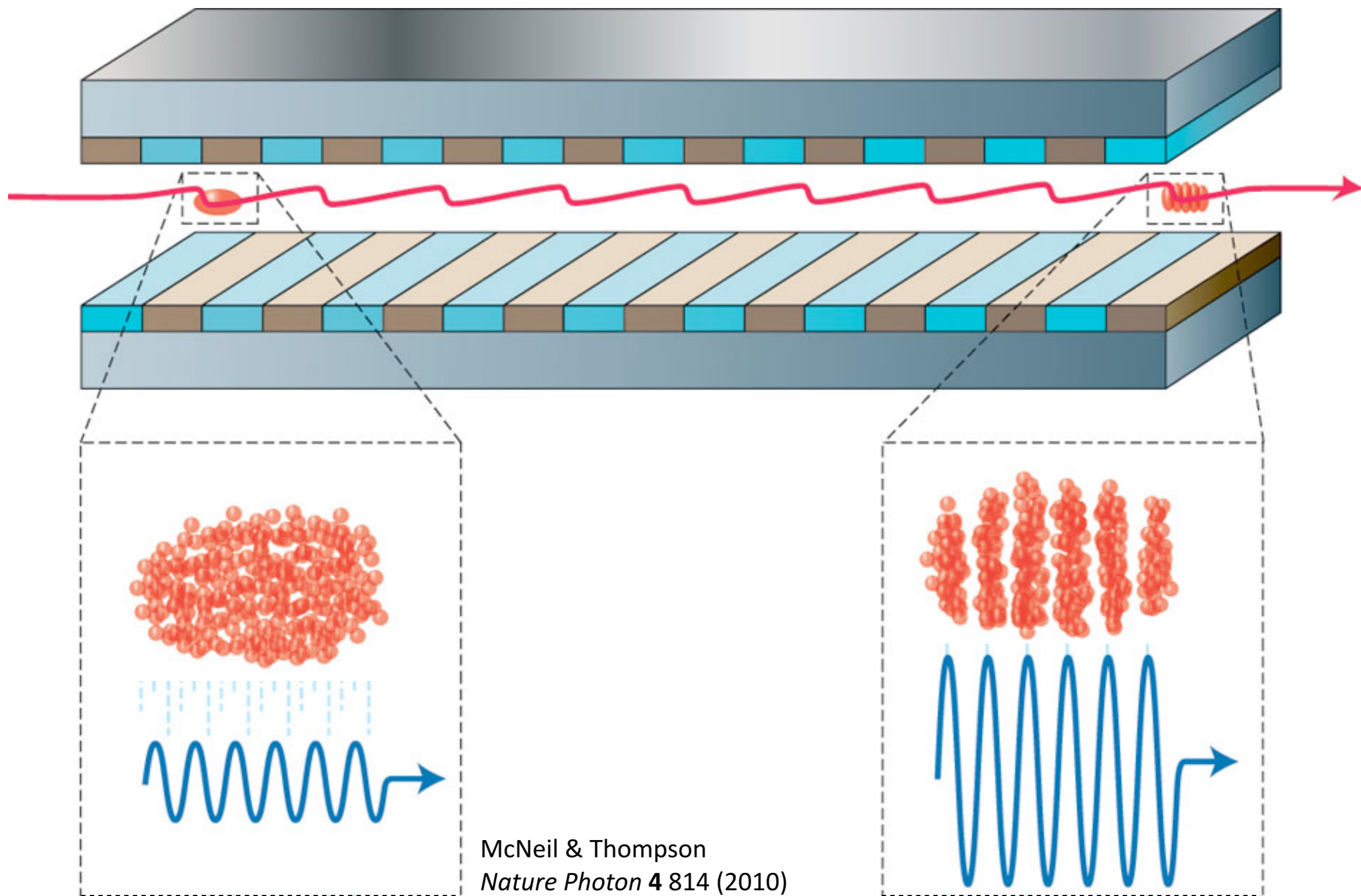
Schenefeld site photo taken on 20 July 2014

The European XFEL has just begun operations



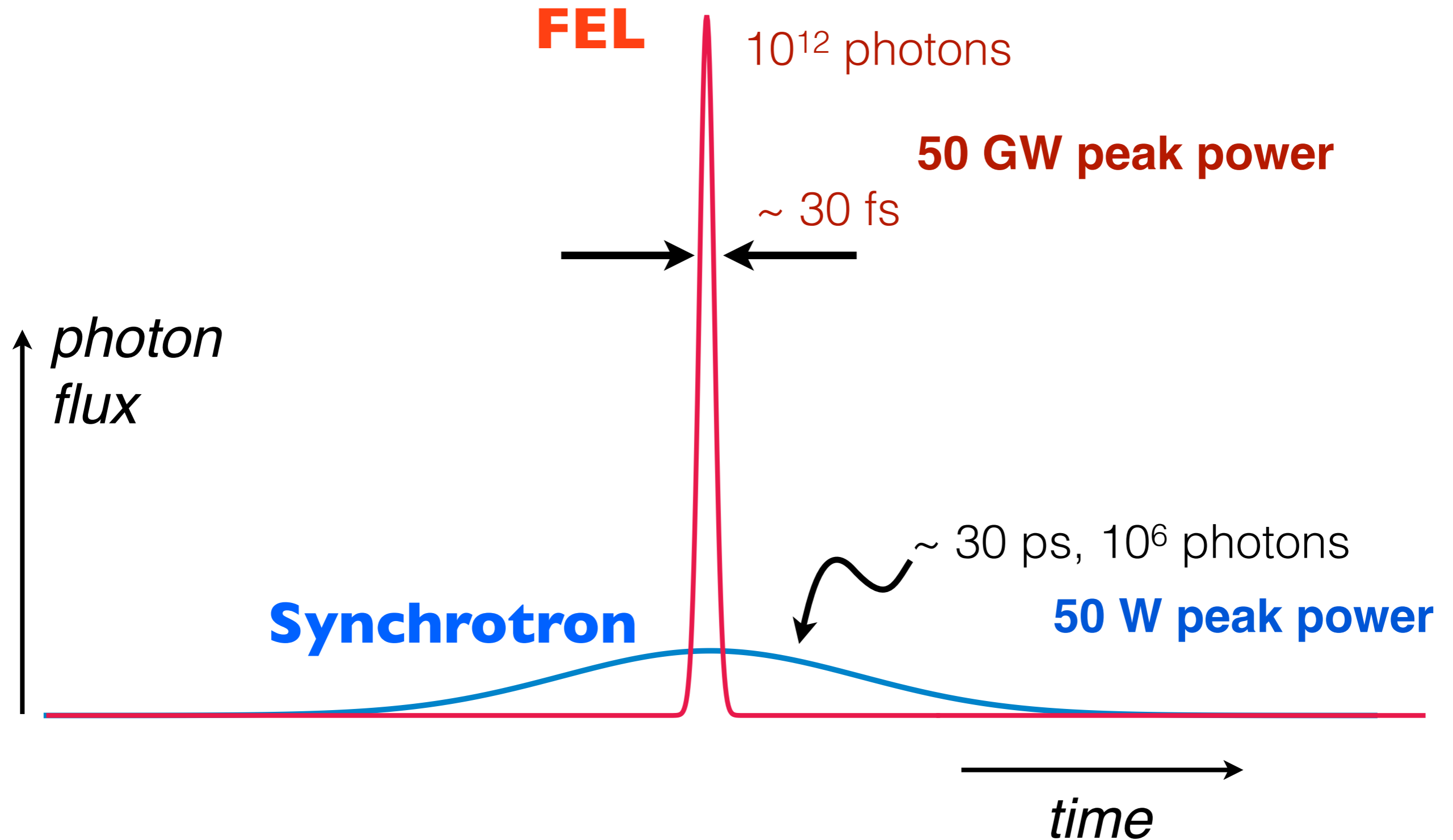
XFEL tunnel photo taken on 11 June 2015

X-rays are produced by a process called SASE

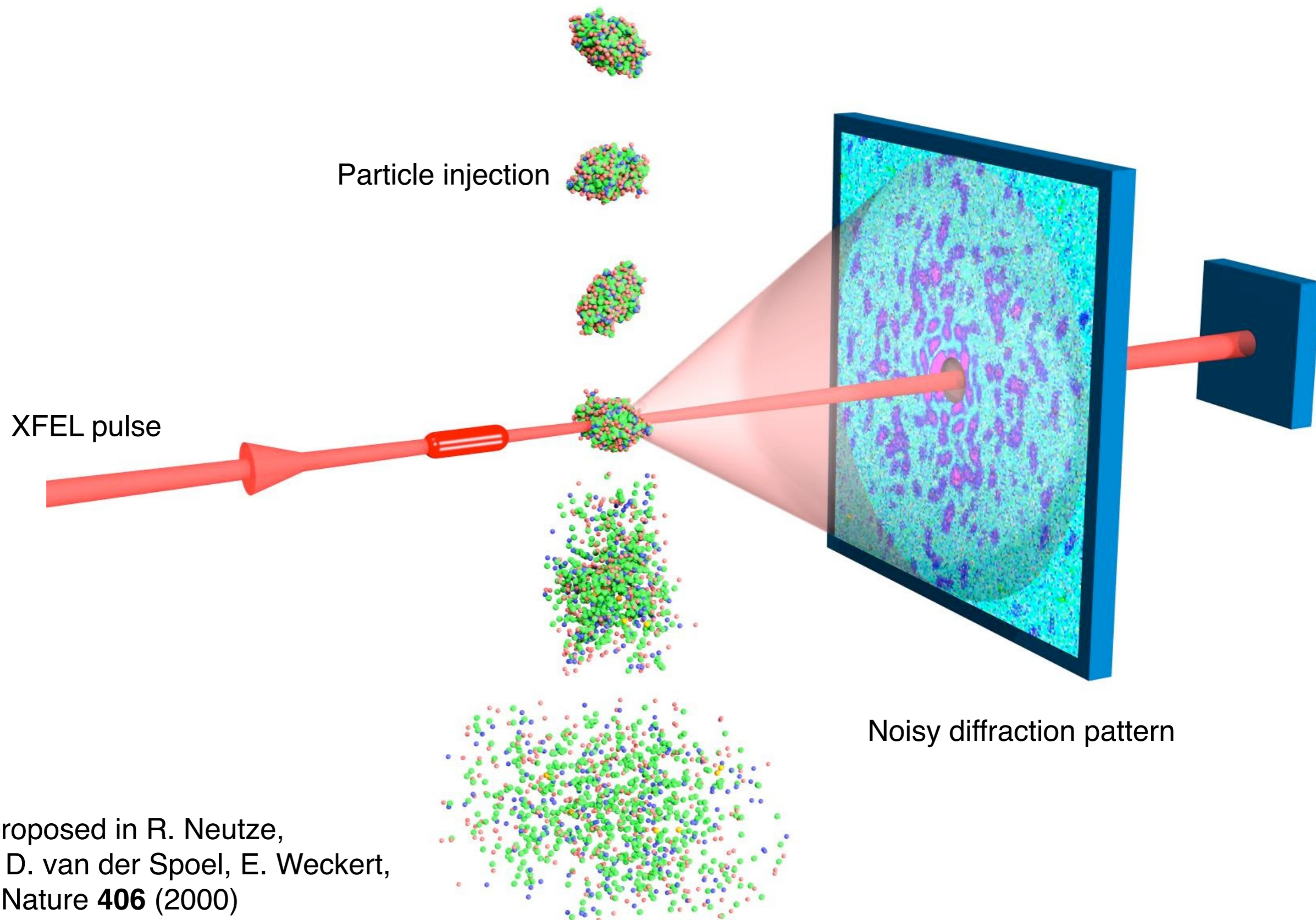


McNeil & Thompson
Nature Photon **4** 814 (2010)

X-ray FELs are a billion times brighter than synchrotrons

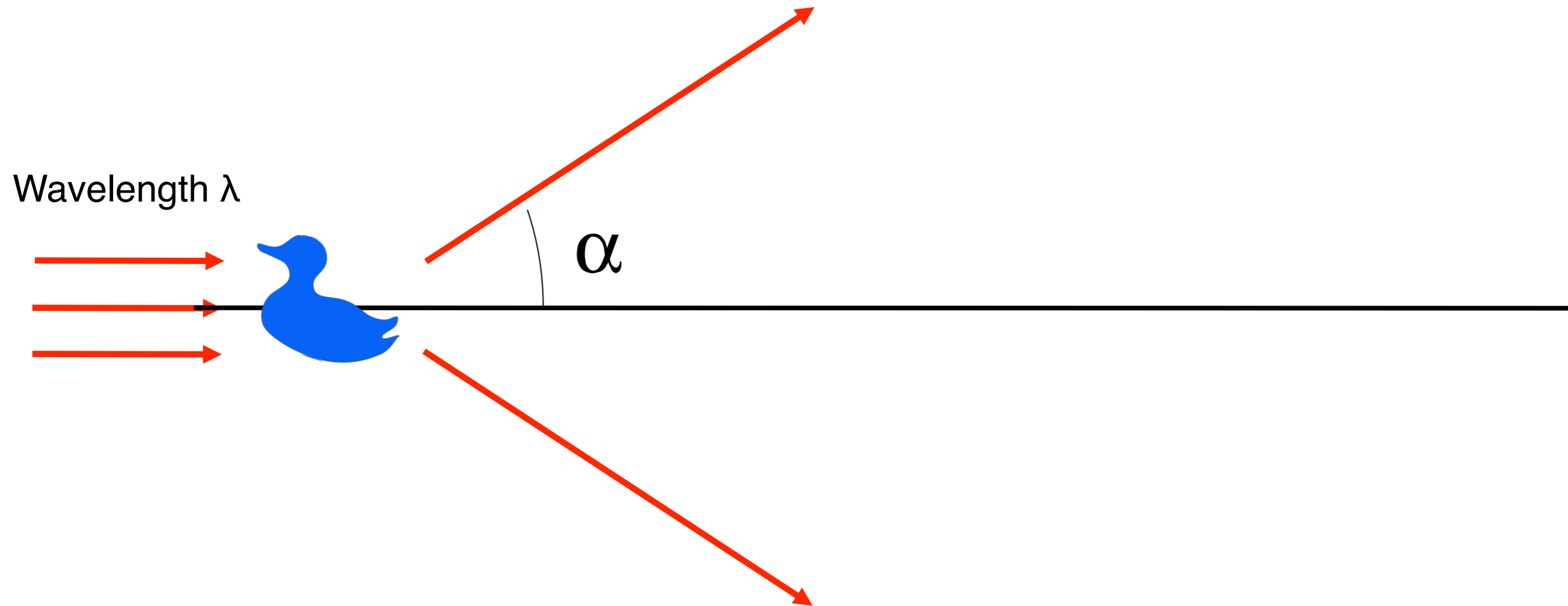


X-ray free-electron lasers may enable atomic-resolution imaging of biological macromolecules



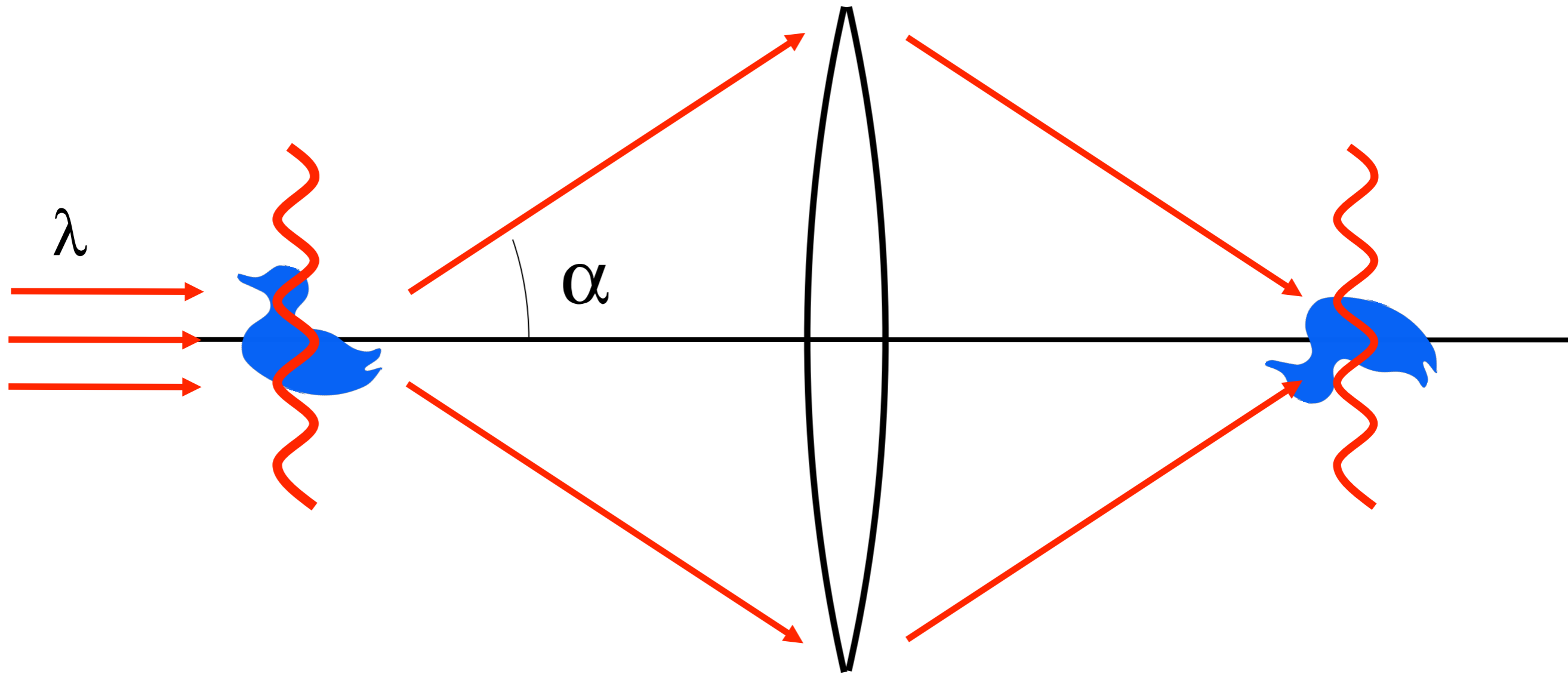
Scheme proposed in R. Neutze,
R. Wouts, D. van der Spoel, E. Weckert,
J. Hajdu, *Nature* **406** (2000)

Imaging can be achieved with a lens



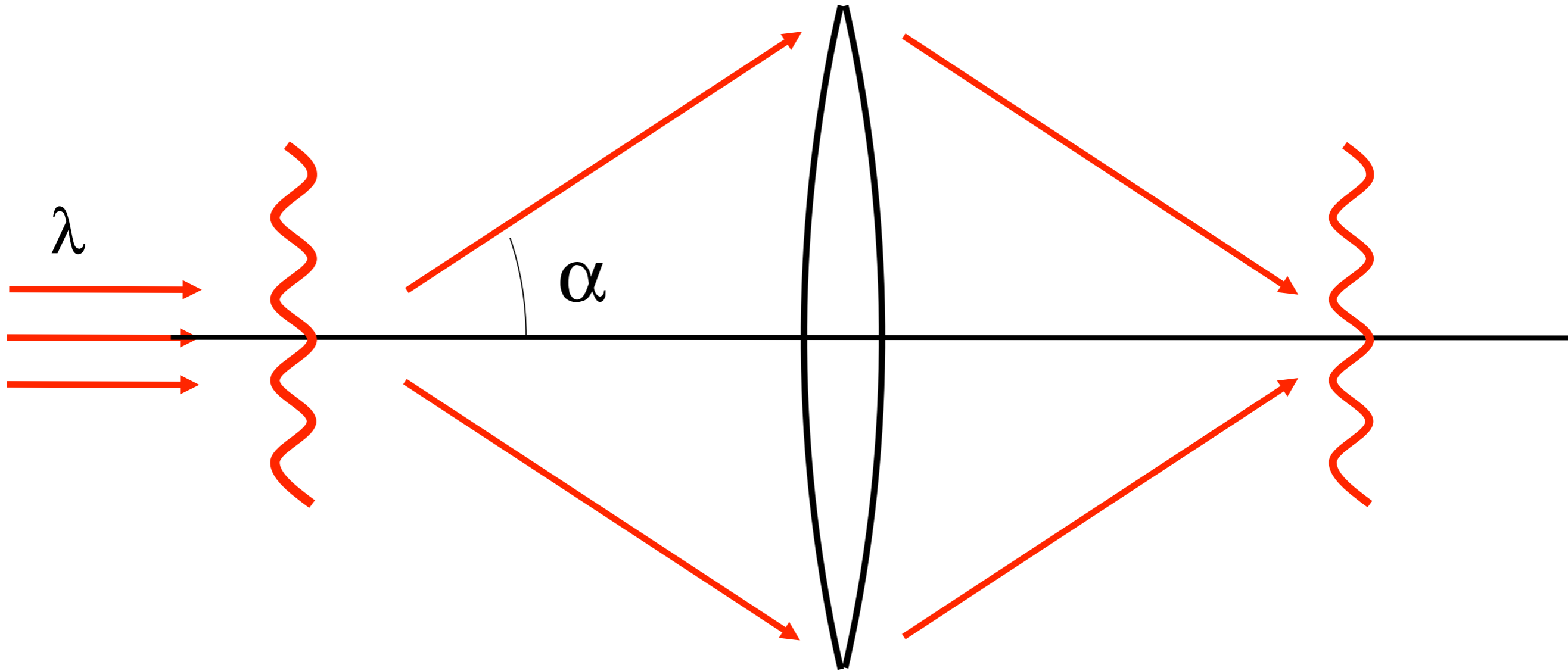
Resolution: $\delta = \lambda / \sin \alpha$

Imaging can be achieved with a lens



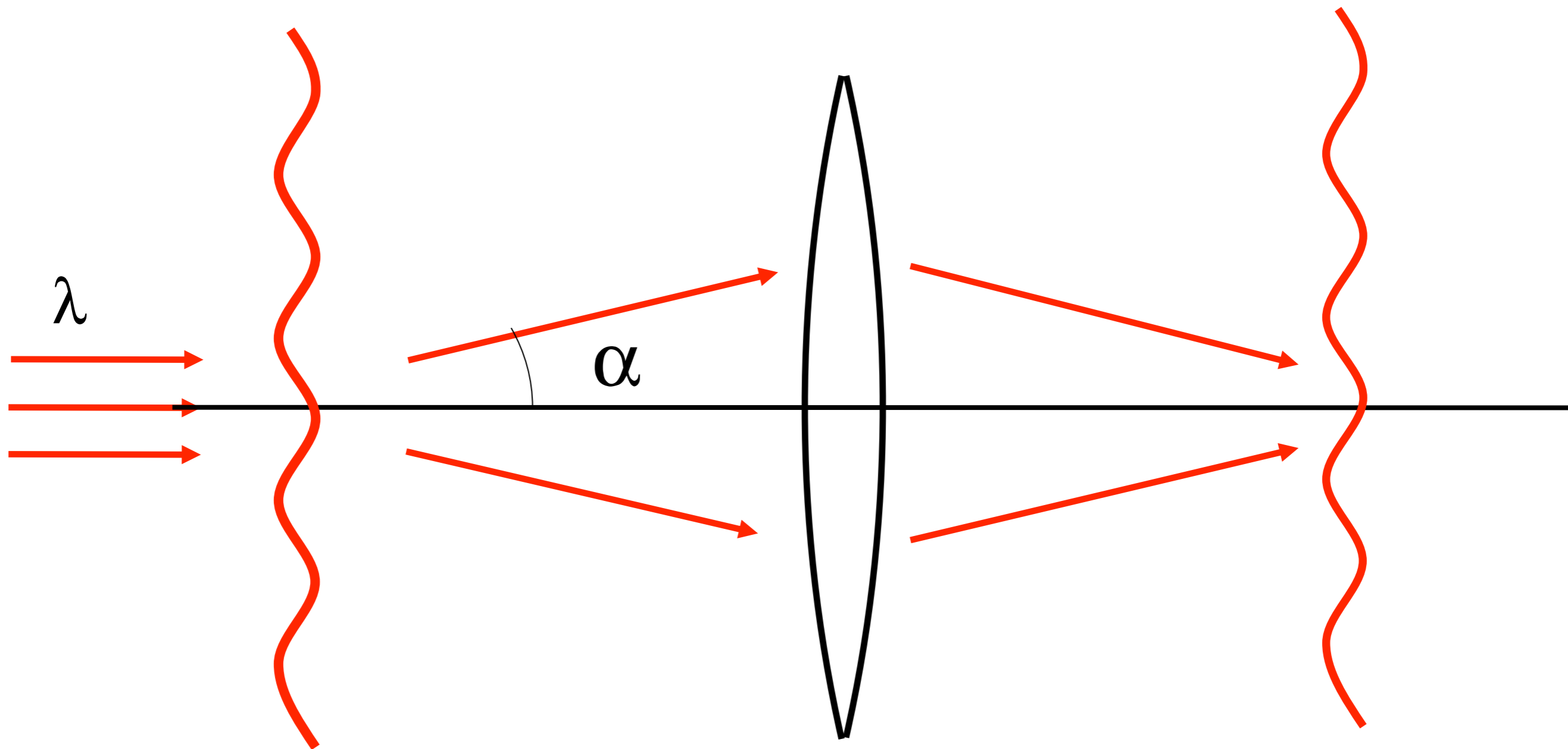
Resolution: $\delta = \lambda / \sin \alpha$

Imaging can be achieved with a lens



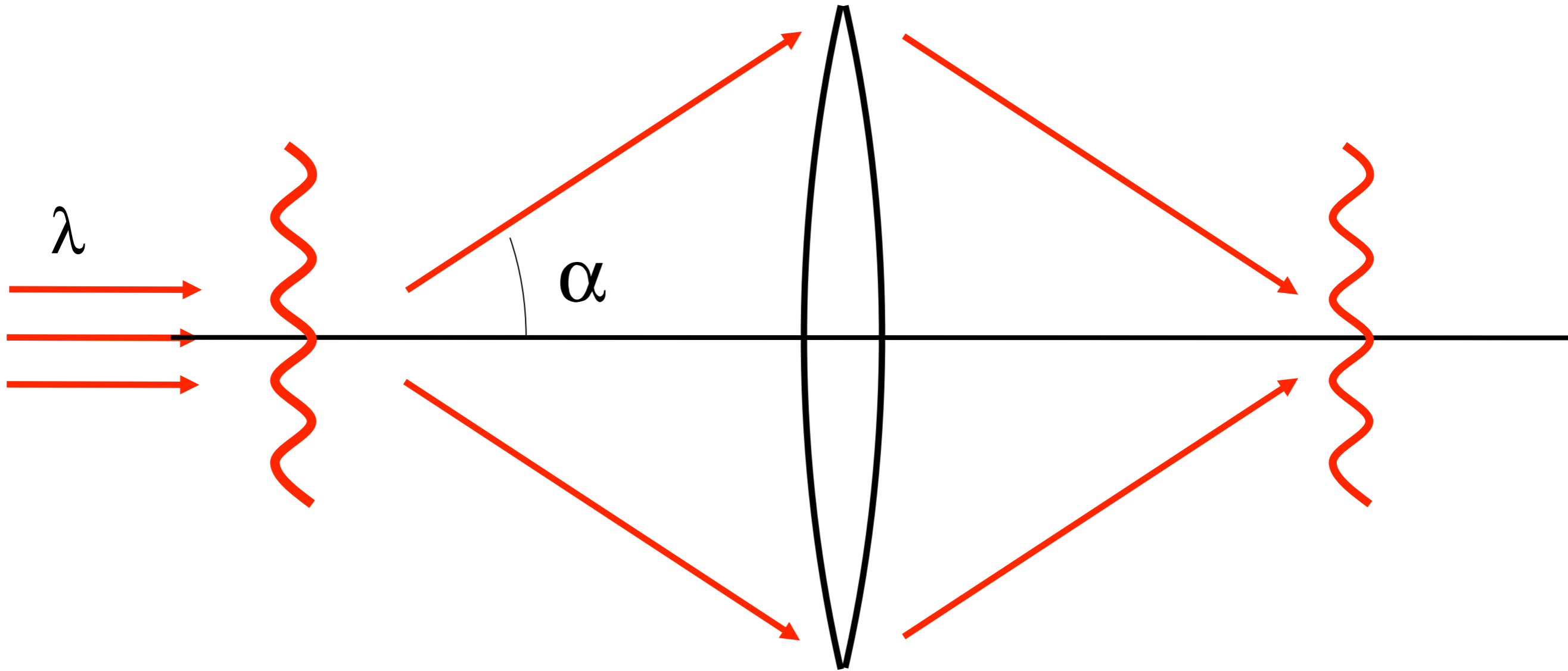
Resolution: $\delta = \lambda / \sin \alpha$

Imaging can be achieved with a lens



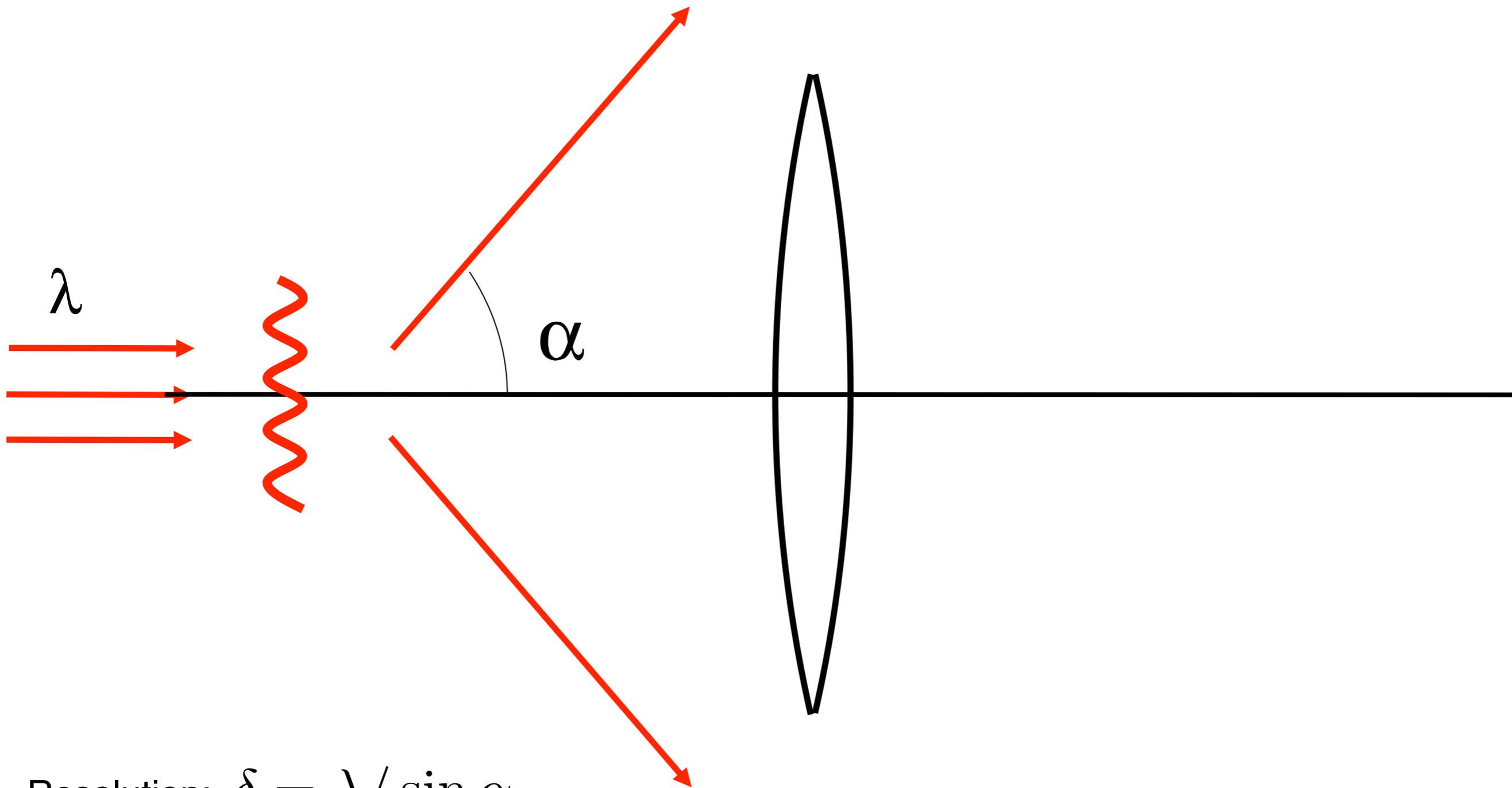
Resolution: $\delta = \lambda / \sin \alpha$

Imaging can be achieved with a lens



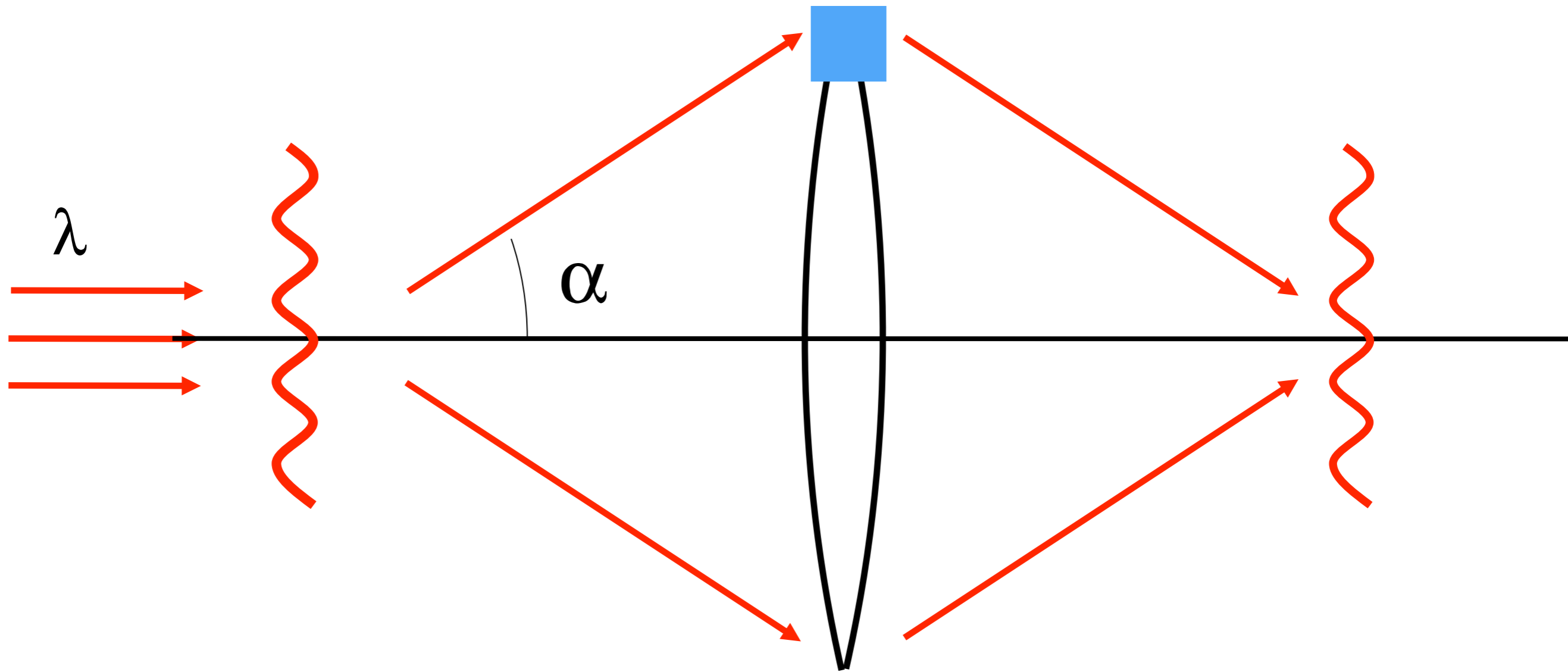
Resolution: $\delta = \lambda / \sin \alpha$

Imaging can be achieved with a lens



Resolution: $\delta = \lambda / \sin \alpha$

Imaging can be achieved with a lens

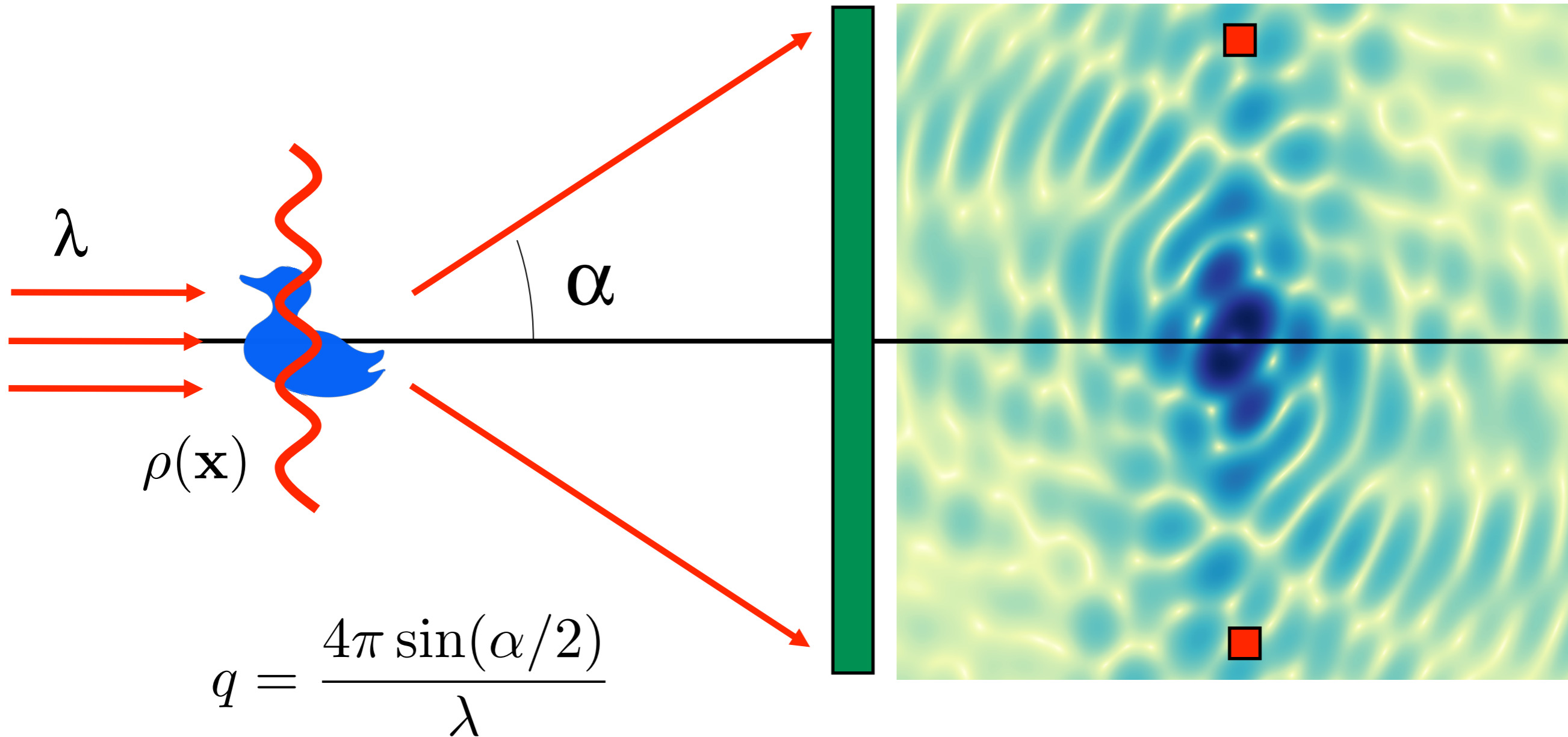


Resolution: $\delta = \lambda / \sin \alpha$

Imaging can be achieved with a lens

$$\hat{\rho}(\mathbf{q}) = -r_e \int \rho(\mathbf{x}) \exp(i\mathbf{q} \cdot \mathbf{x}) d\mathbf{x}$$

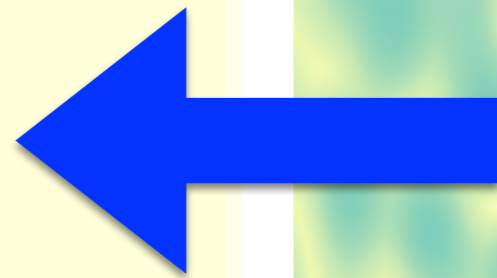
$$I(\mathbf{q}) = |\hat{\rho}(\mathbf{q})|^2$$



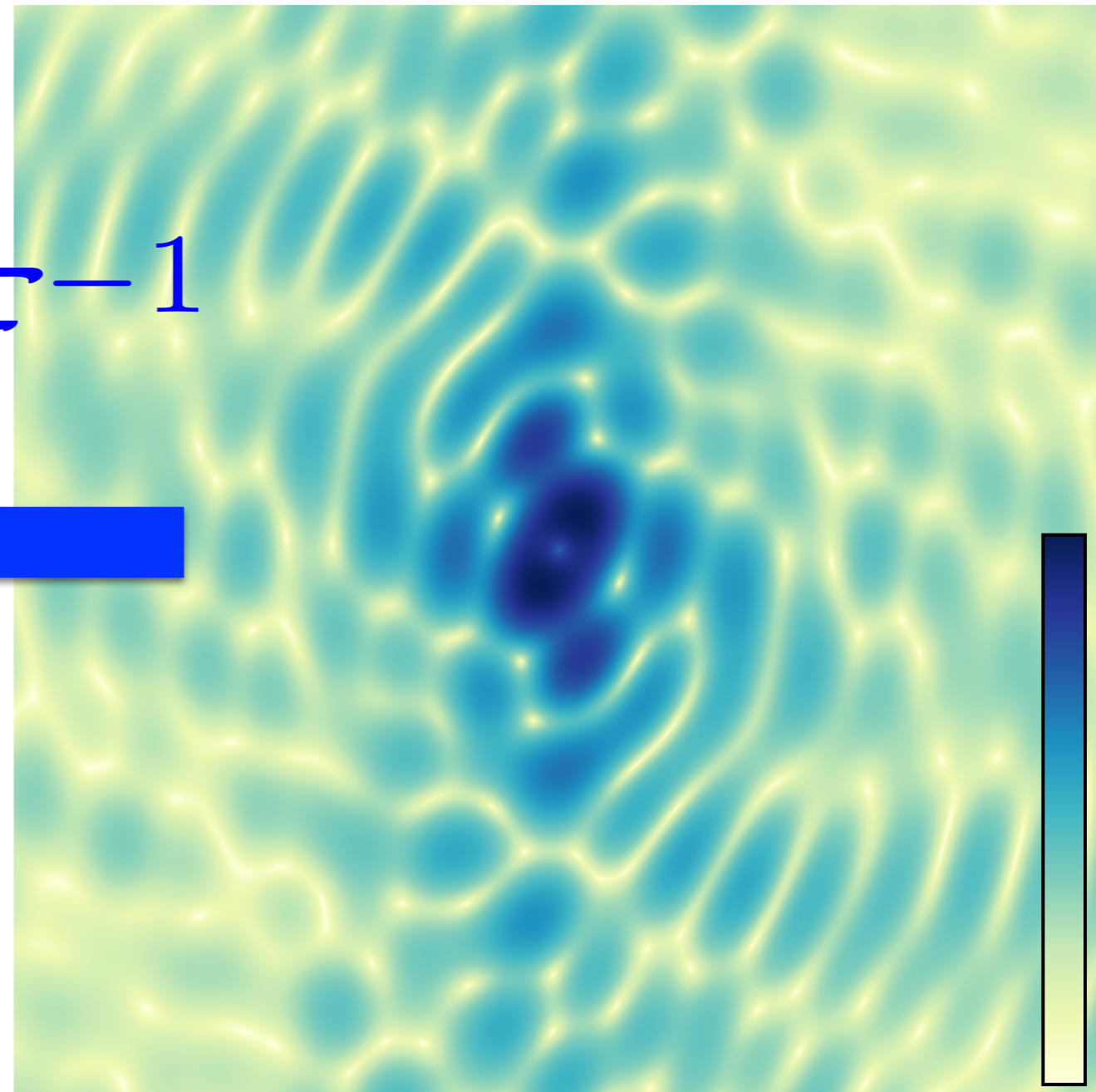
Single particles give continuous diffraction patterns

$$\mathcal{F}^{-1}\{I(\mathbf{q})\} = \rho(\mathbf{x}) \otimes \rho^*(-\mathbf{x})$$

$$I(\mathbf{q}) = |\hat{\rho}(\mathbf{q})|^2$$

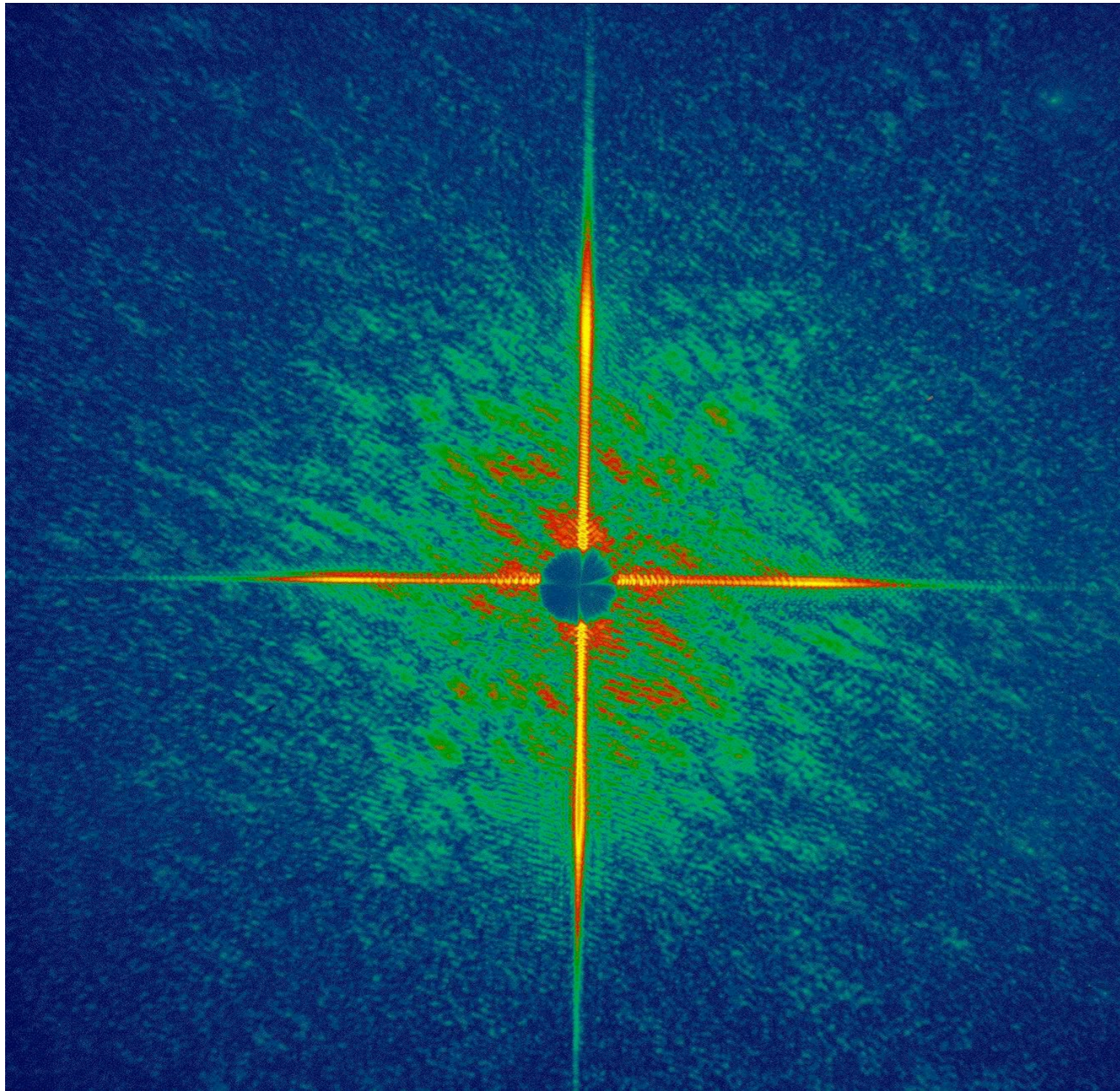


\mathcal{F}^{-1}

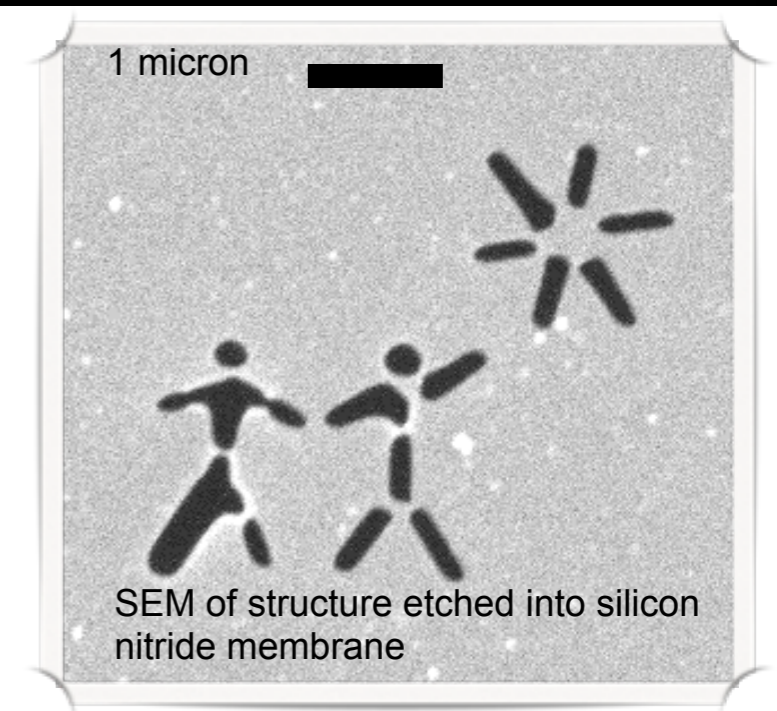
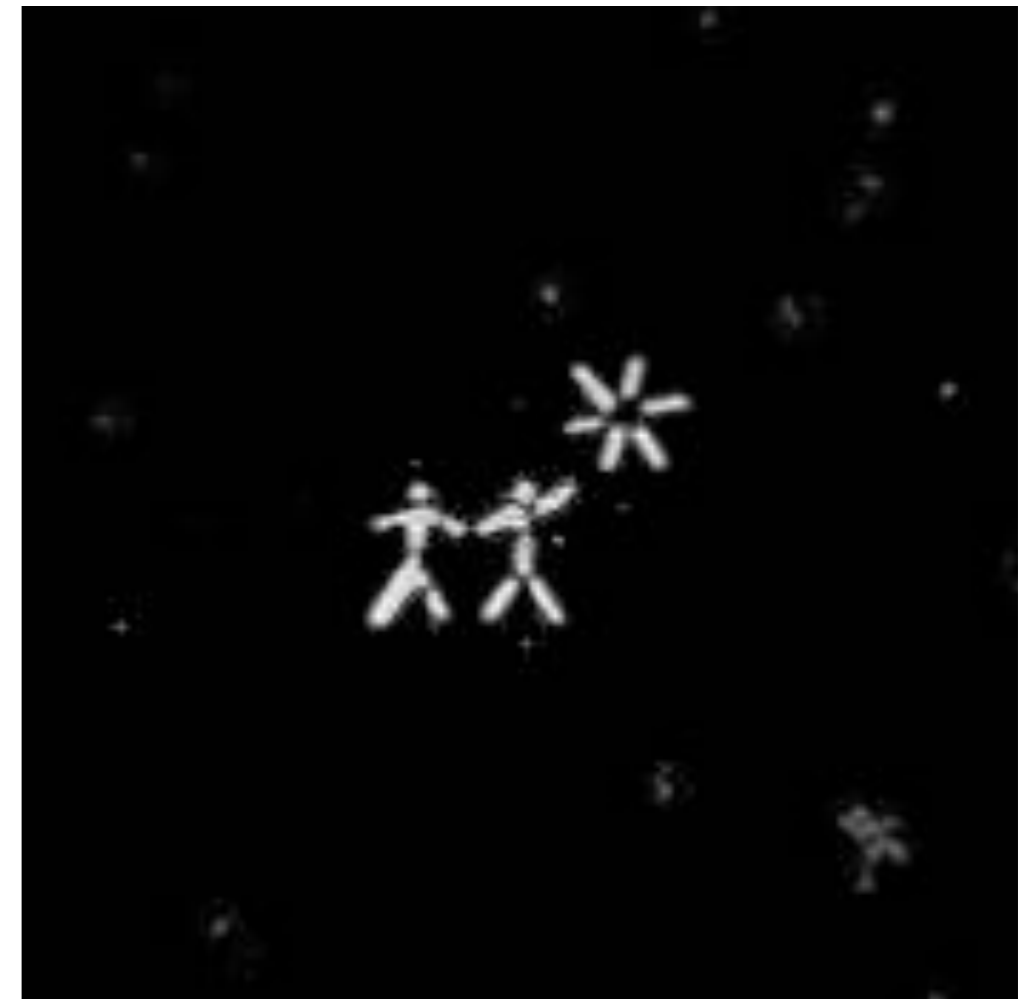


Over-constrained: more knowns than unknowns

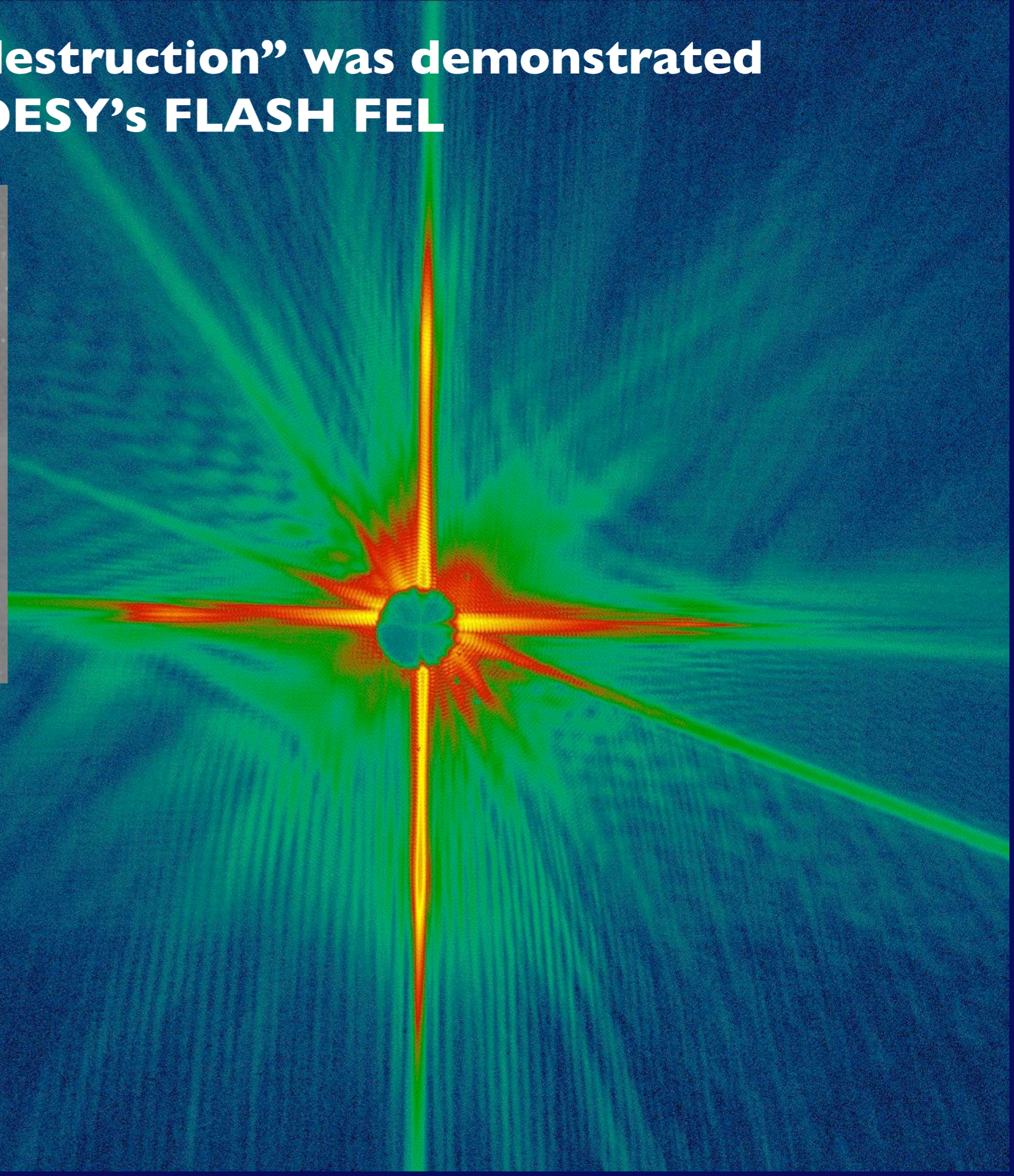
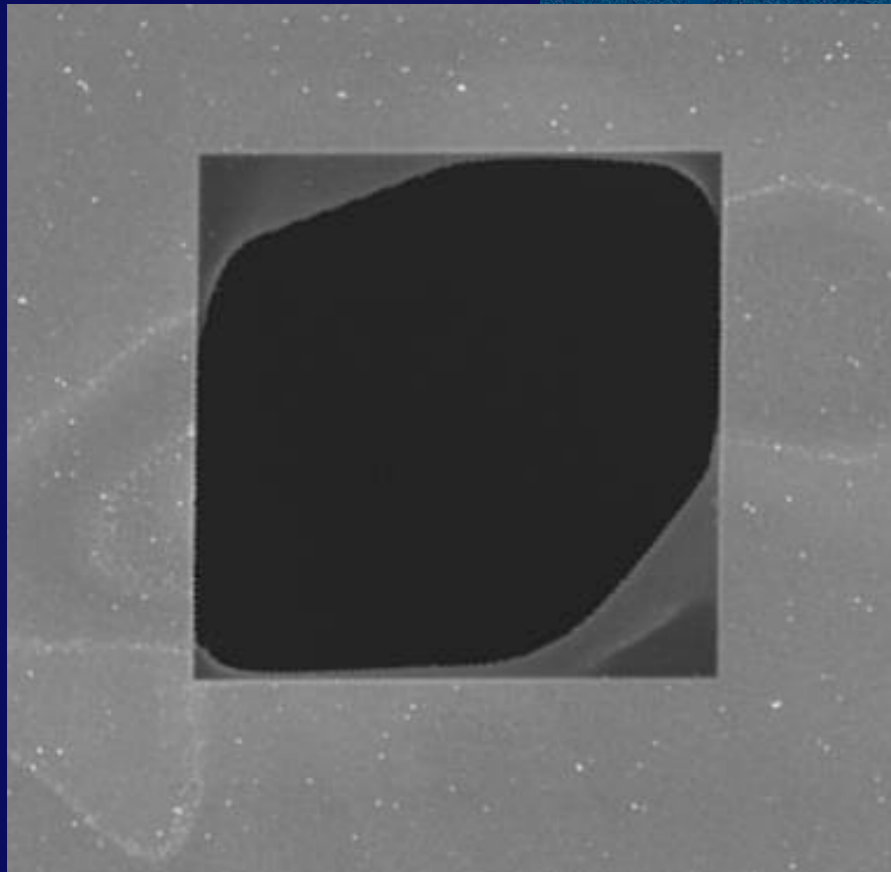
Phasing is achieved using iterative algorithms



Chapman et al. Nature Physics 2 839 (2006)

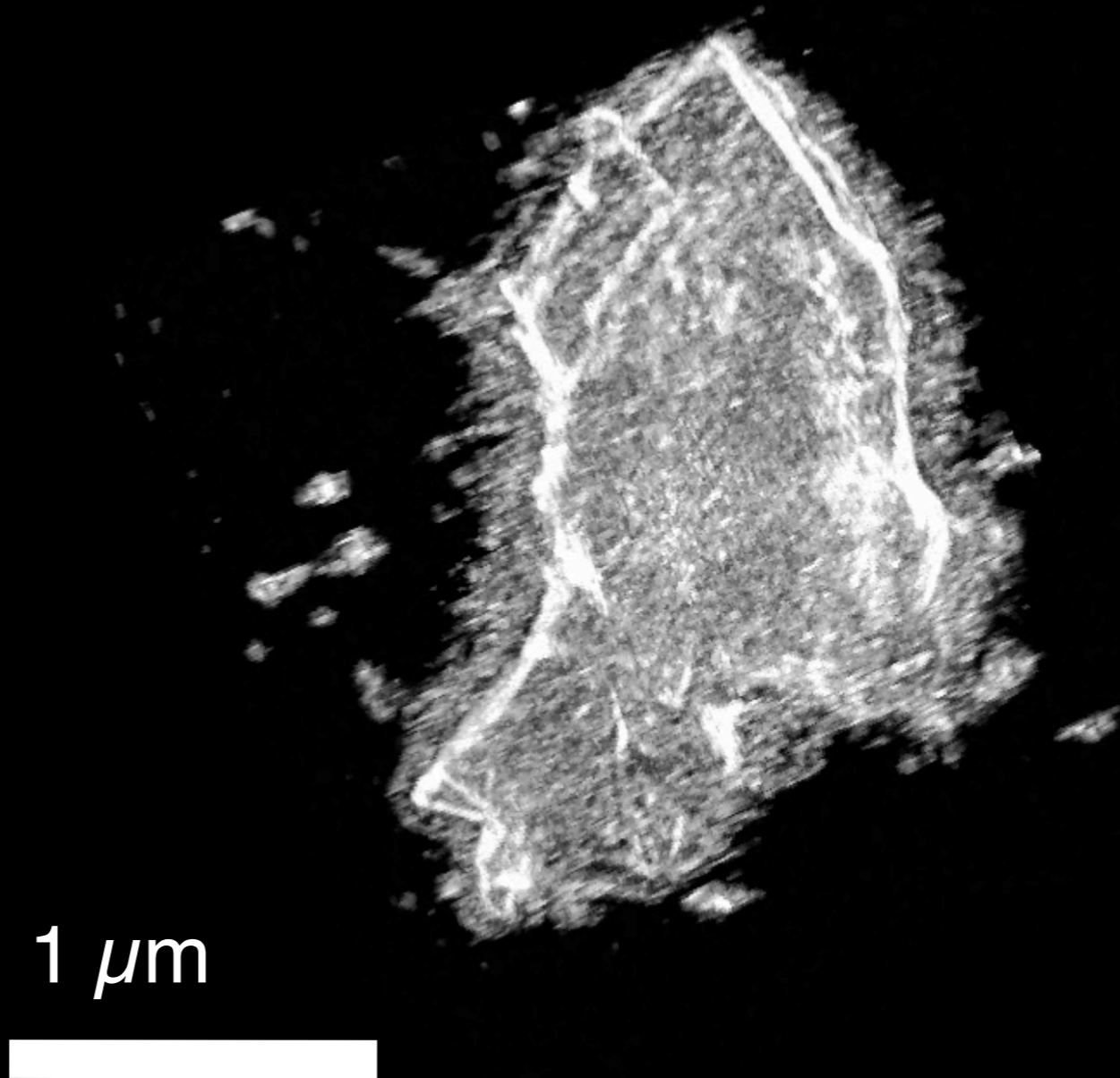
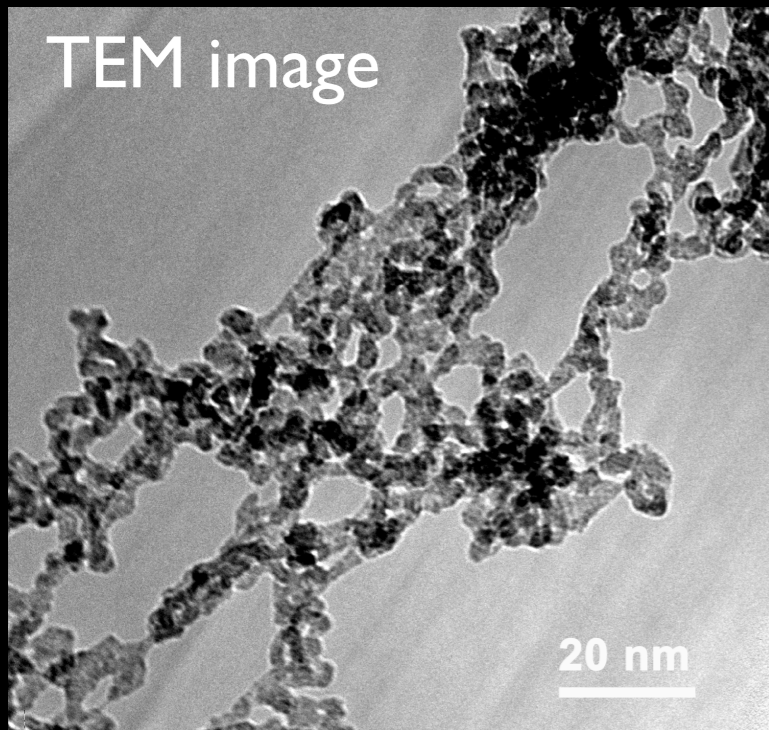


“Diffraction before destruction” was demonstrated with soft X-rays at DESY’s FLASH FEL

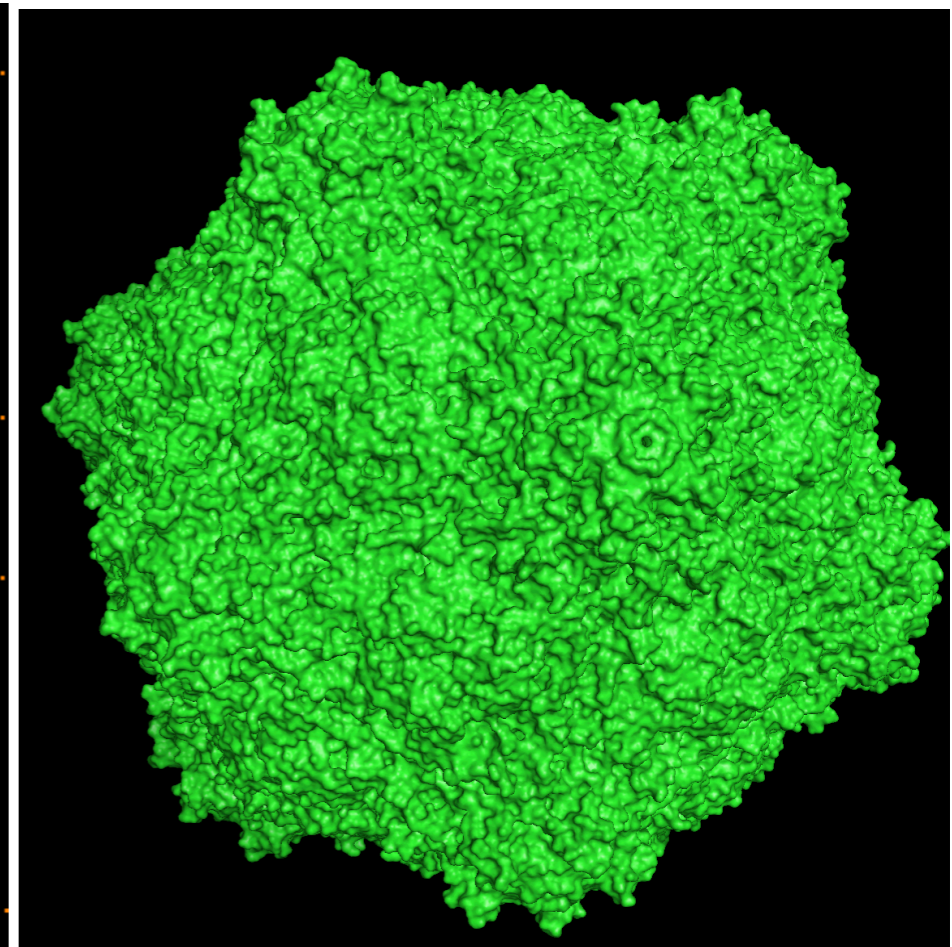
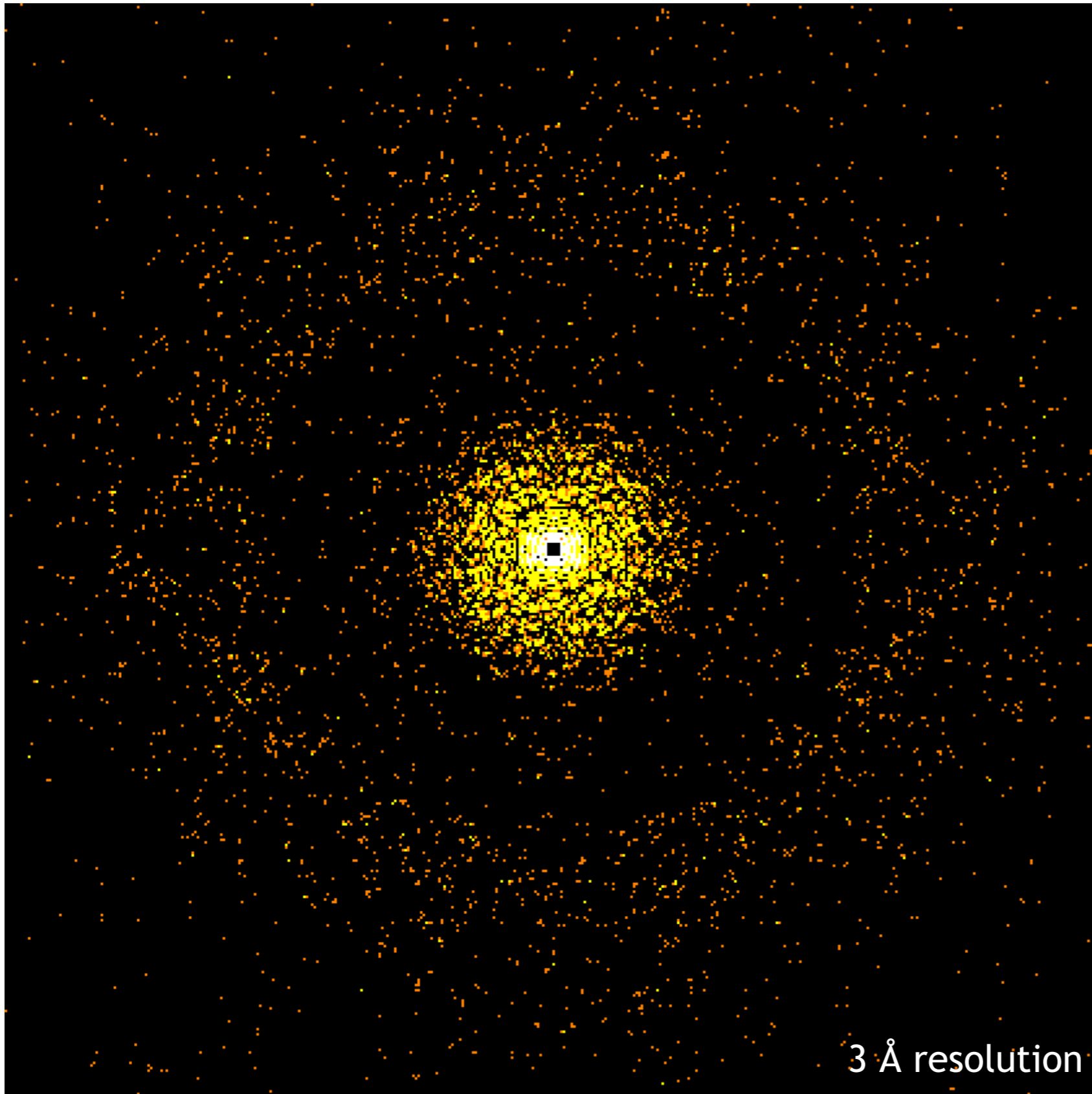


We have performed 3D X-ray imaging of Aerogel foam at 10 nm resolution

Analysis of the 3D image reveals anisotropy in the structure. Other characterization techniques (TEM, SAXS) could not reveal this



Atomic-resolution diffraction from single particles requires focused intensities of more than 10^{14} ph/ μm^2



← 28 nm →

10^{14} ph/ μm^2

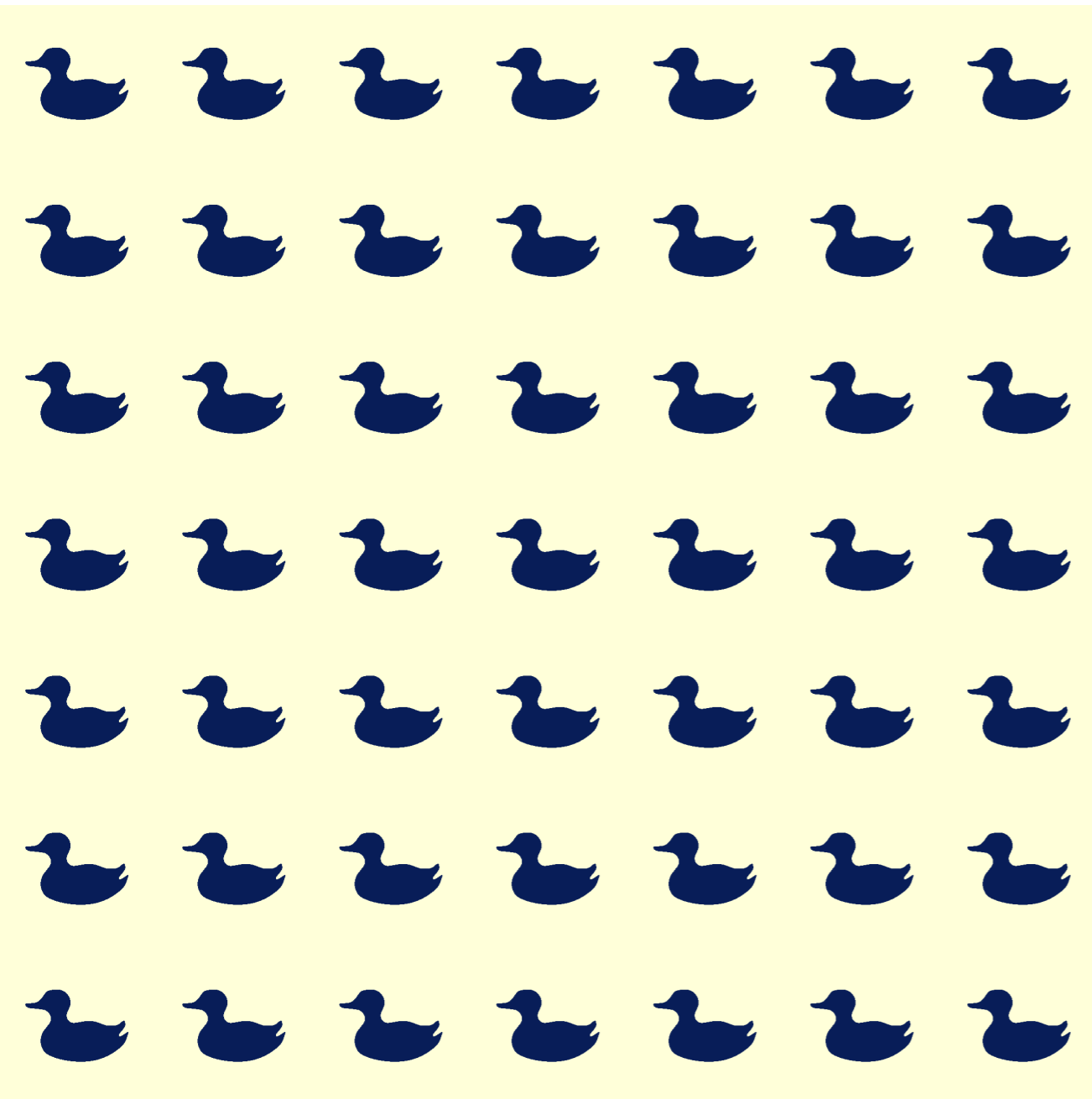
60 GGy

6000 MGy/fs × 10 fs

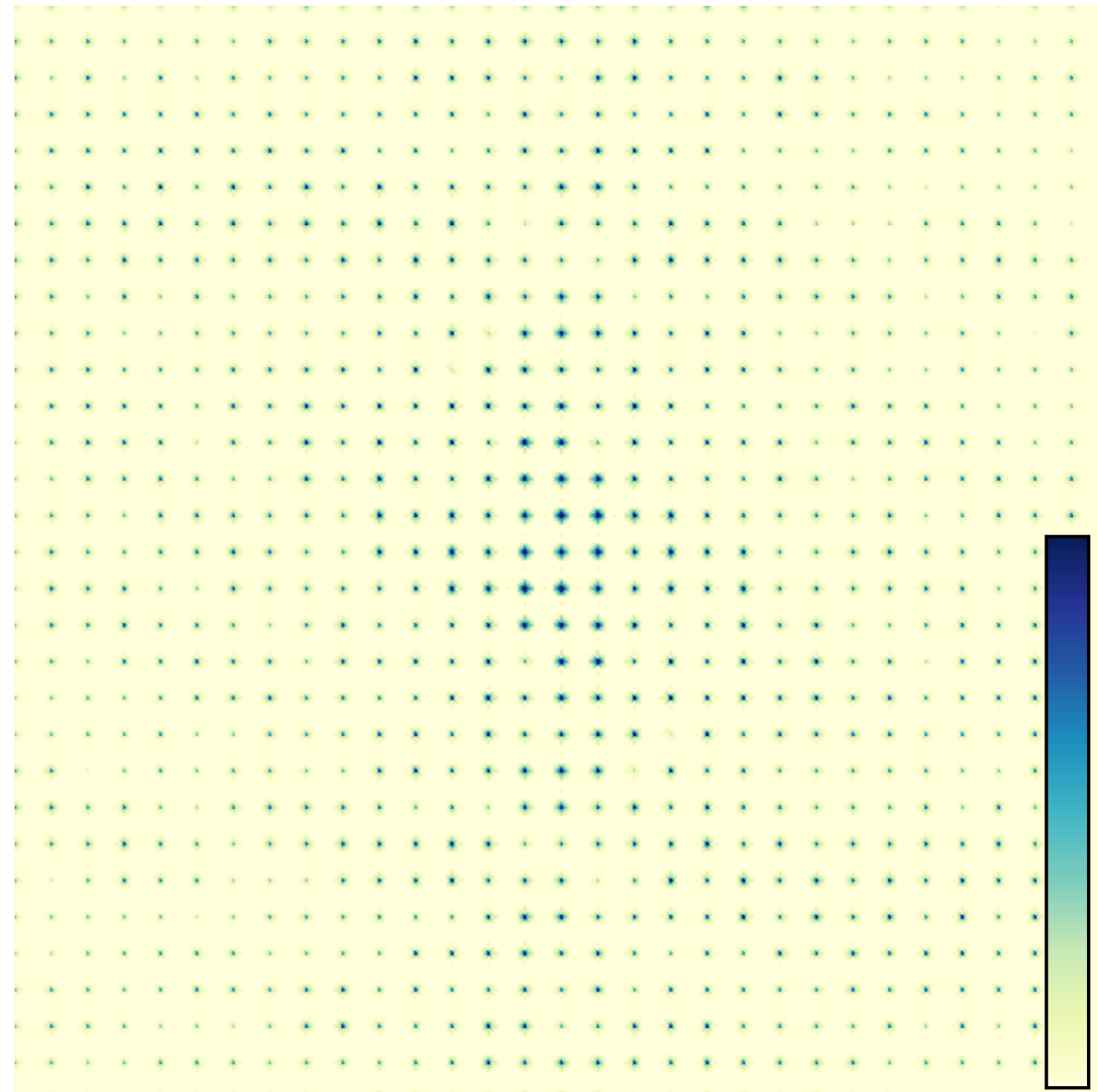
RMS displacement: 0.5 Å
half electrons ionized

Crystals give Bragg spots

$$\rho(\mathbf{x})$$



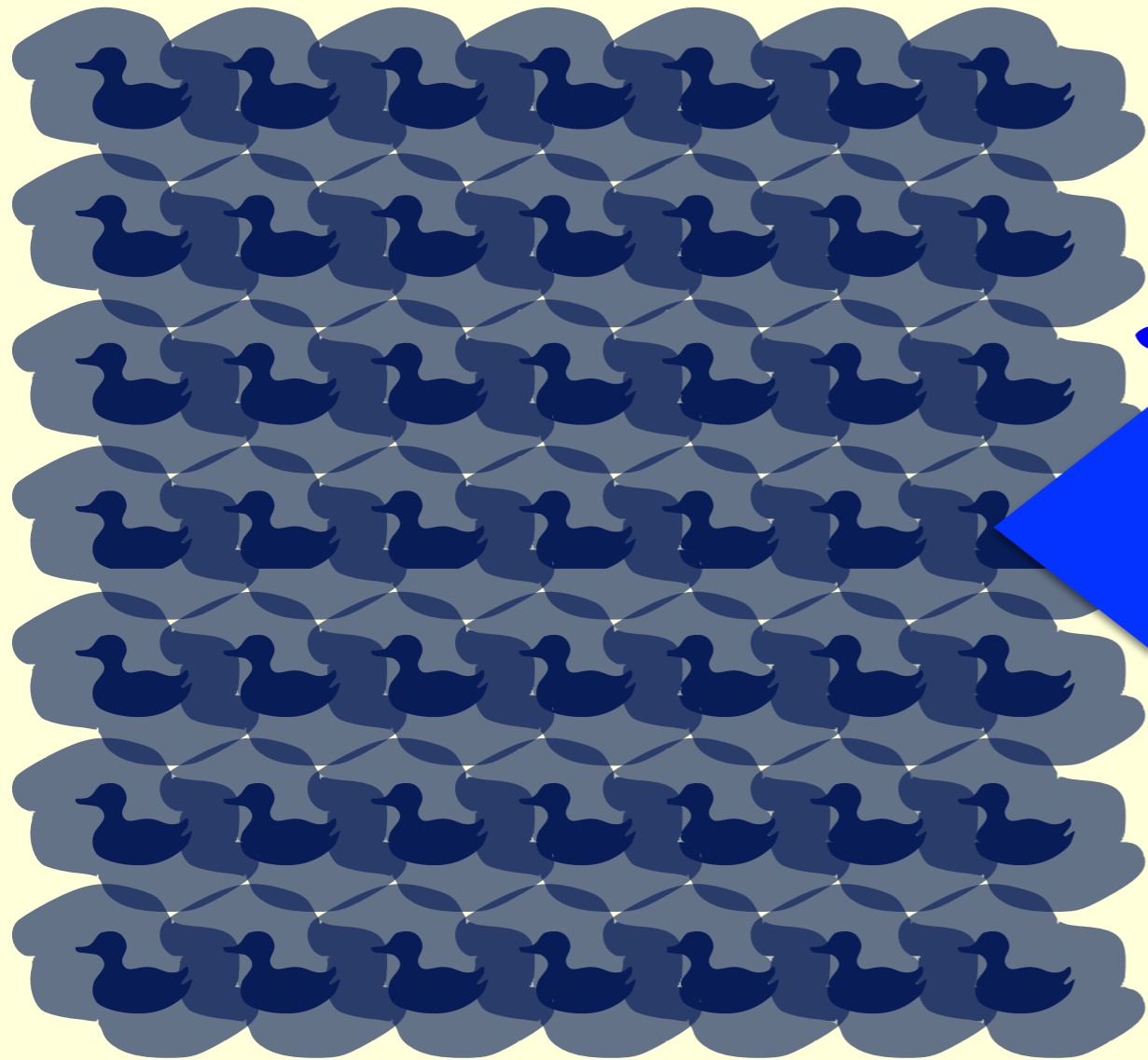
$$I(\mathbf{q}) = |\hat{\rho}(\mathbf{q})|^2$$



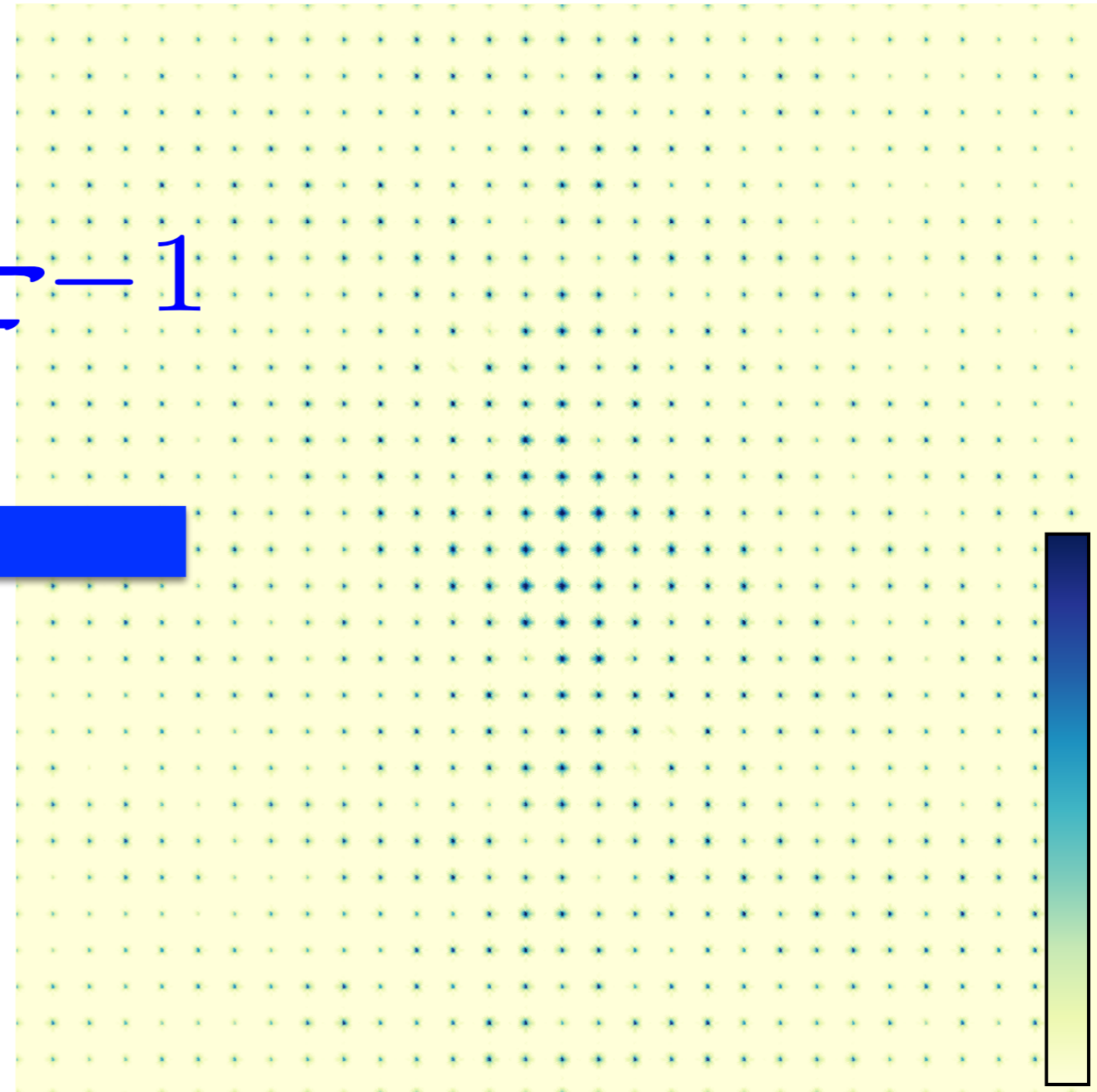
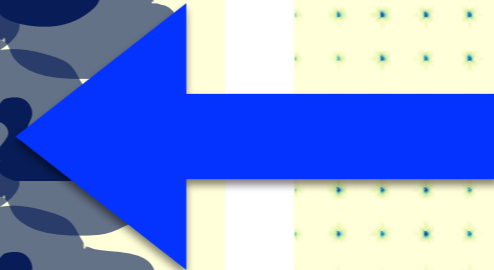
Crystals give Bragg spots

$$\mathcal{F}^{-1}\{I(\mathbf{q})\} = \rho(\mathbf{x}) \otimes \rho^*(-\mathbf{x})$$

$$I(\mathbf{q}) = |\hat{\rho}(\mathbf{q})|^2$$



\mathcal{F}^{-1}



Under-constrained: fewer knowns than unknowns

Recent hard X-ray experiments show high-resolution diffraction

Photosystem I

9.3 keV

Single shot pattern

~ 1 mJ (5×10^{11} photons)

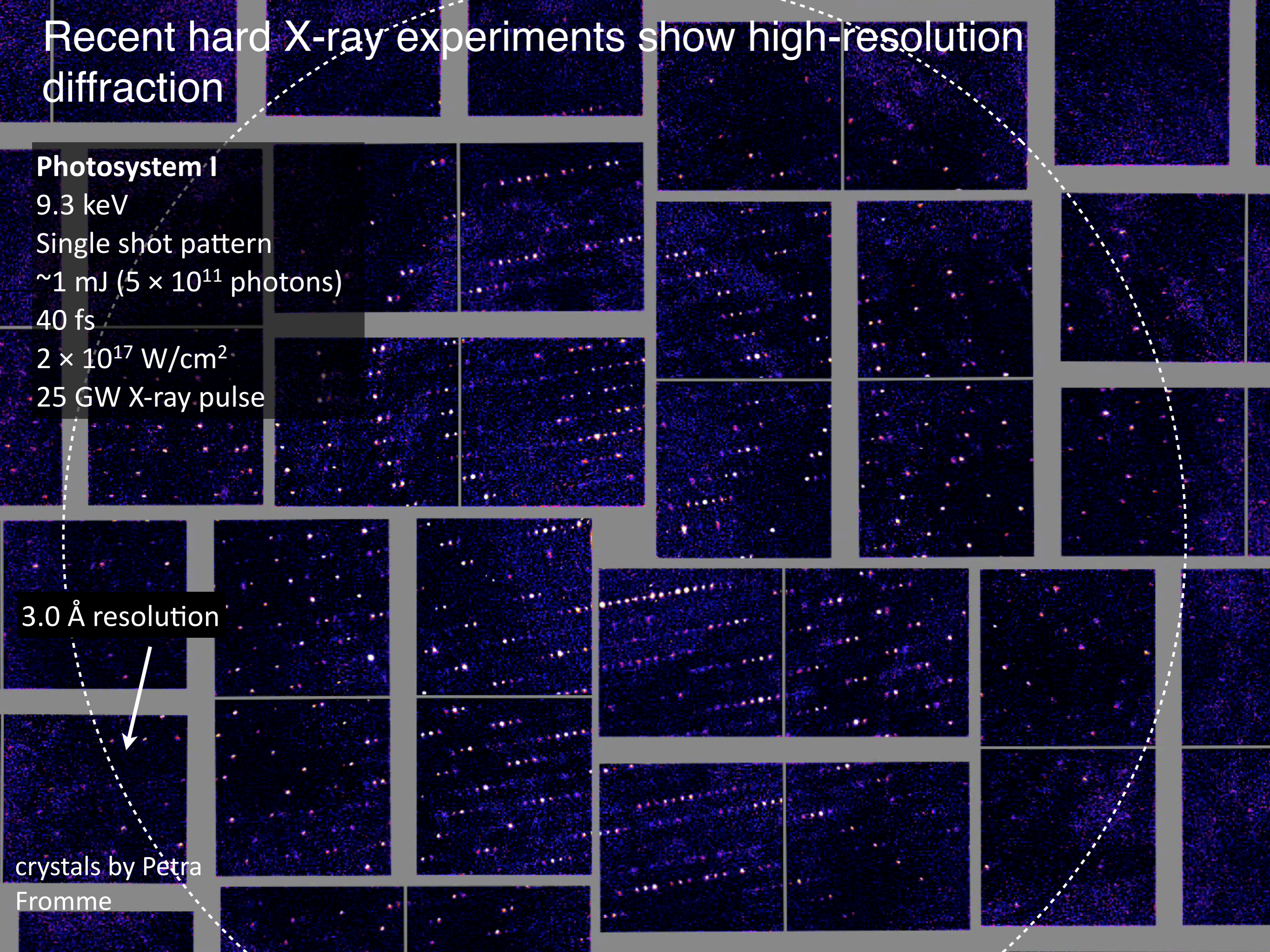
40 fs

2×10^{17} W/cm²

25 GW X-ray pulse

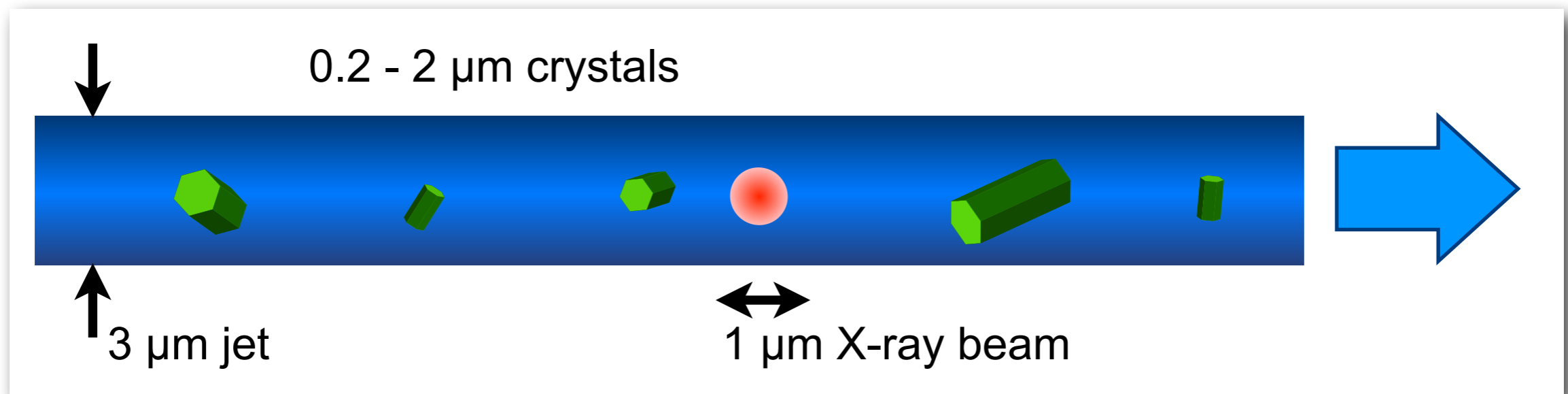
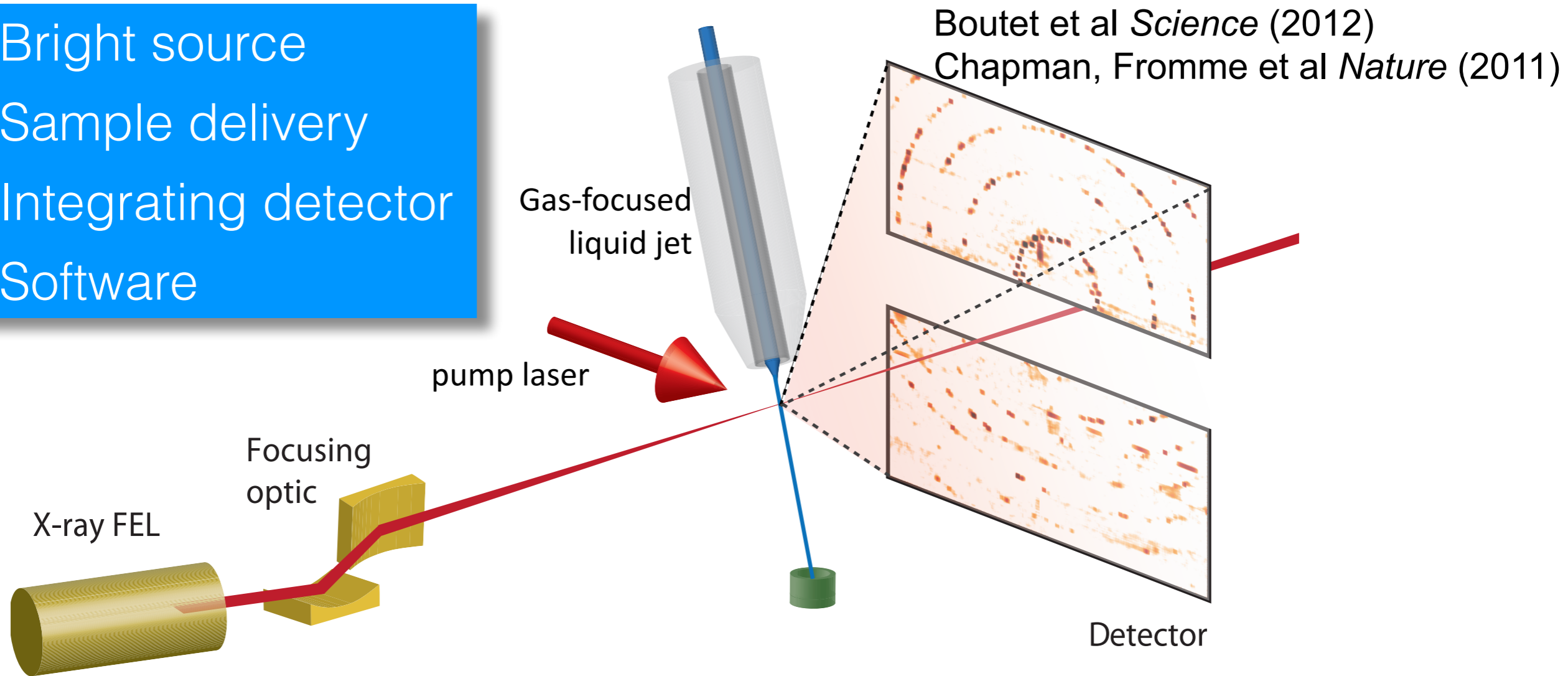
3.0 Å resolution

crystals by Petra
Fromme



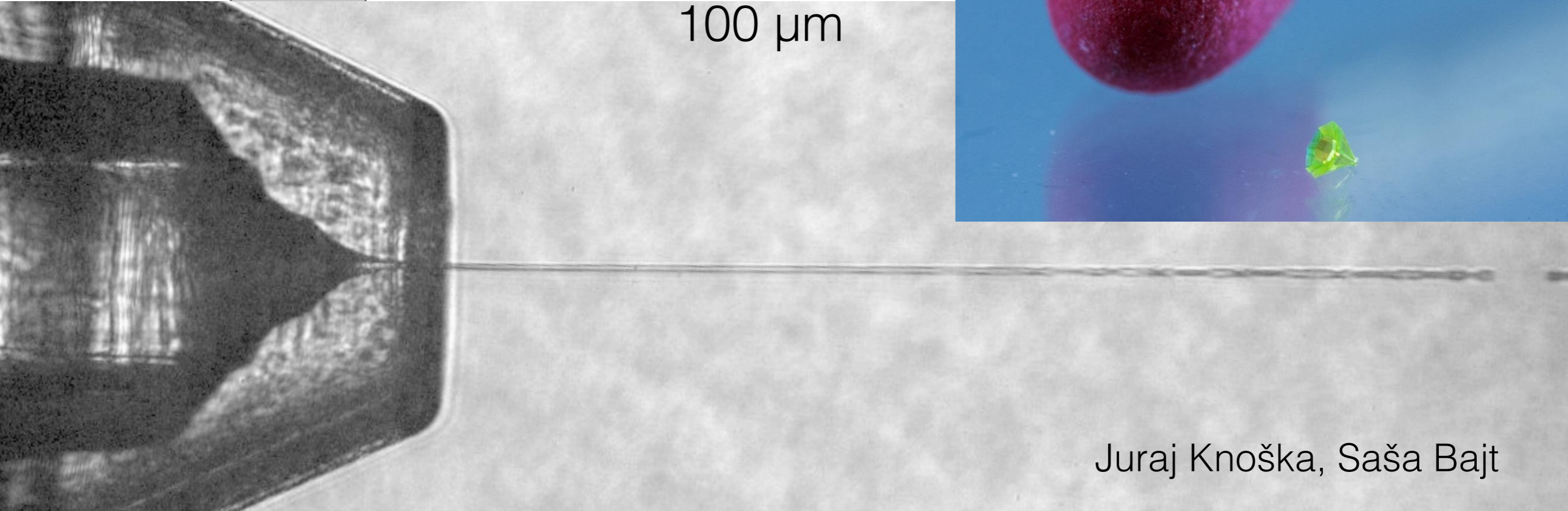
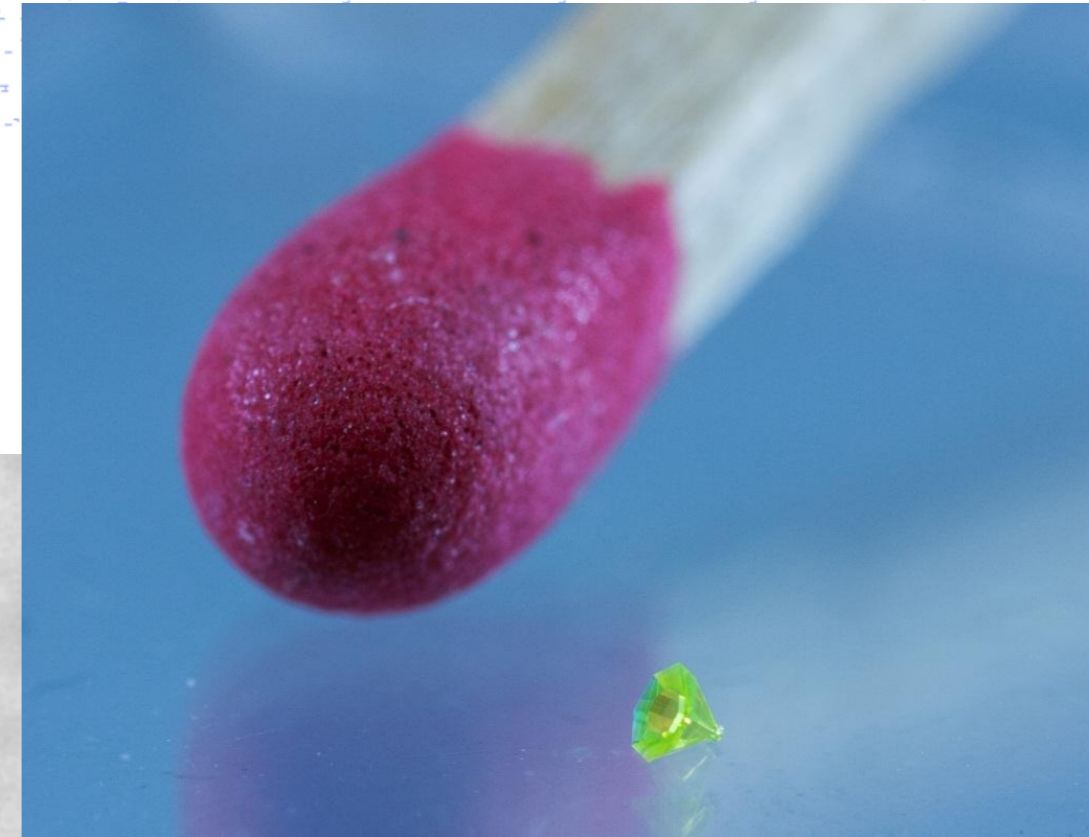
Serial crystallography is made possible by four key technologies

1. Bright source
2. Sample delivery
3. Integrating detector
4. Software



Micrometer-diameter jets are formed by fluid and gas focusing

Božidar Šarler

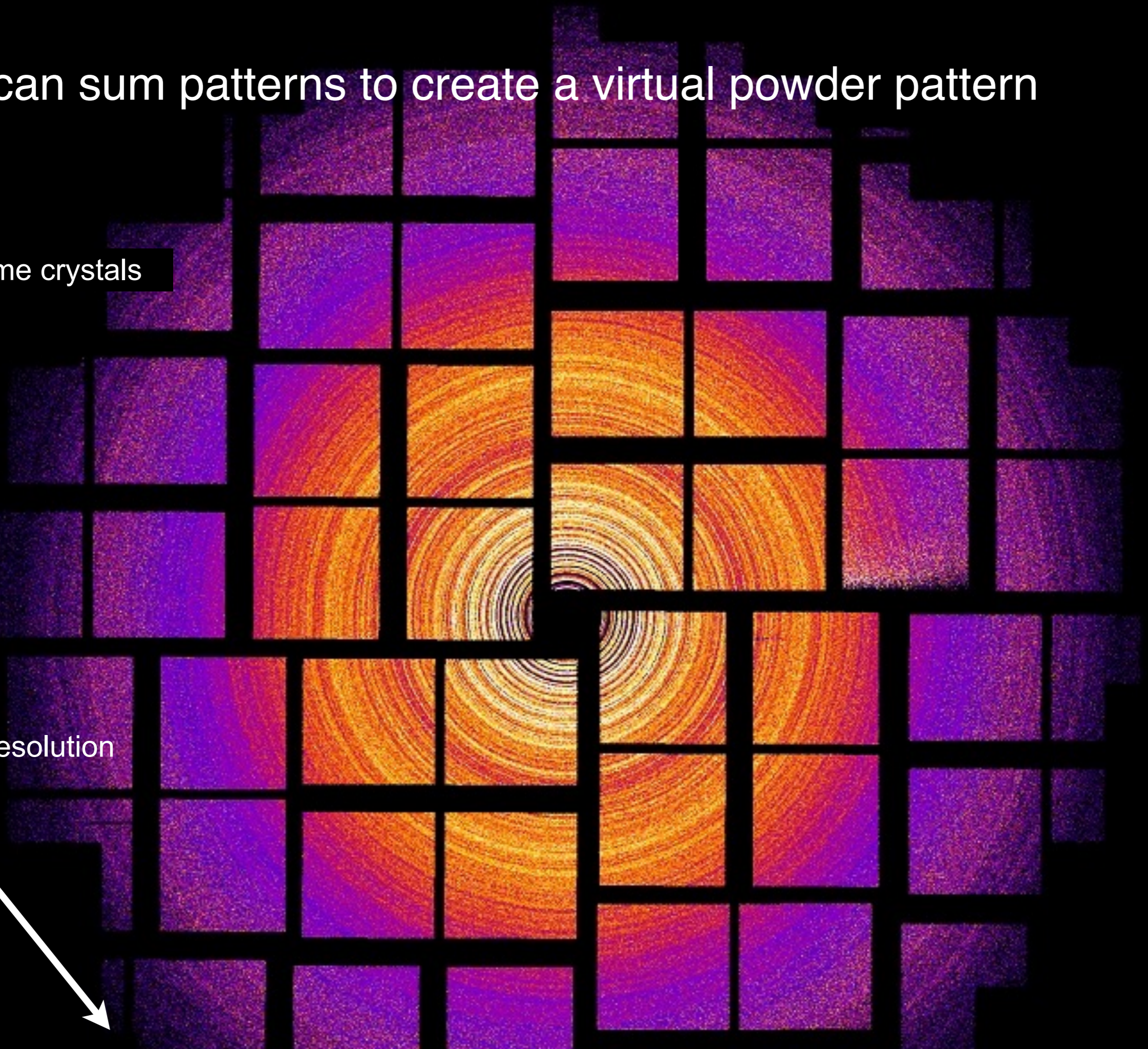


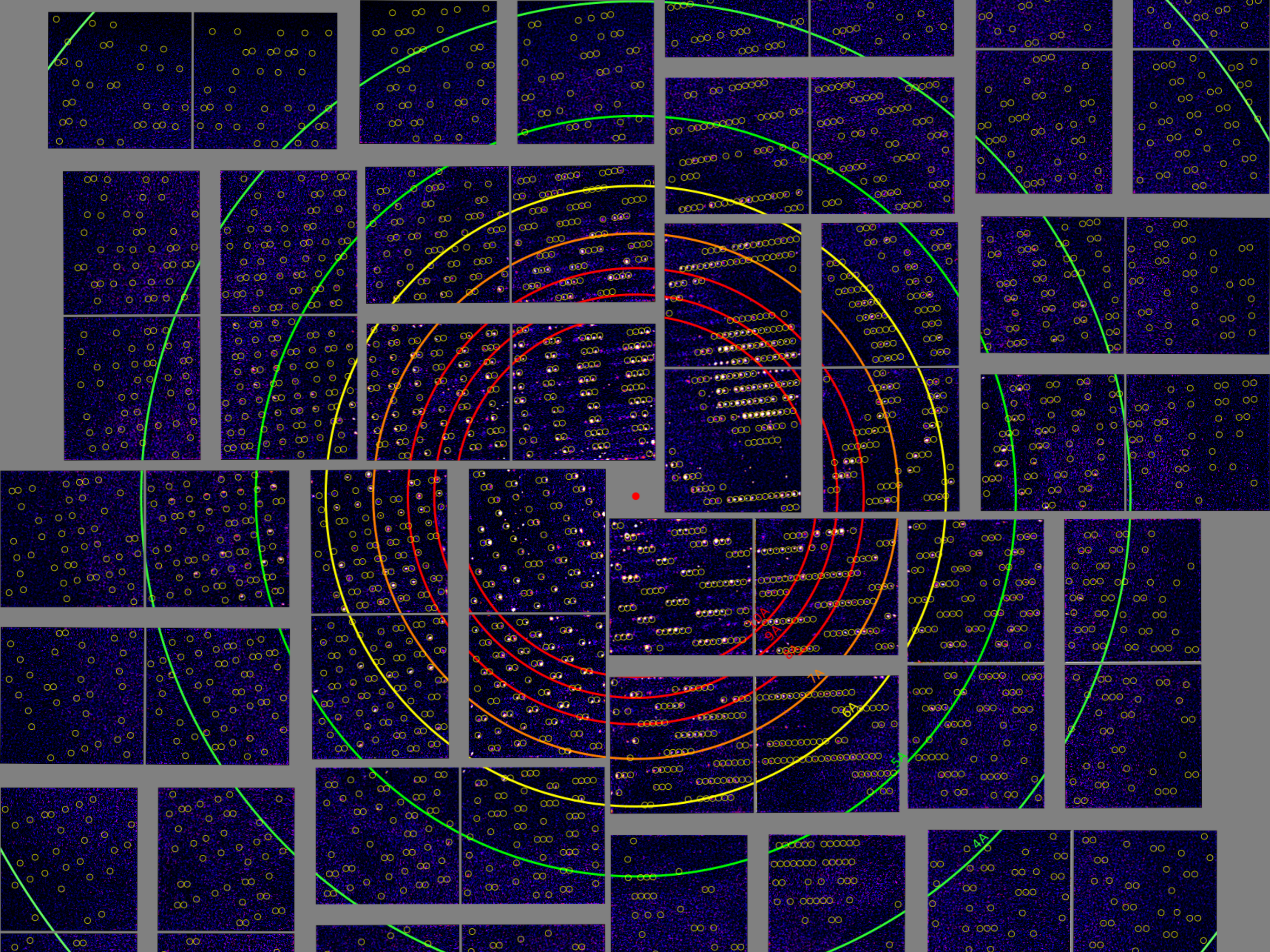
Juraj Knoška, Saša Bajt

We can sum patterns to create a virtual powder pattern

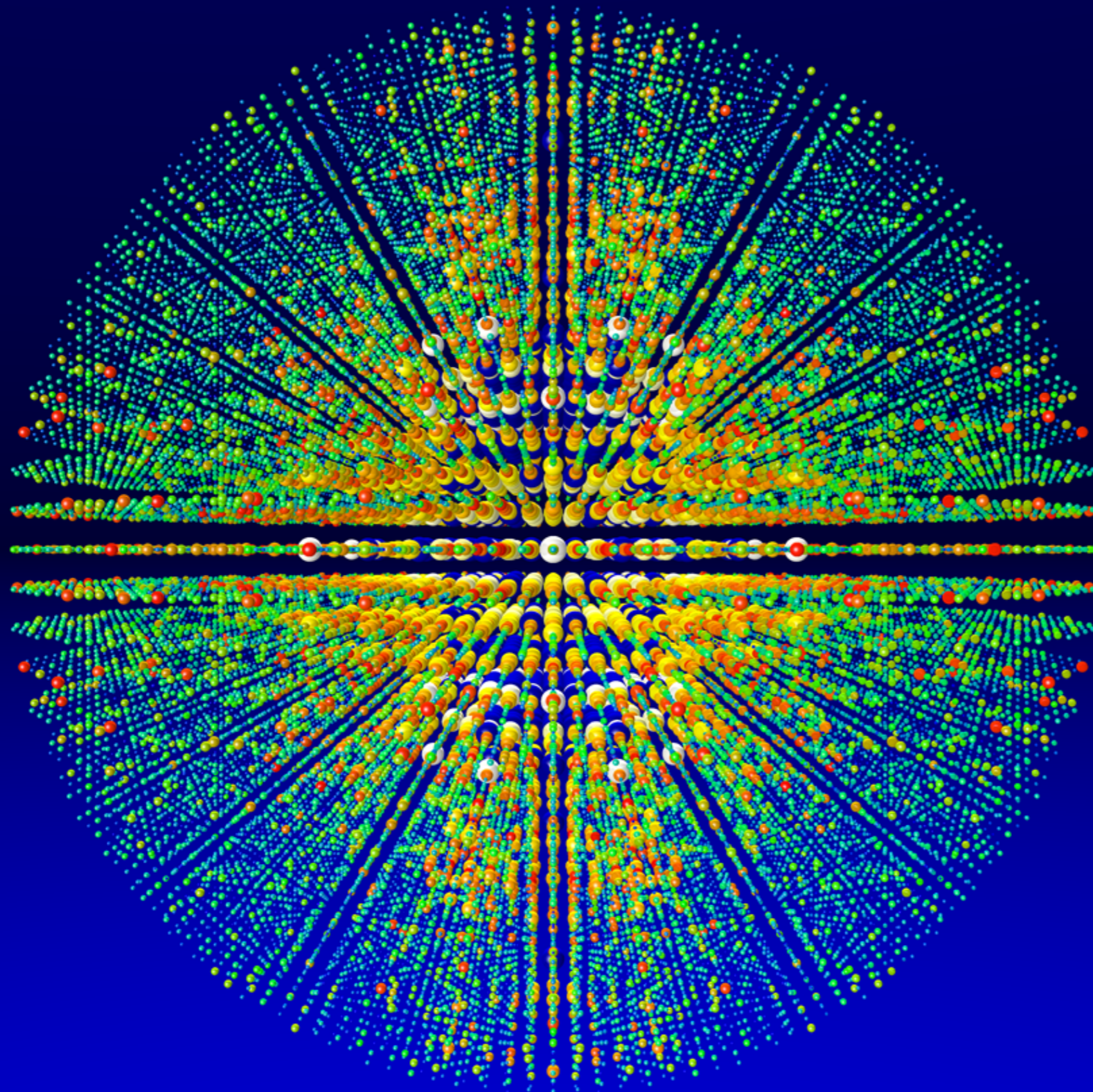
Lysozyme crystals

1.9 Å resolution

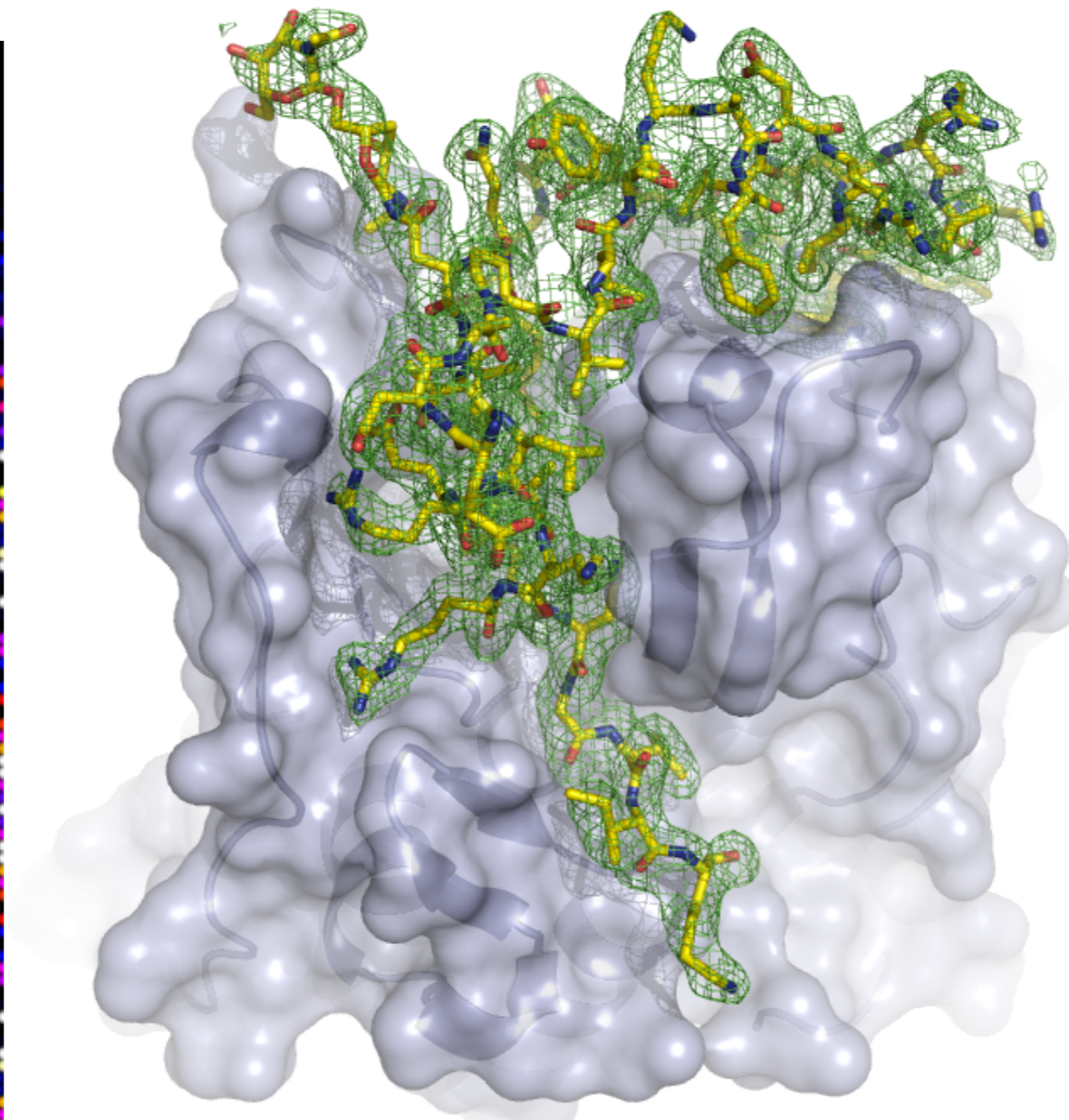
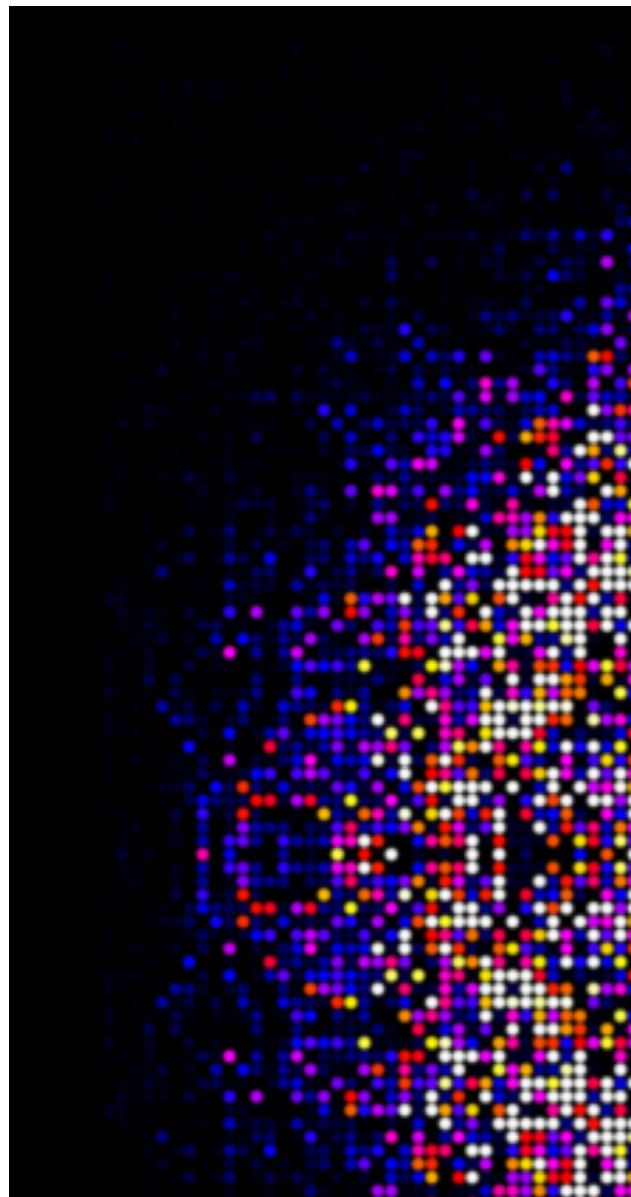




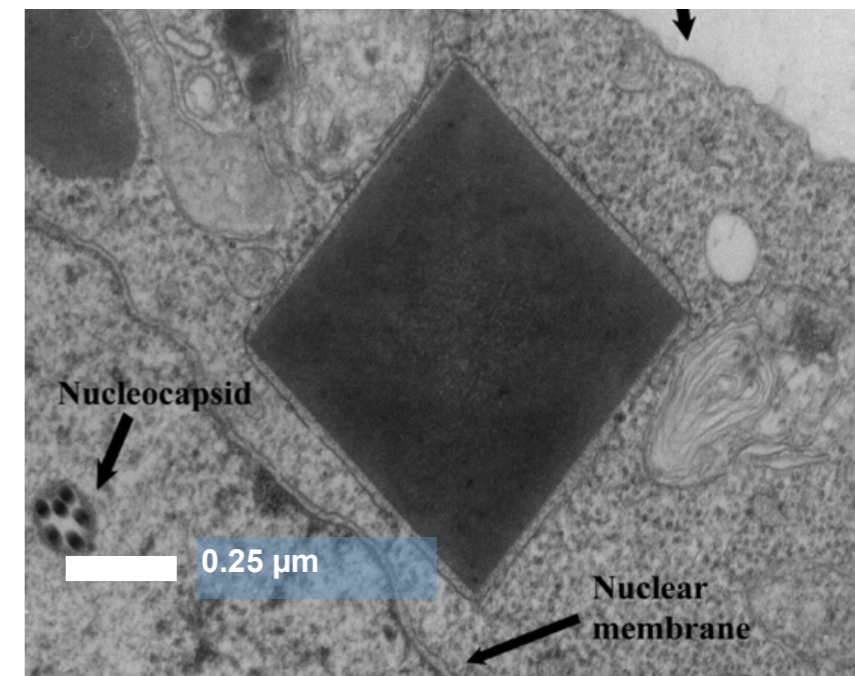
Intensities are merged into a “3D powder” pattern



Structures have been obtained by in vivo grown crystals



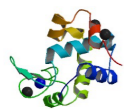
Trypanosoma brucei cathepsin B obtained from in vivo grown crystals



Redecke, Nass et al. Science (2013)

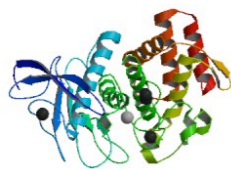
Merged structure factors from 175,000 single-shot patterns

Over 100 XFEL structures have been solved



Lysozyme

4ZIX, 5C6I, 5C6J, 5C6L,
4RWI, 4RW2, 4N5R



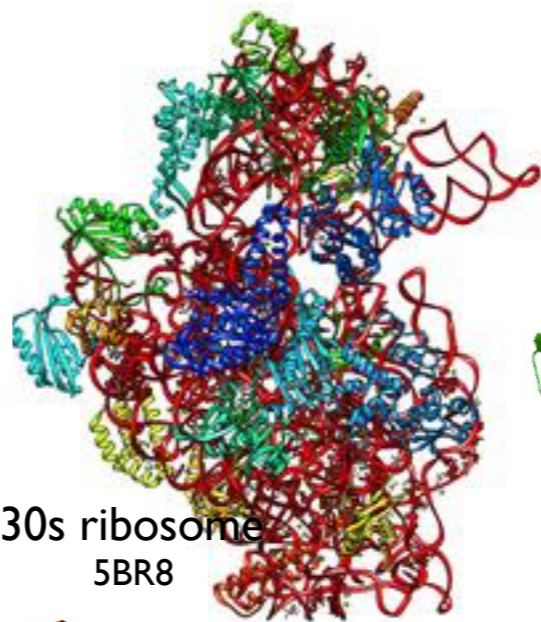
Thermolysin

4OW3,
4TNL, 5DLH



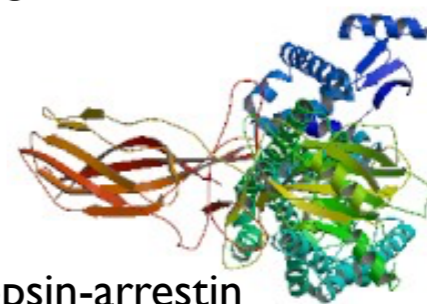
ATPase

4XOU



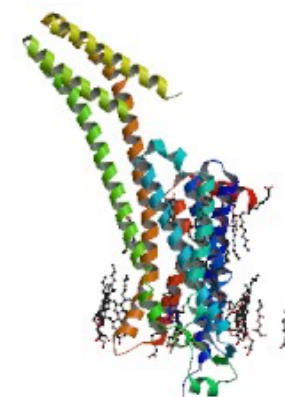
30s ribosome

5BR8



Rhodopsin-arrestin

4ZWJ



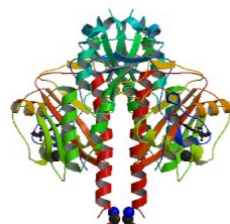
A2a

5K2D, 5K2C,
5K2B, 5K2A



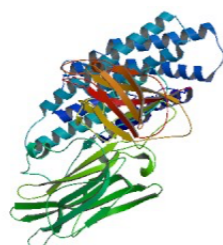
SNARE complex

5CCG



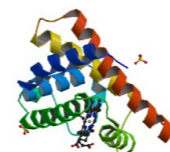
Phytochrome

5MG0, 5MGI, 5L8I



Cry toxin

4QX3,
4QX2,
4QX1, 4QX0



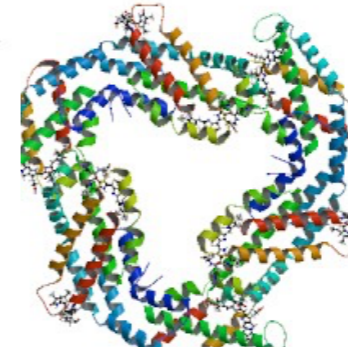
Myoglobin (x15)

4PNJ, 5CNG, 5CNF,
5CNE, 5CND, 5CNC
5CNB, 5CN9, 5CN8,
5CN7, 5CN6, 5CN5,
5CN4, 5CMV, 5JOM



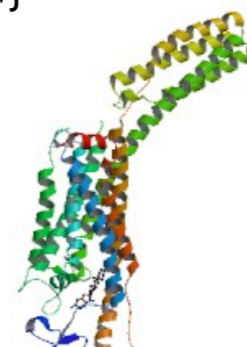
BinAB

5FOY, 5FOZ, 5G37,



Phycocyanin

4Q70, 4Z8K, 4ZIZ



Smoothed

4O9R



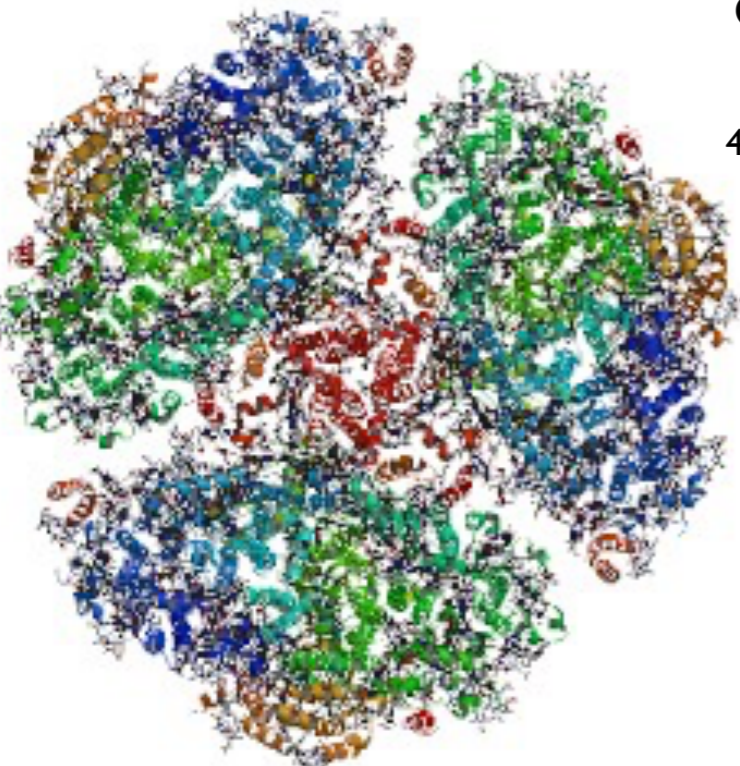
Angiotensin

4YAY



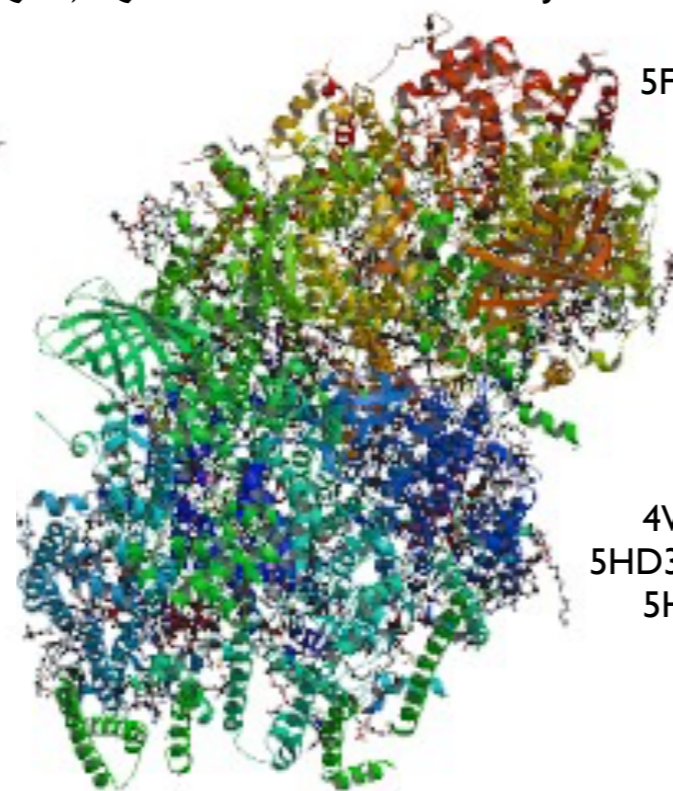
d-opioid

4RWD



Photosystem I+II

3PCQ, 4FBY, 4IXR, 4IXQ,
4TNK, 4TNJ, 4TNI, 4TNH, 4PBU,
4RVY, 5E7C, 5TIS, 5KAI, 5KAF,



PYP

4WLA, 4WL9,
5HD3, 5HDS, 5HDD,
5HDC, 5HD5,

Reaction centre

4AC5, 4CAS,
5M7K, 5M7J



Bacteriorhodopsin

5J7A



DgkA

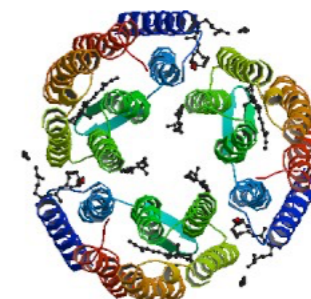
4UYO

CathepsinB

4HWY



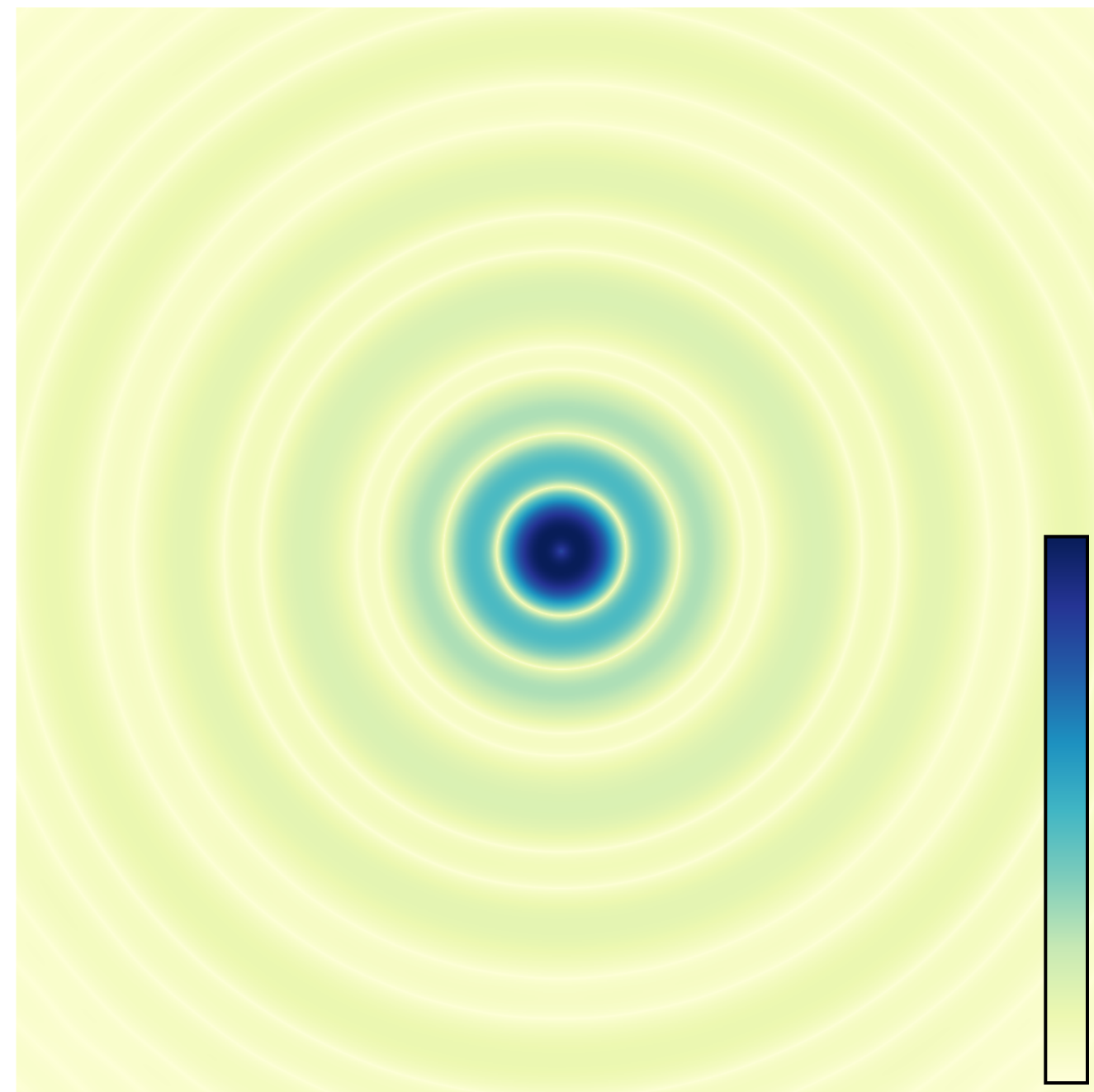
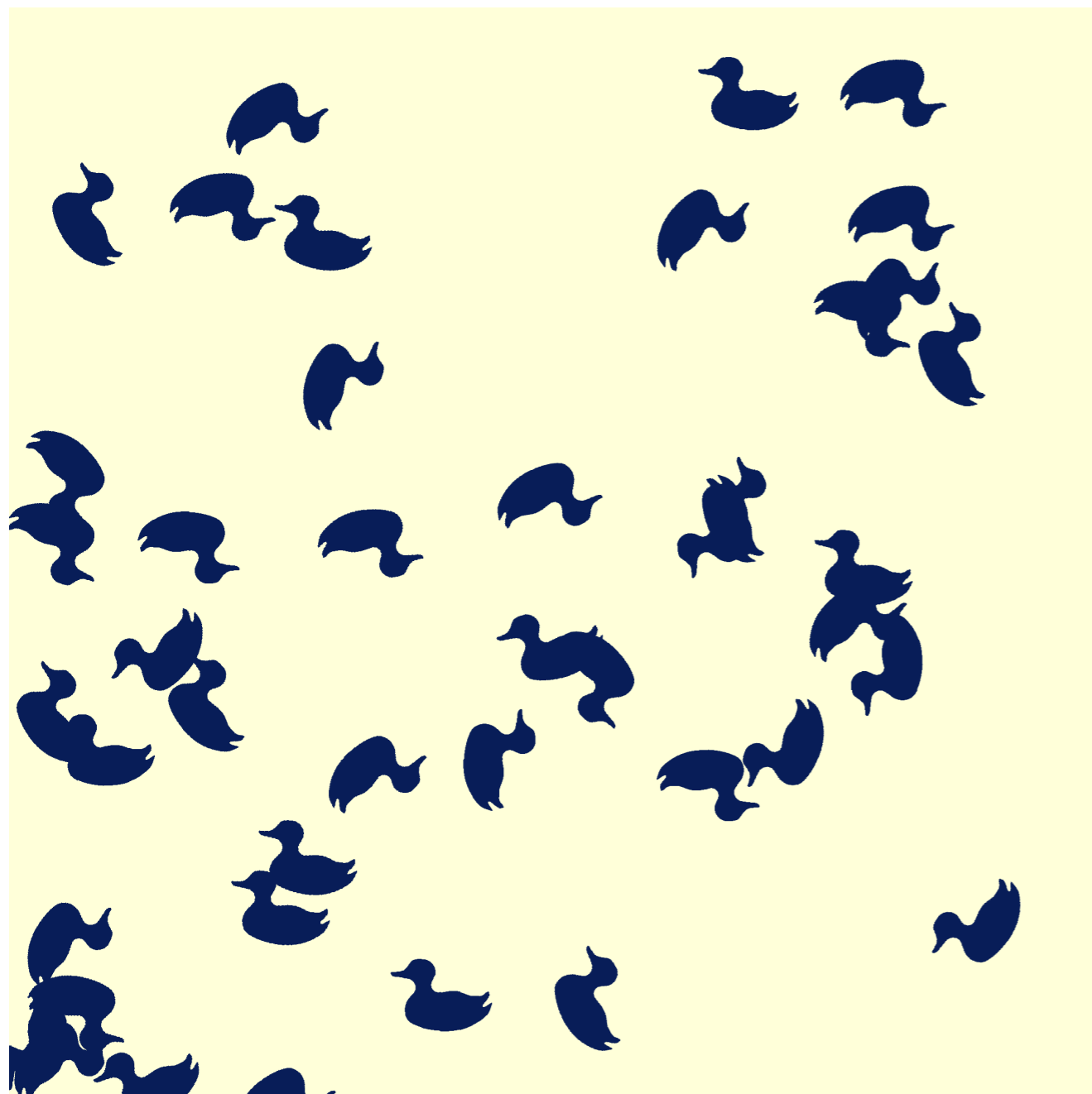
4ZQX



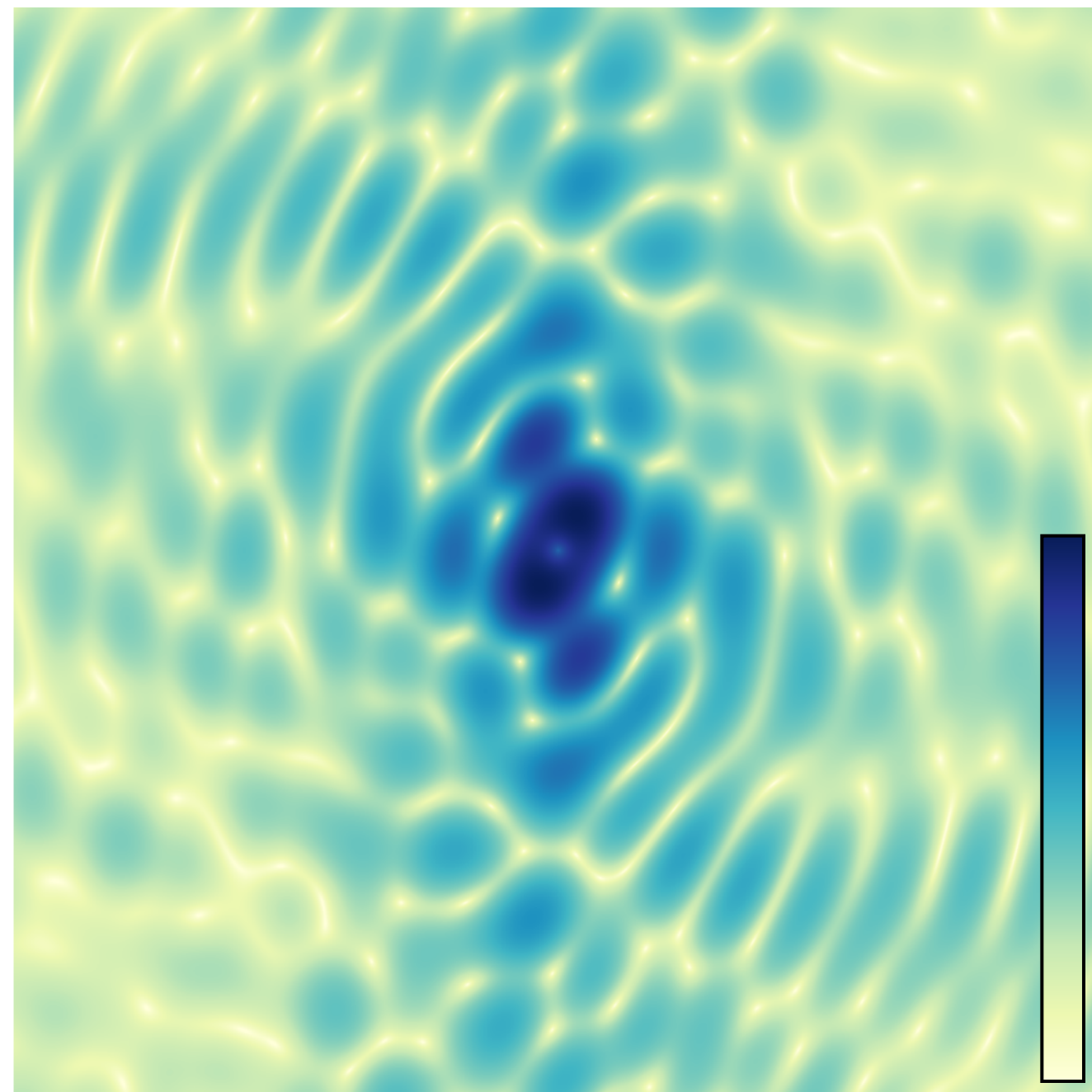
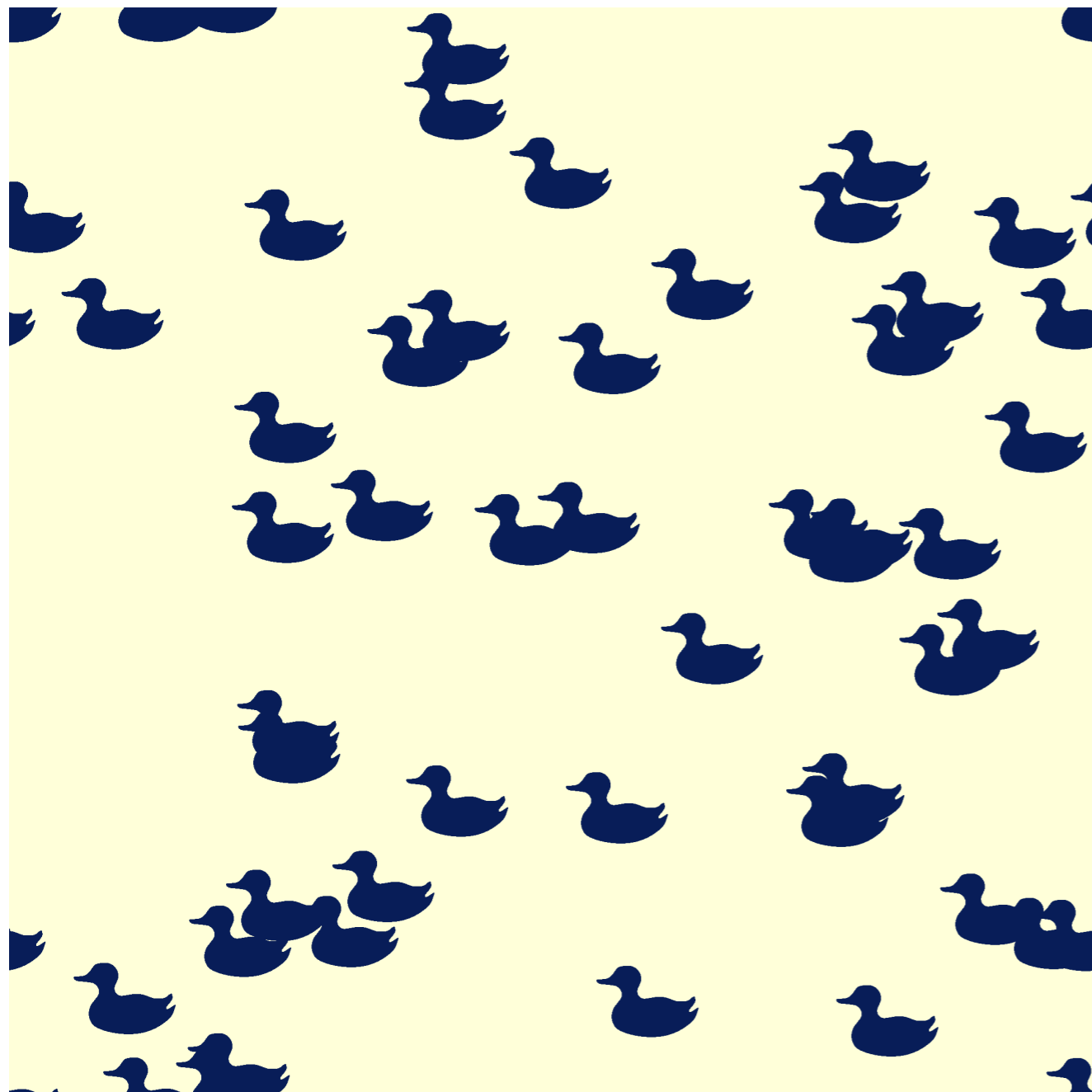
Riboswitch

5SWE, 5SWD, 5E54

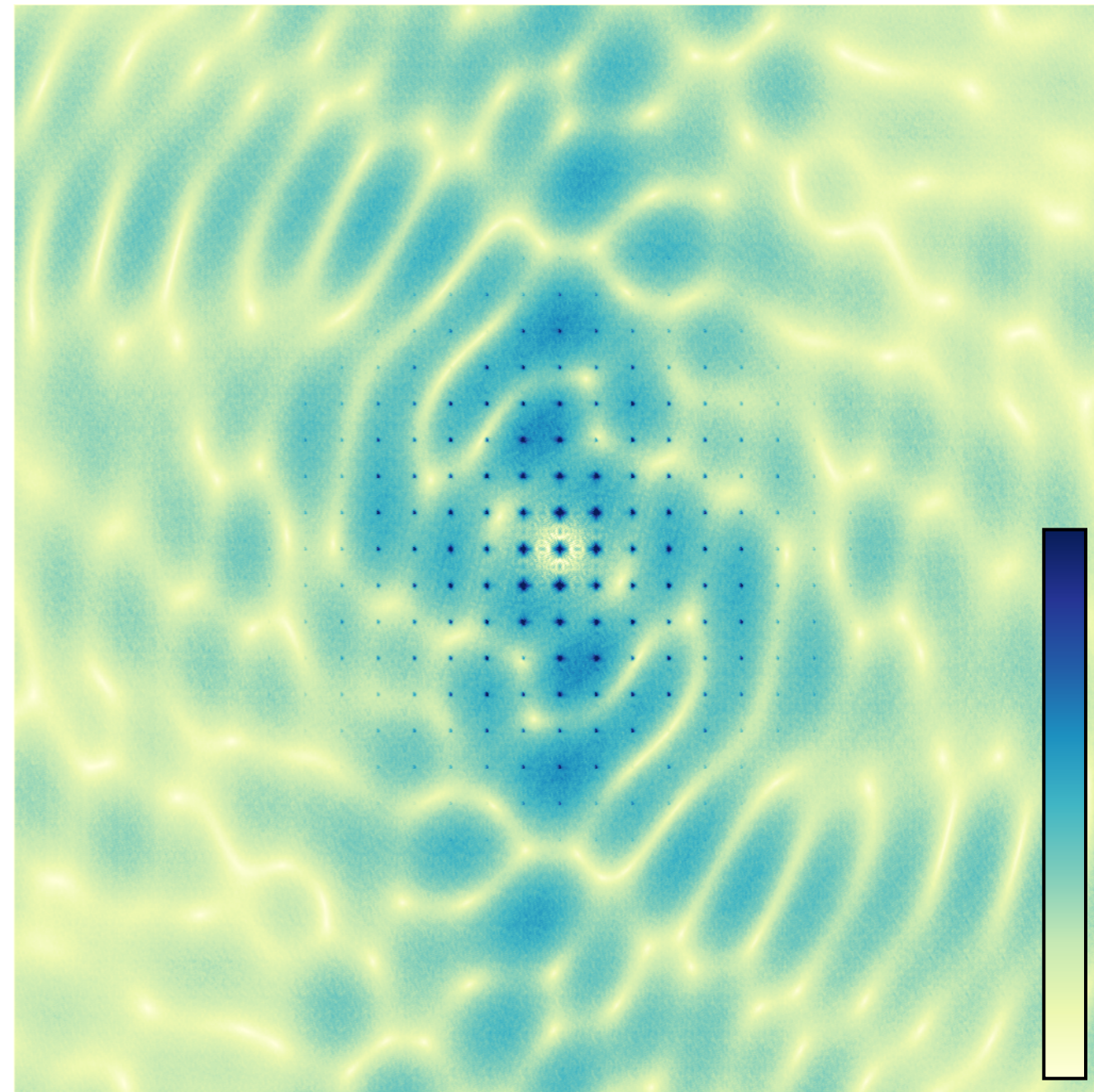
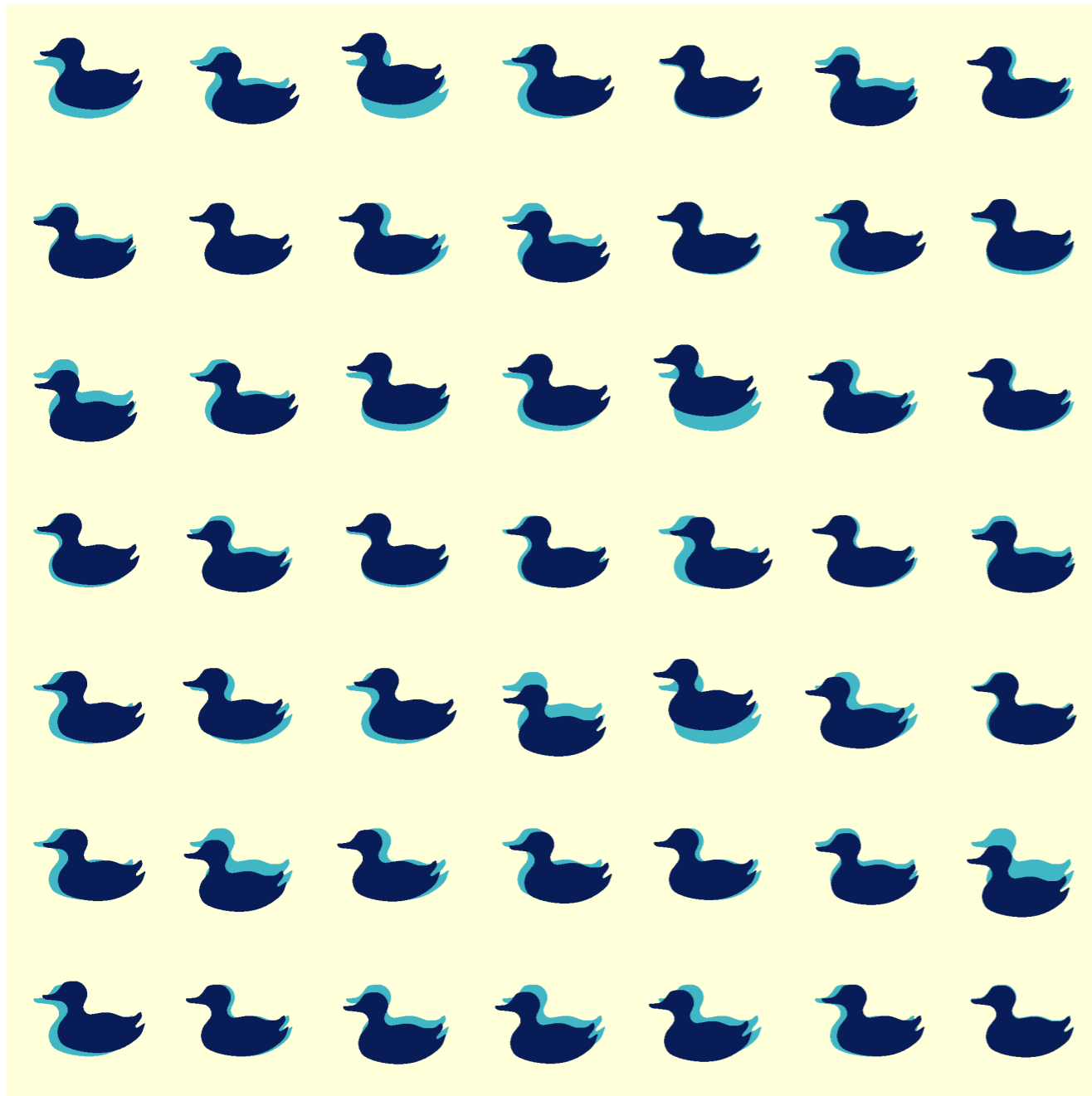
Solution scattering gives single-molecule diffraction, but orientationally averaged



Aligned molecules yield a single-molecule pattern

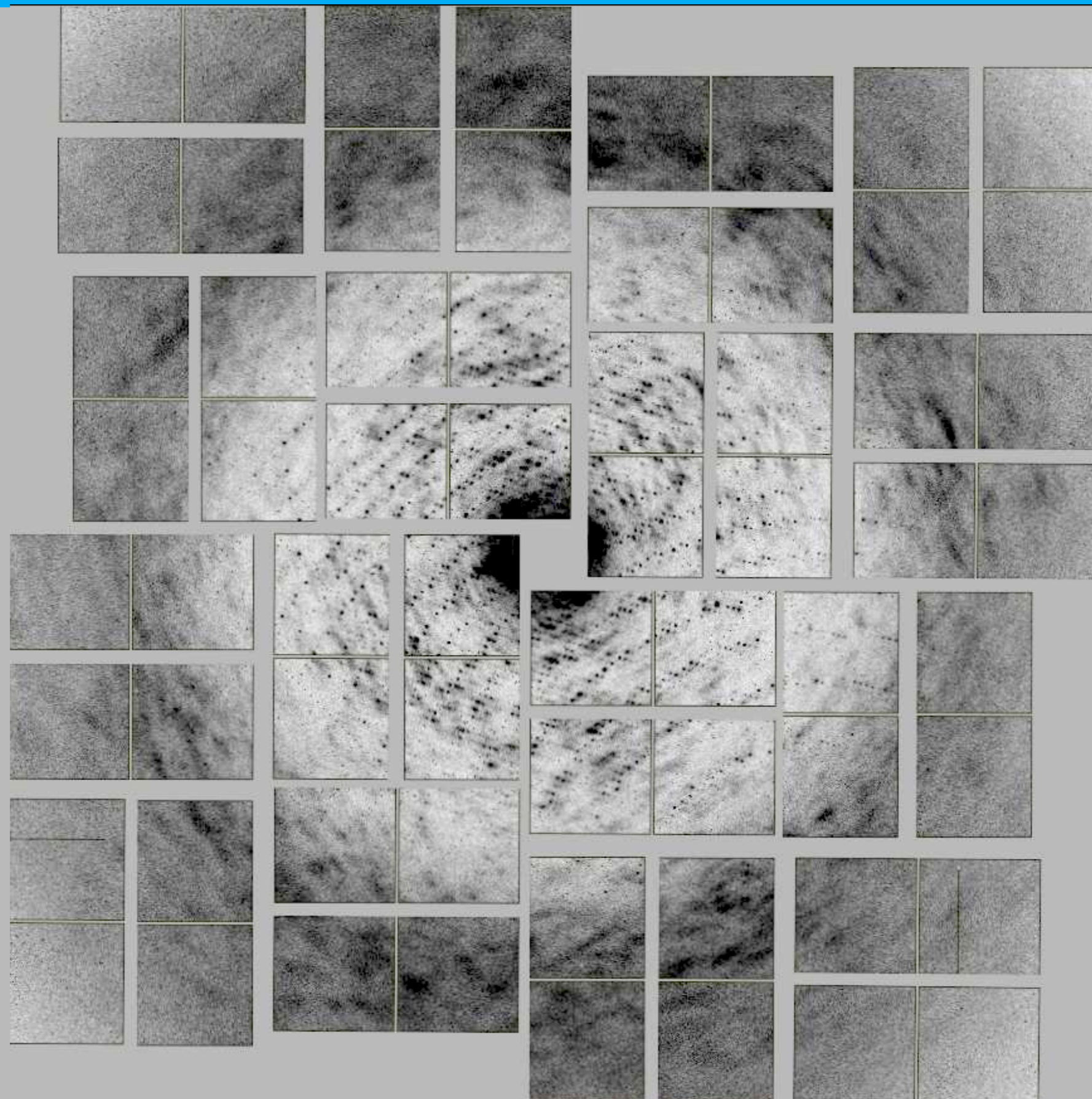


Crystals provide a very high degree of alignment

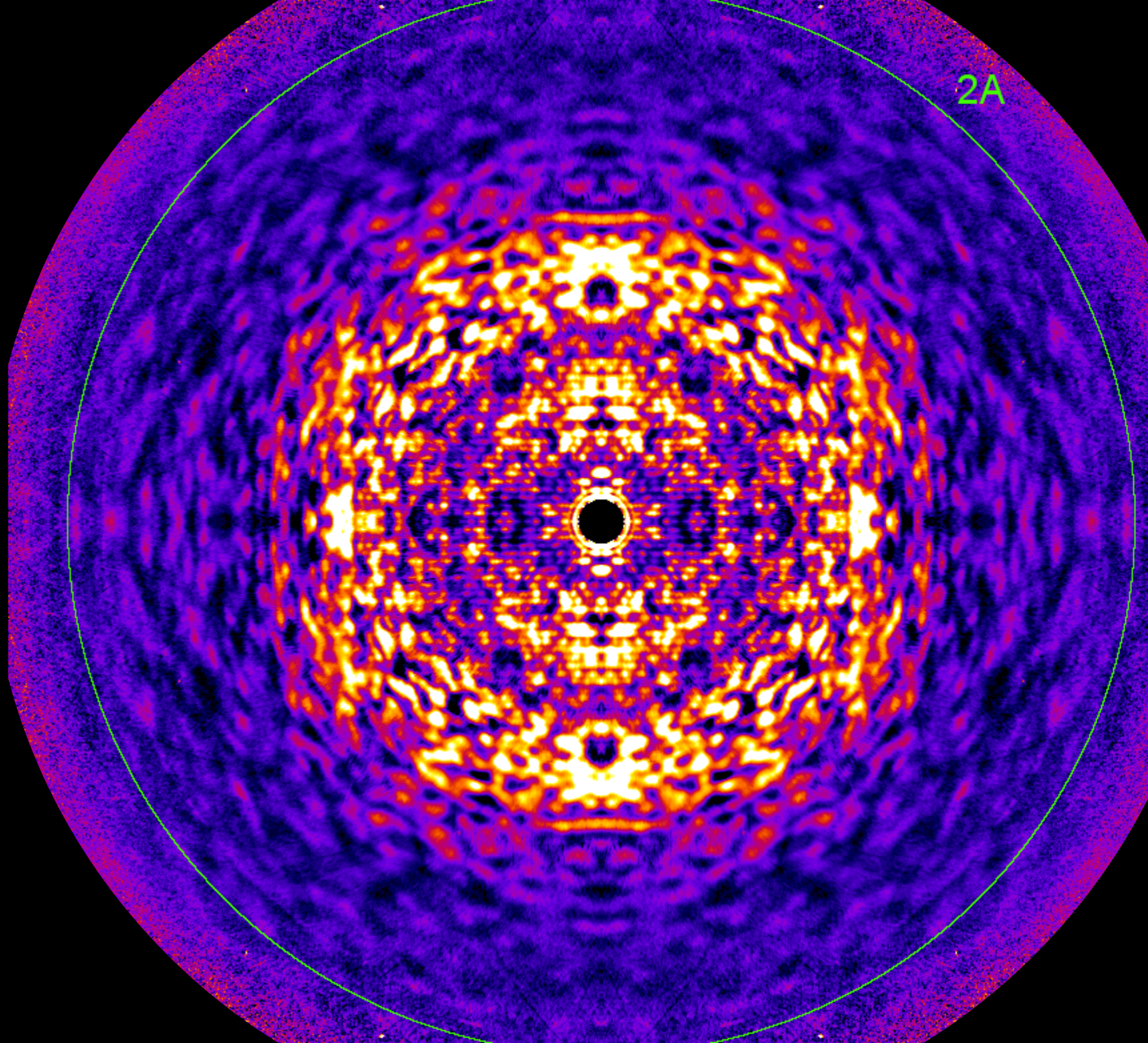


$$\langle I(\mathbf{q}) \rangle = \left| \sum_i \hat{\rho}_i(\mathbf{q}) \right|^2 \exp(-q^2 \sigma^2) + \sum_i |\hat{\rho}_i(\mathbf{q})|^2 (1 - \exp(-q^2 \sigma^2))$$
$$\sigma^2 = \langle D^2 \rangle$$

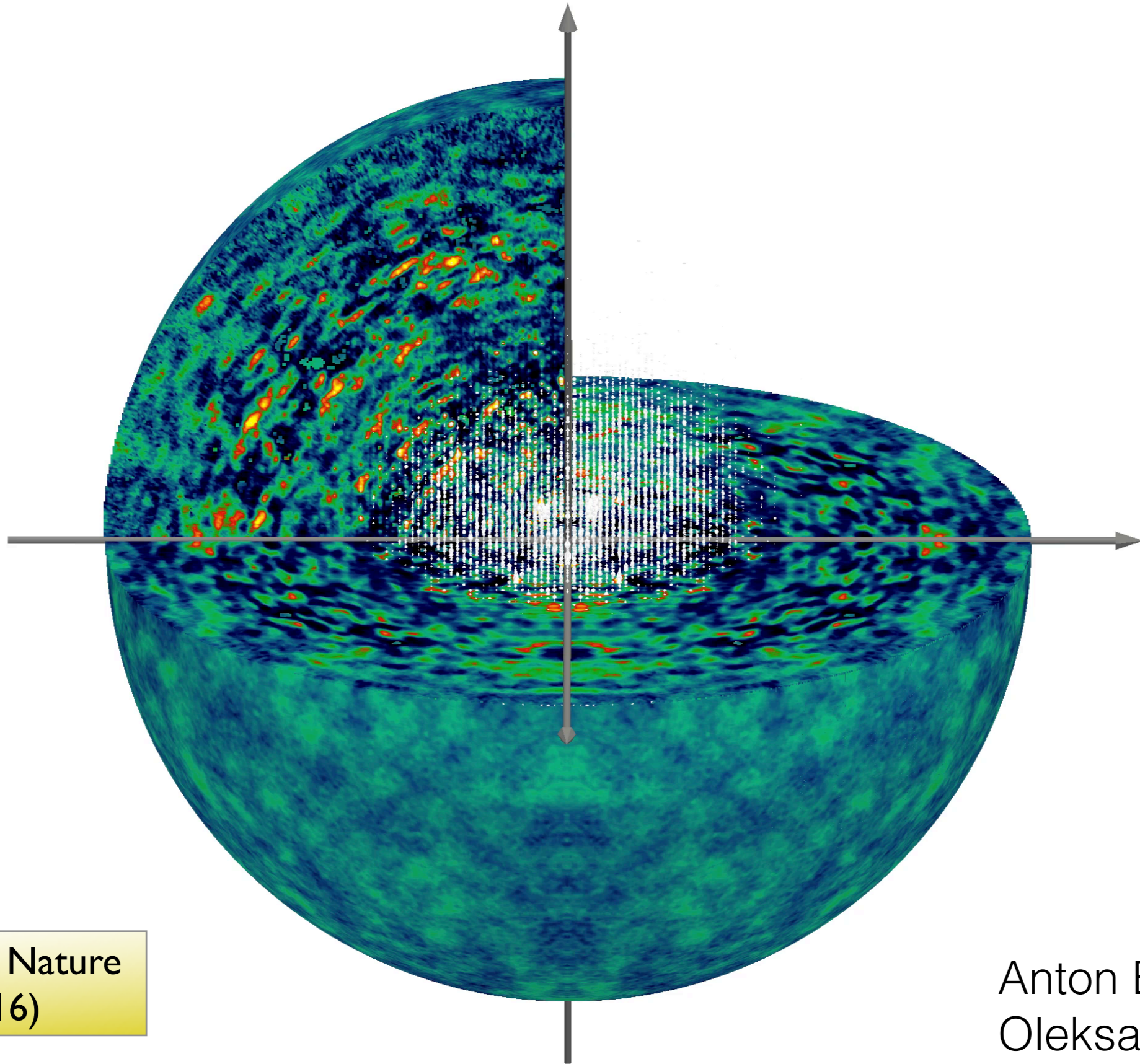
You can see a lot just by looking



2A



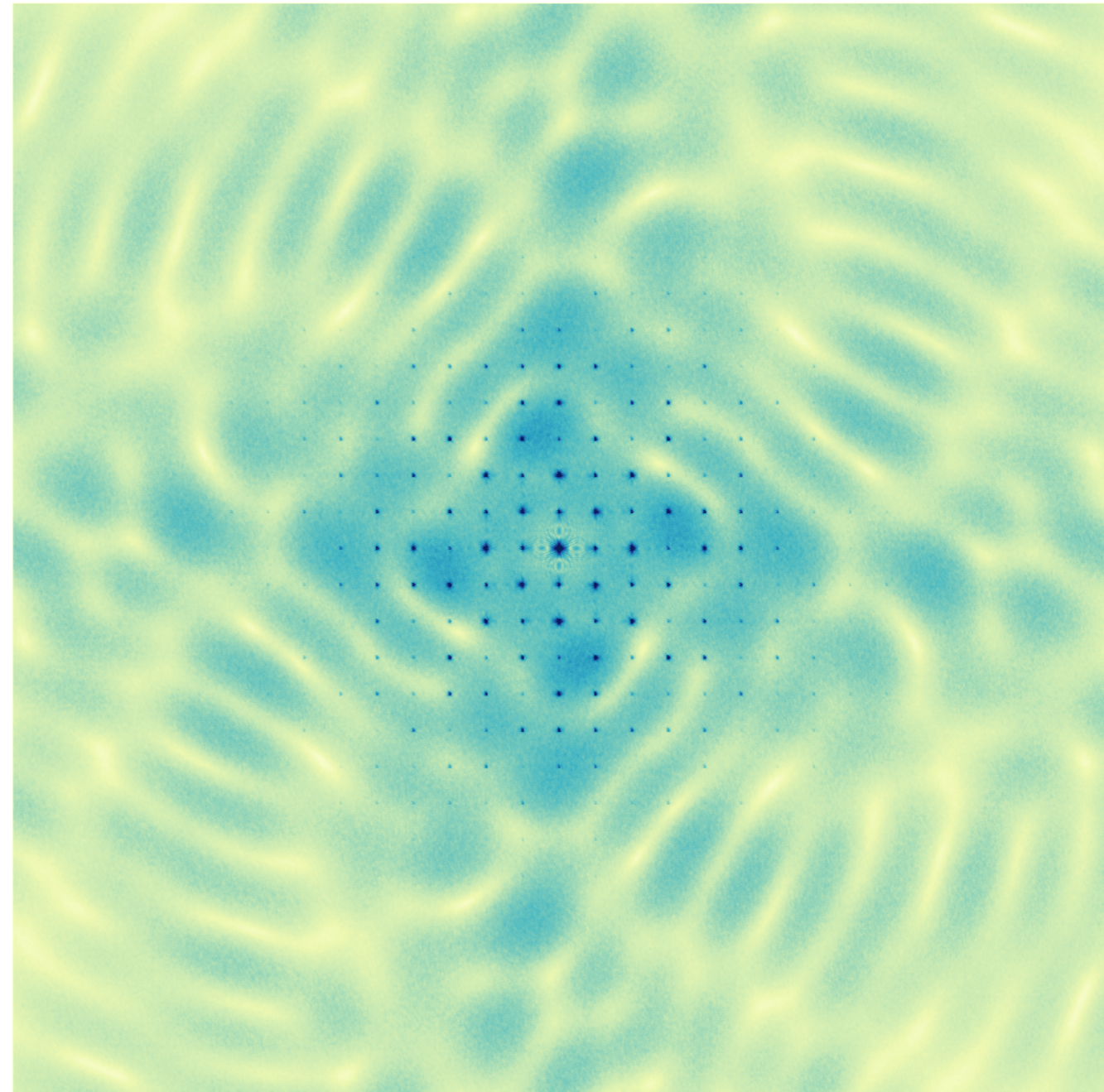
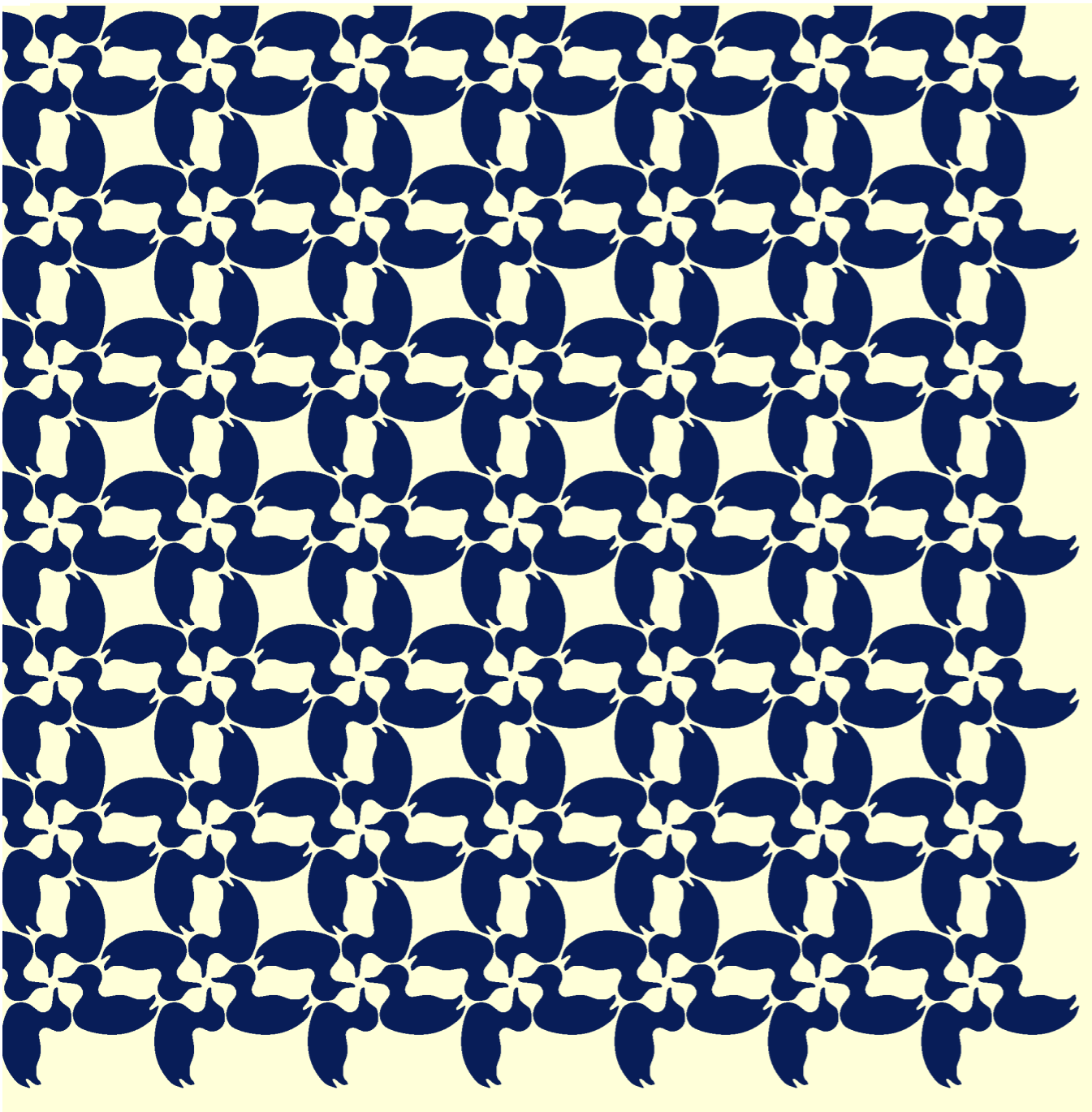
By averaging thousands of patterns a strong single molecule diffraction pattern emerges



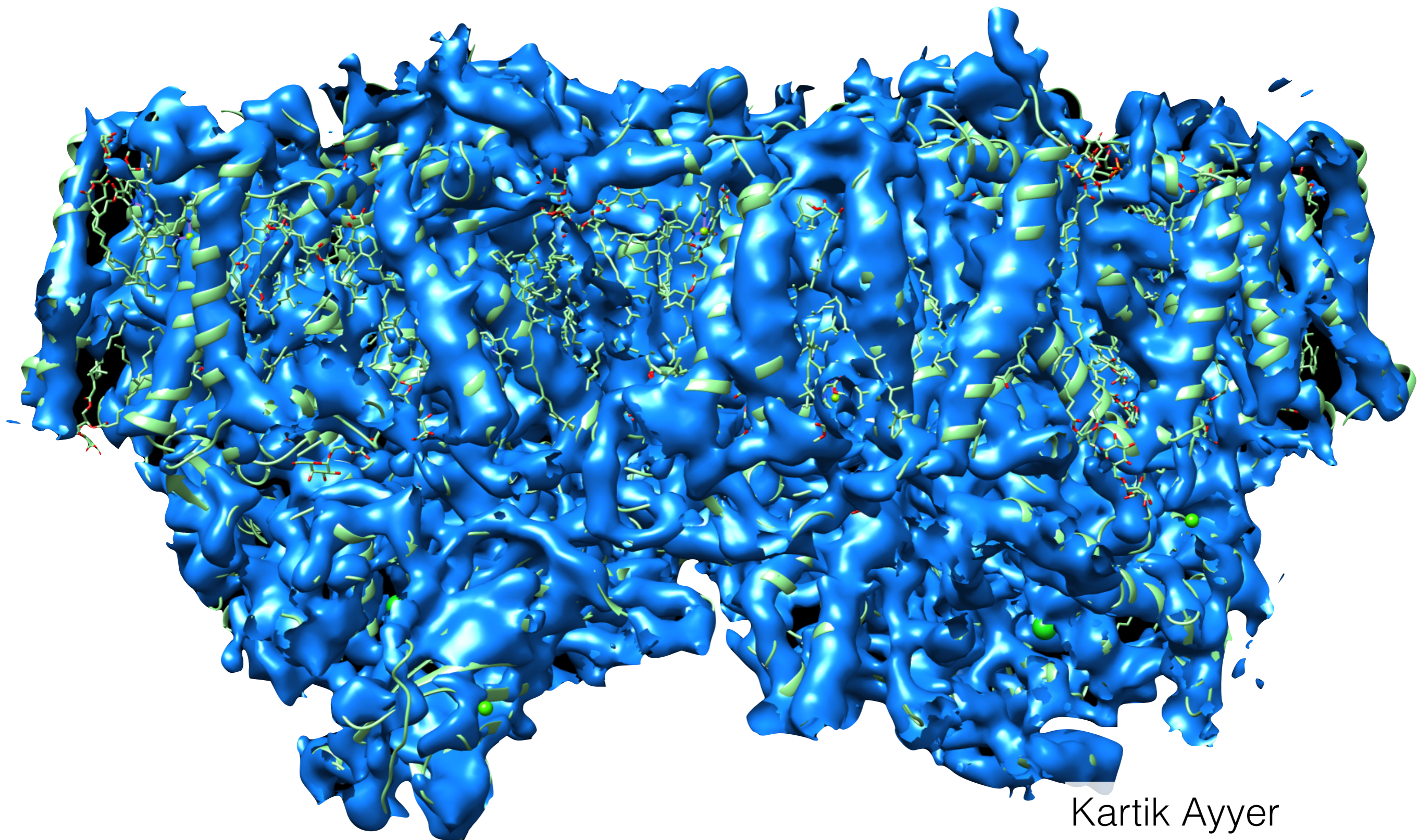
K. Ayyer et al. Nature
530, 202 (2016)

Anton Barty
Oleksandr Yefanov

The orientational symmetry of the crystal is preserved,
but not the translational symmetry

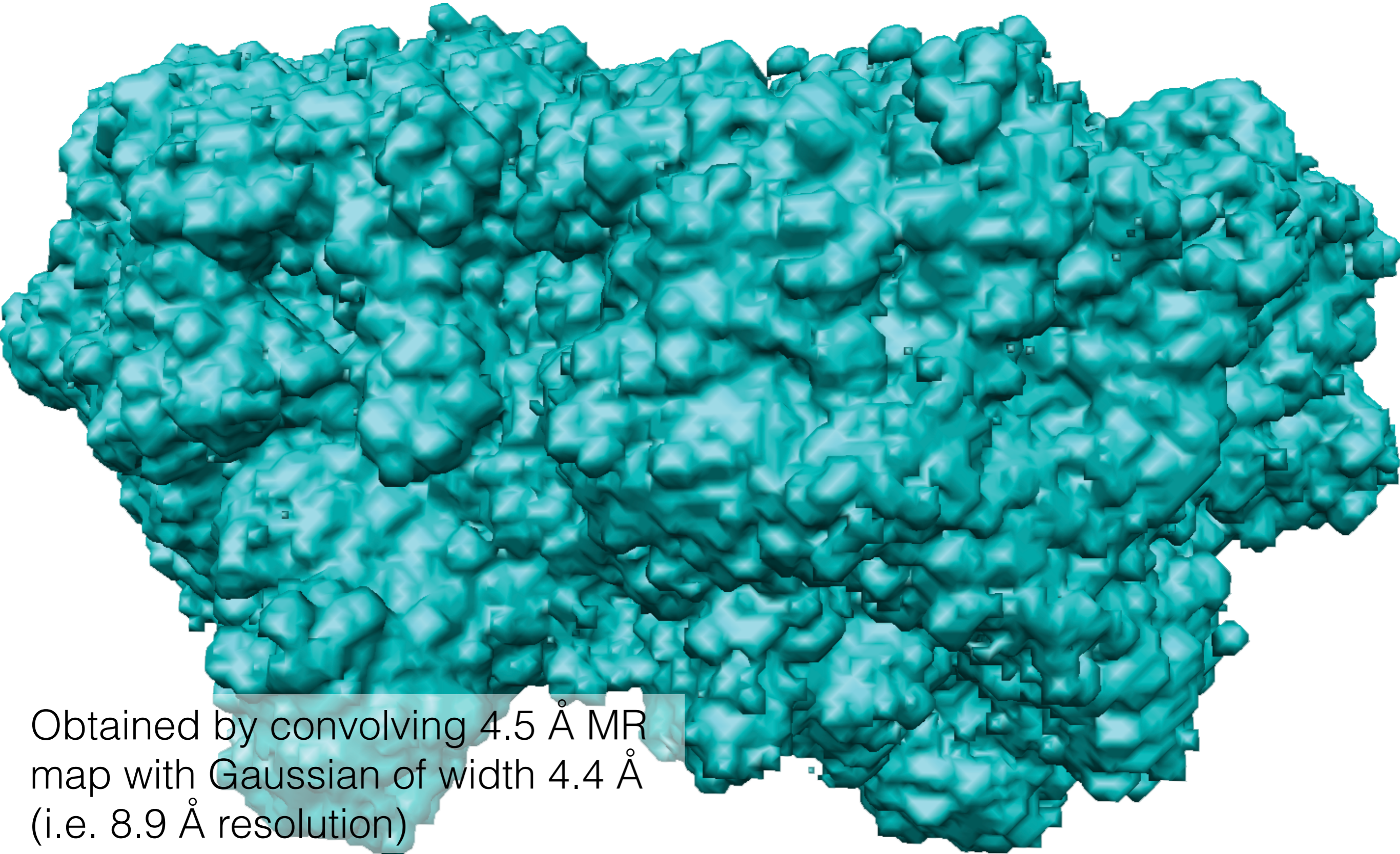


Electron density map from Bragg peaks alone (4.5 Å)

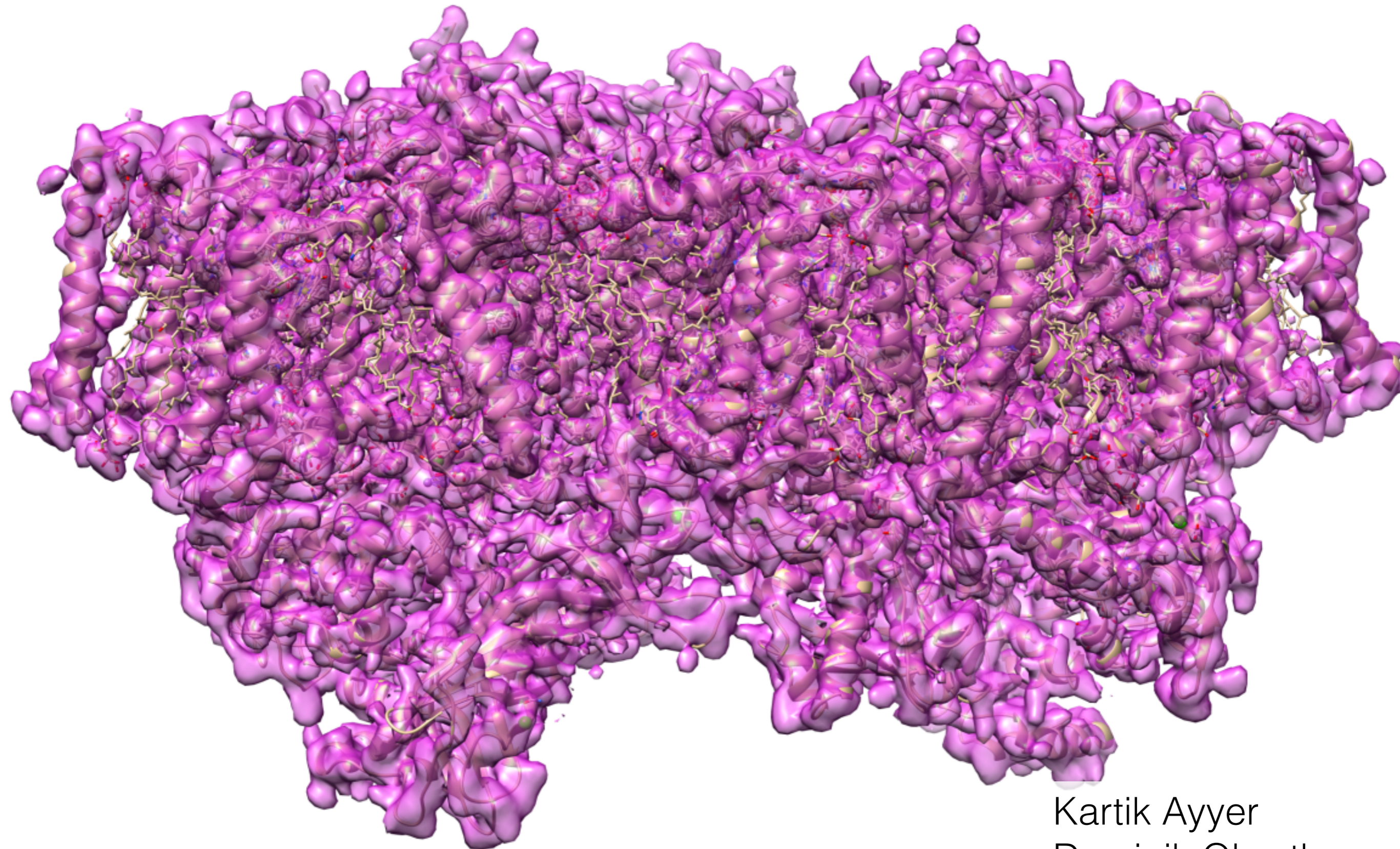


Kartik Ayyer
Dominik Oberthuer

The low-resolution support constrains the phases



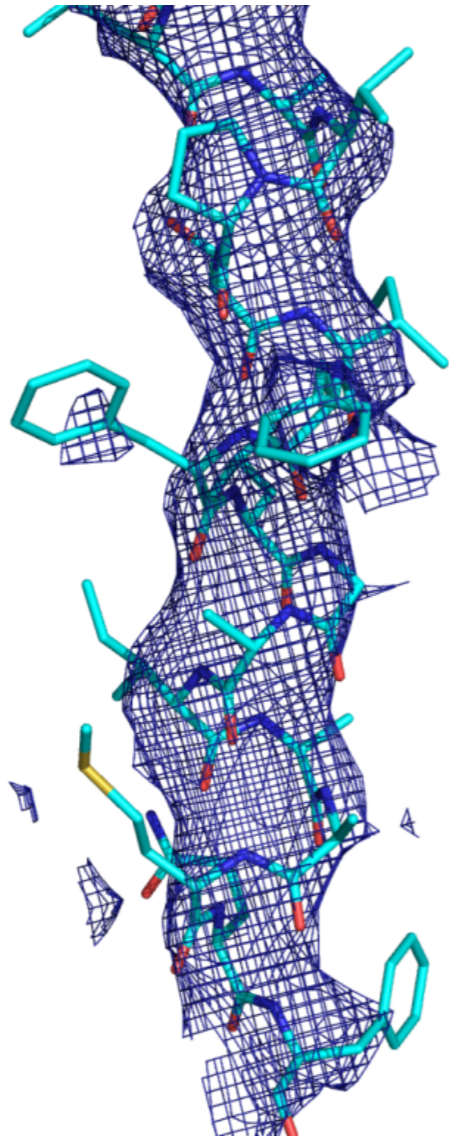
Electron density map including continuous diffraction



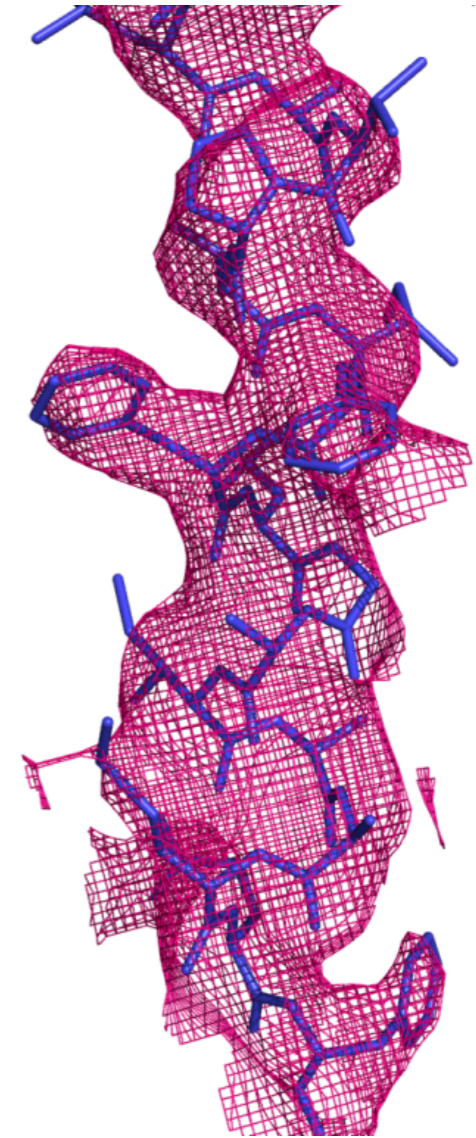
Kartik Ayyer
Dominik Oberthuer

The extended-resolution structure is superior

Bragg only
(4.5 Å)



Bragg and
continuous
(3.5 Å)



Higher diffraction sampling

— model free phasing

— more reliable structure determination

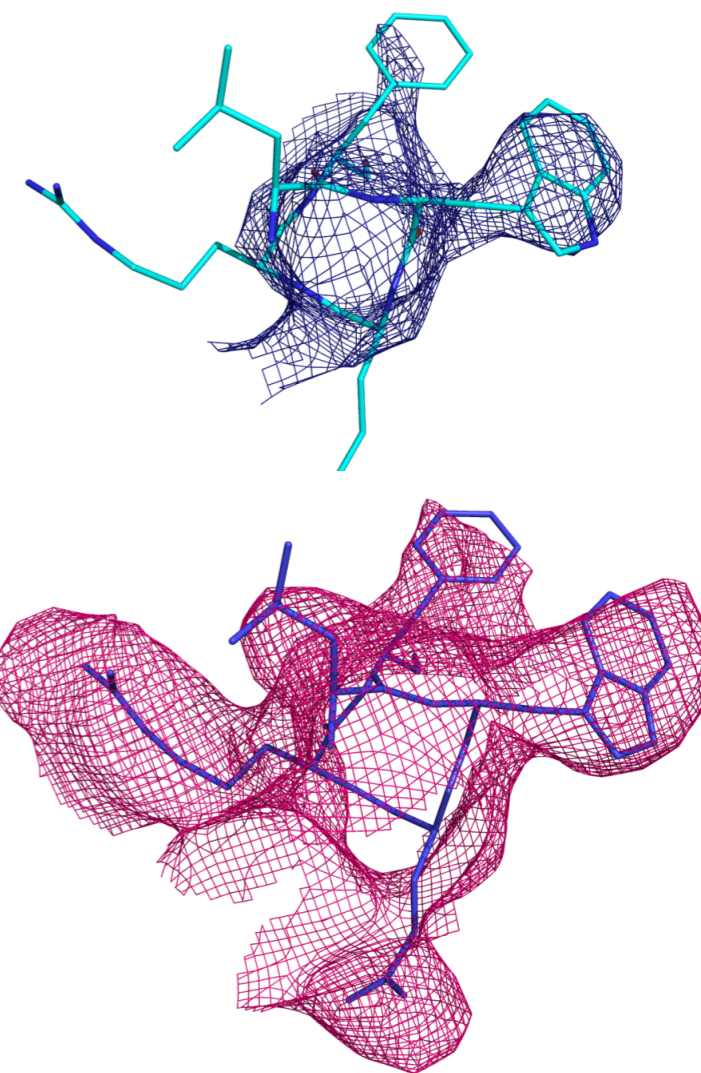
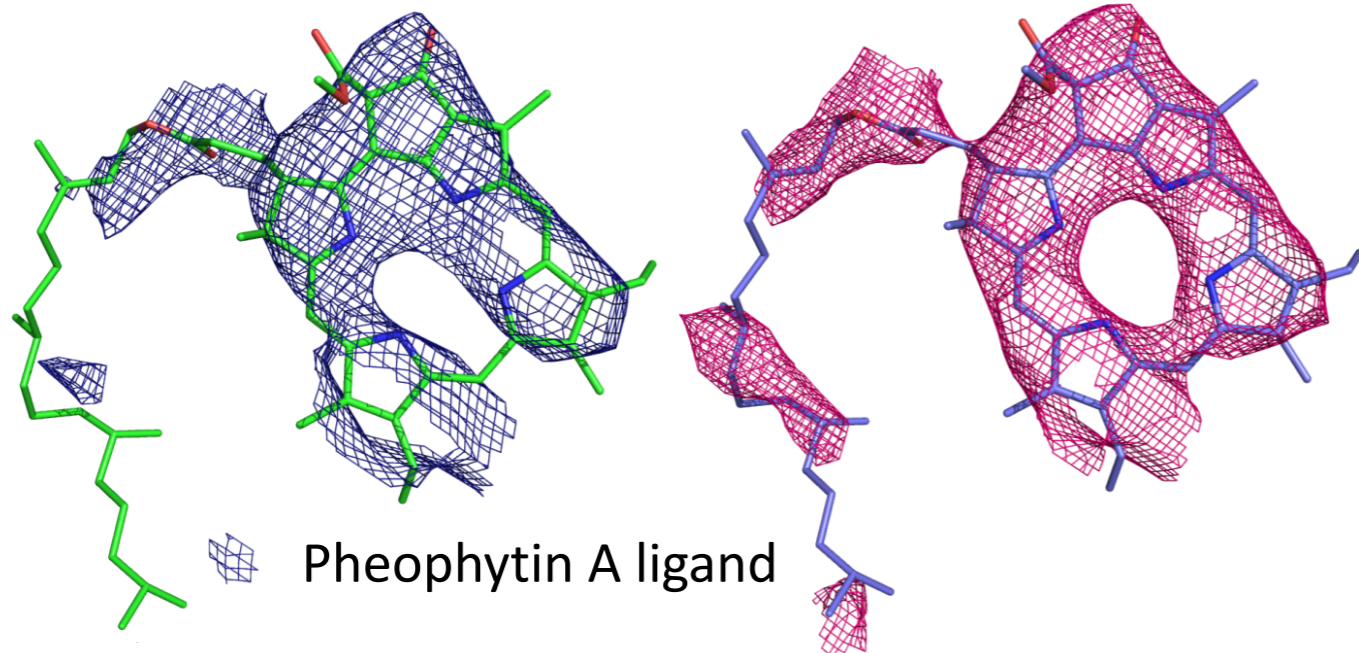
Resolution not limited by the crystal, just detector extent and shots

Number of molecules per shot: $1 \mu\text{m}^3 \times 4 / (9.2 \times 10^6 \text{ \AA}^3) = 4 \times 10^5$

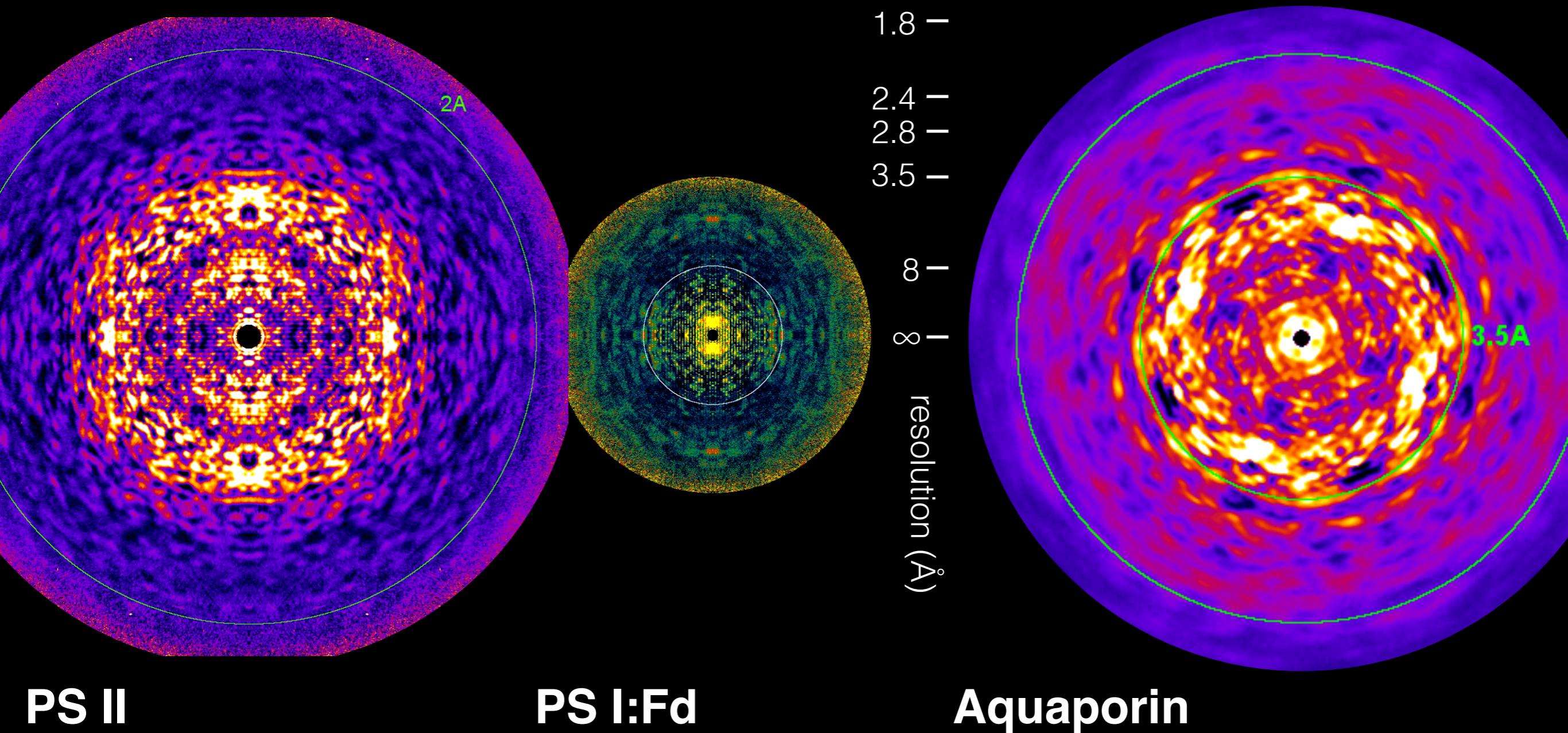
The extended-resolution structure is superior

Bragg only (4.5 Å)

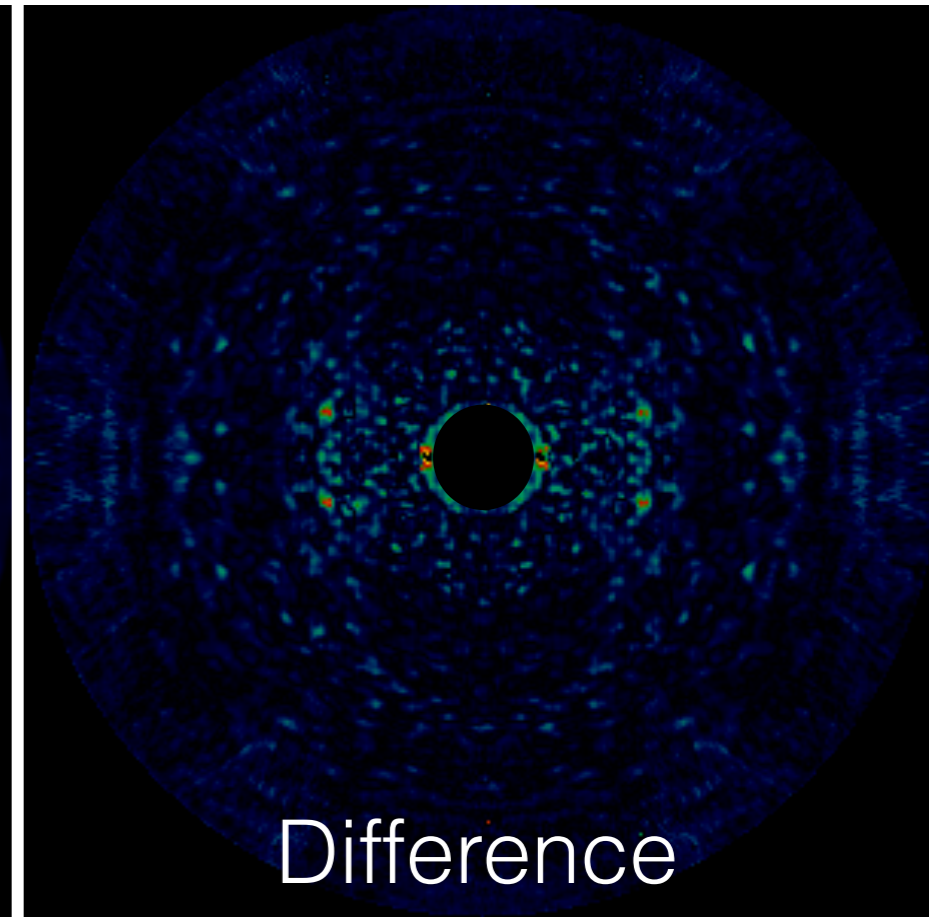
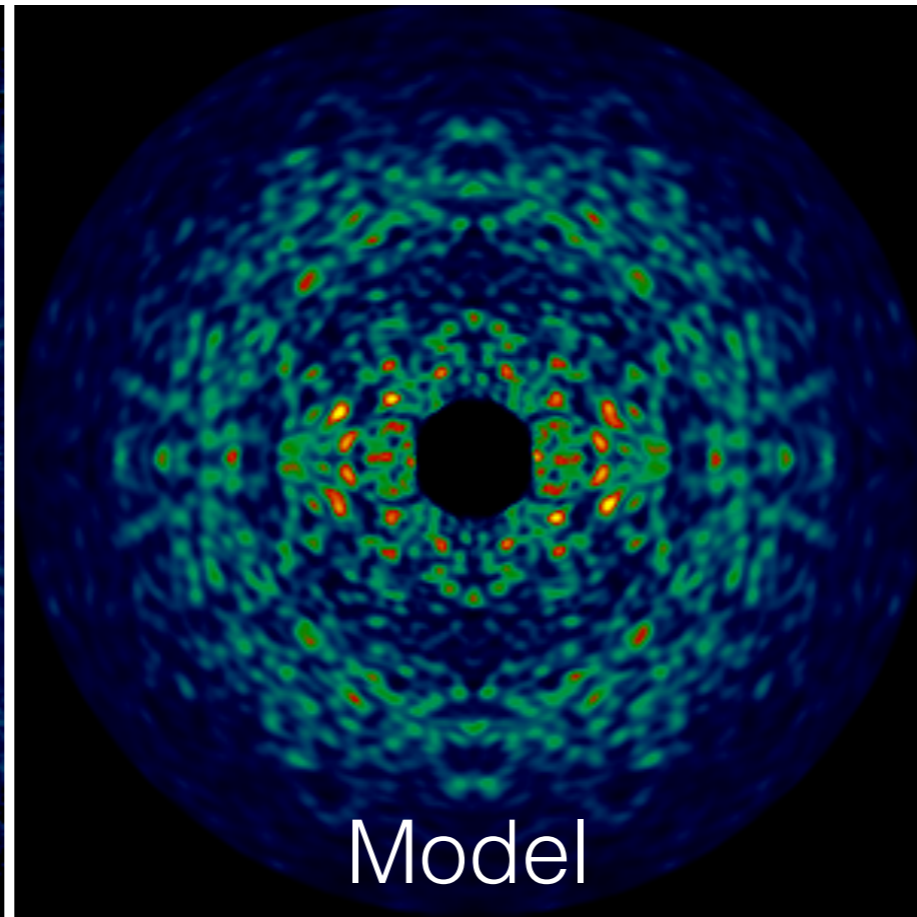
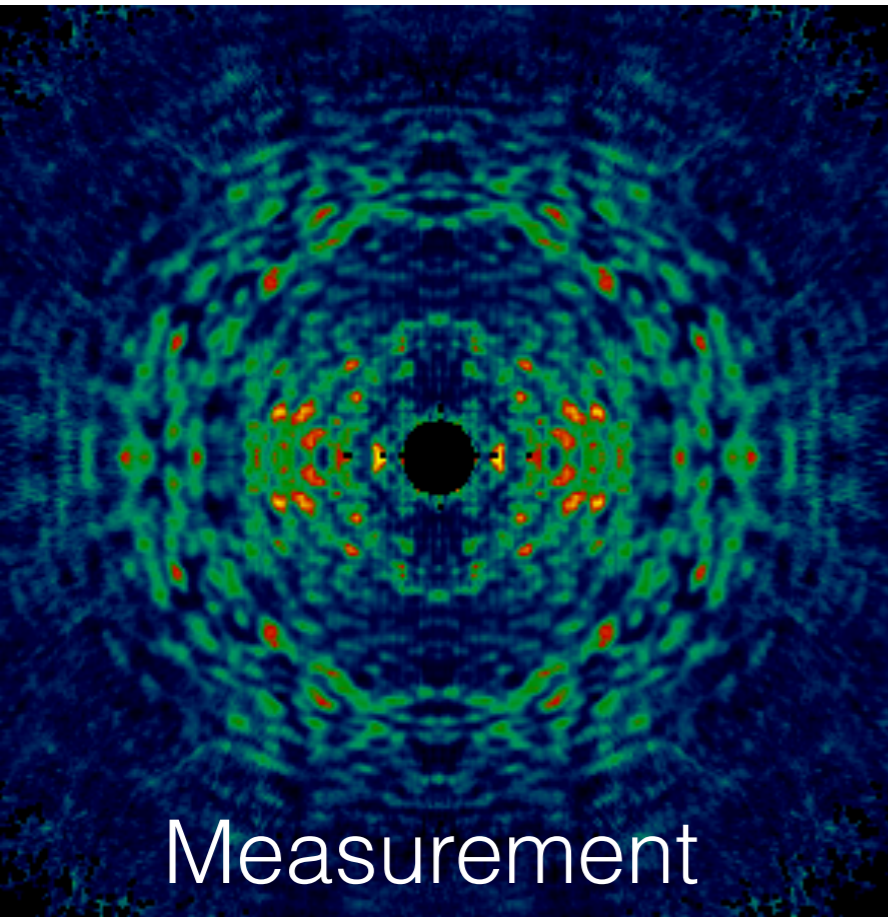
Bragg and continuous (3.5 Å)



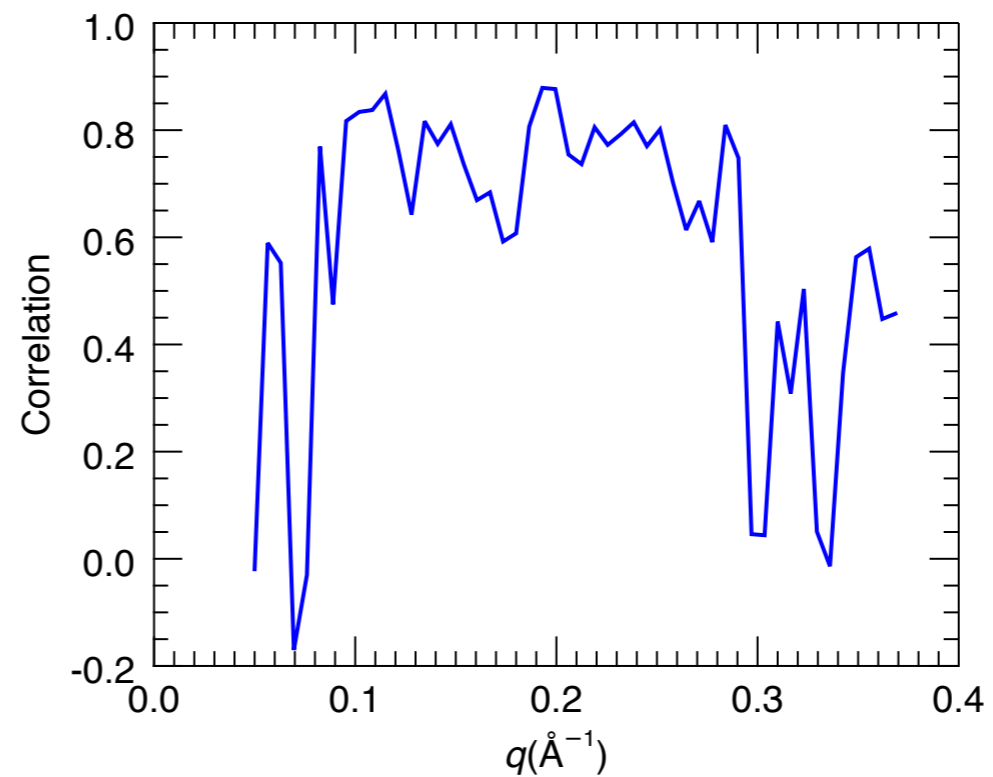
We observe continuous diffraction in other systems, and have extended observation of PS II to 1.9 Å



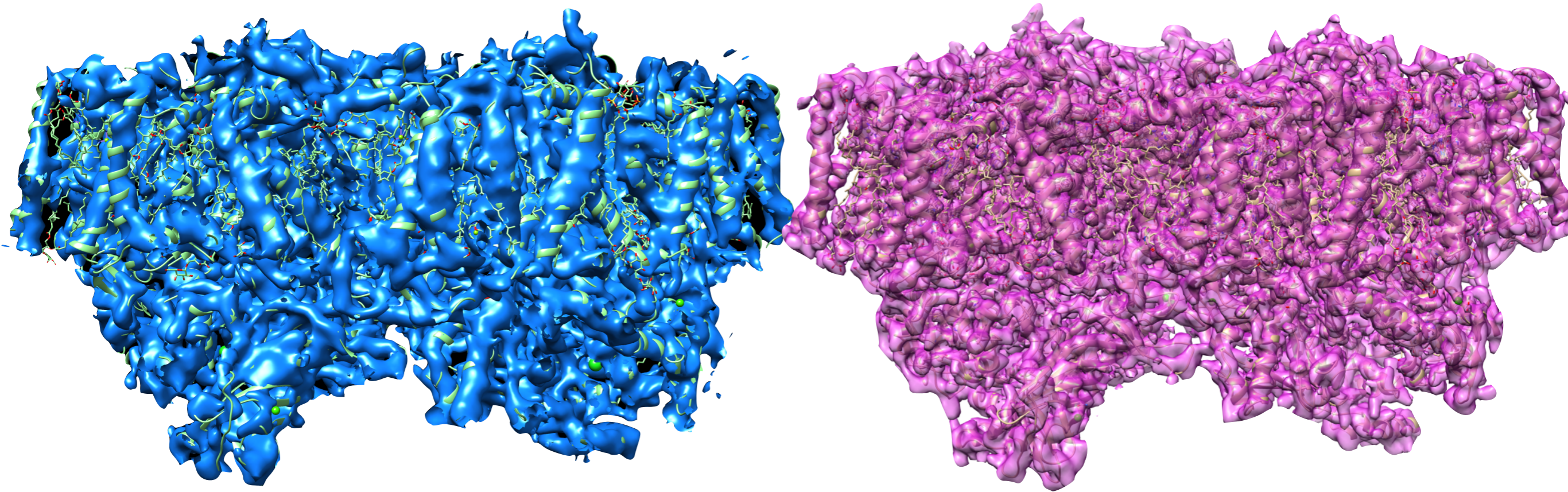
The continuous diffraction agrees with the simulated diffraction from the atomic model



Cross Correlation = 75%



There are many opportunities for extending imaging concepts to X-ray diffraction at the atomic scale

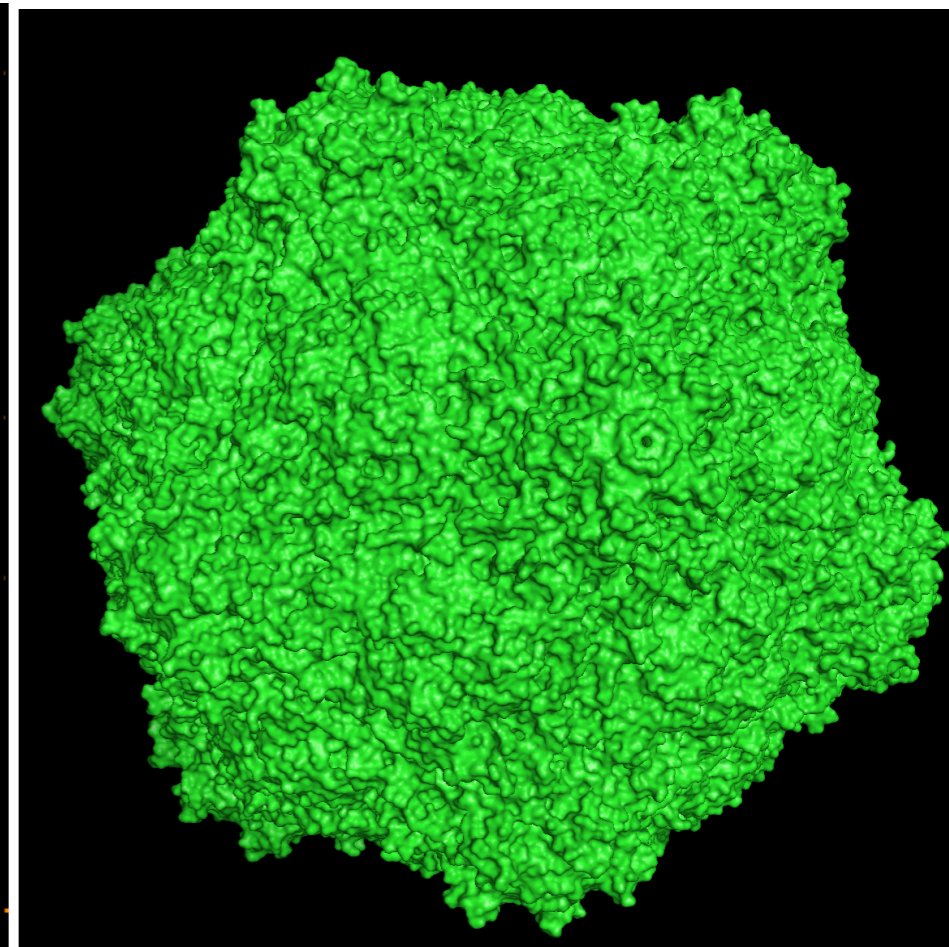
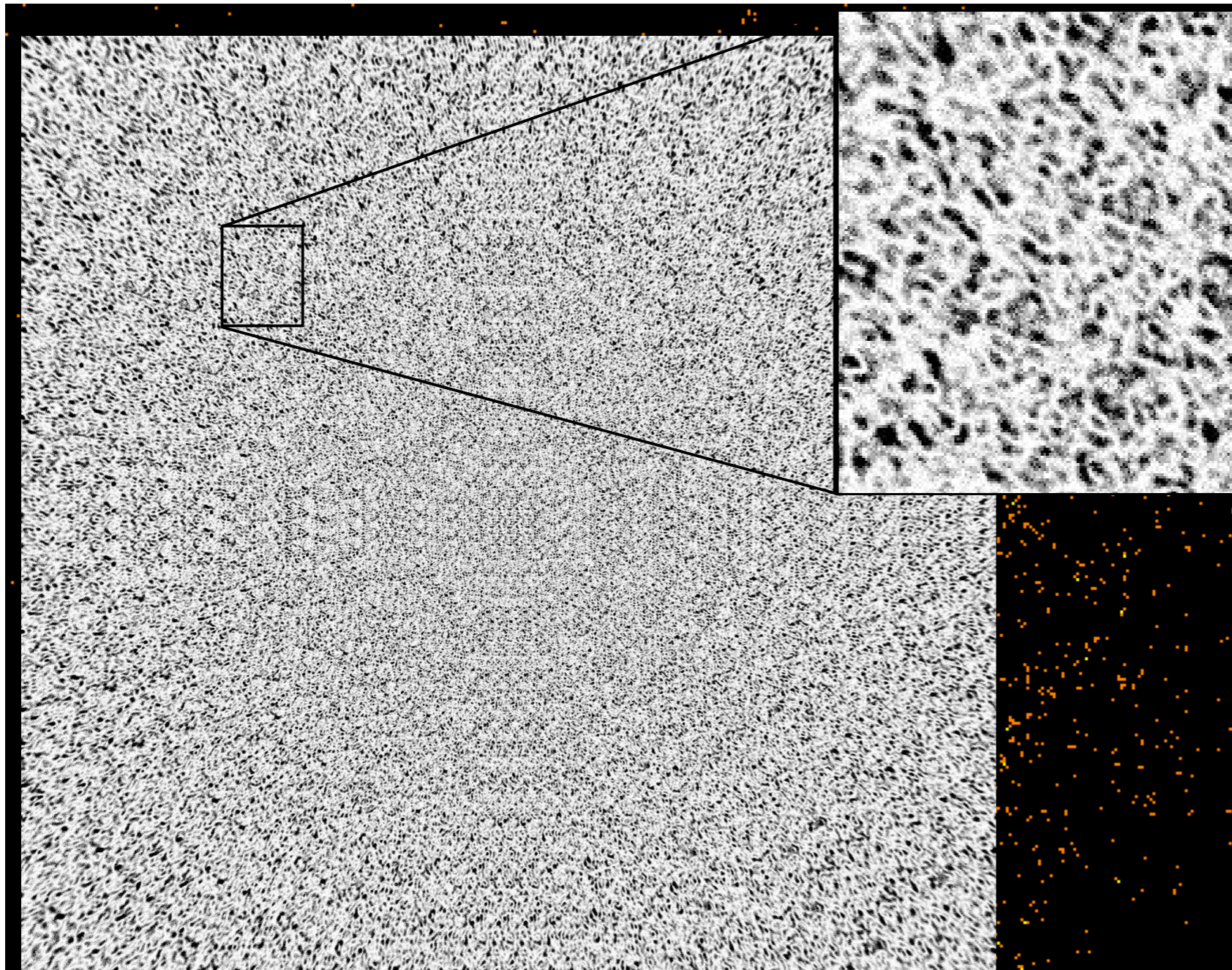


Measurements require care to eliminate background and record weak continuous diffraction

Poorly diffracting crystals are better!

- More information than required to describe the object
- model free phasing
- more reliable structure determination
- first new phasing since MAD
- resolution better than you think

Atomic-resolution diffraction from single particles requires focused intensities of more than 10^{14} ph/ μm^2



← 28 nm →

10^{14} ph/ μm^2

60 GGy

6000 MGy/fs \times 10 fs

RMS displacement: 0.5\AA
half electrons ionized

A. Classen *et al* [arXiv.org:abs/1705.08677](https://arxiv.org/abs/1705.08677)

Measure interference of fluorescence
during the coherence time

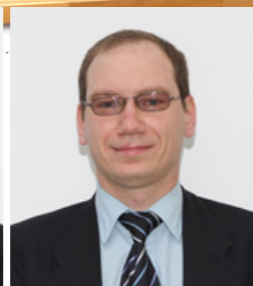
Coherent X-ray Imaging at CFEL



Kartik
Ayyer



Anton
Barty



Oleksandr
Yefanov



Dominik
Oberthür



Tom
White



Valerio
Mariani



Lorenzo
Galli



Kanupriya
Pande



Andrew
Morgan

Funding:



European Research Council
Established by the European Commission



Bundesministerium
für Bildung
und Forschung



LCLS experiments and analyses are carried out as a large collaboration

CFEL-DESY/UHH

A. Barty, T. White, S. Stern, C. Caleman, K. Beyerlein, R. Bean, R. Kirian, F. Wang, H. Fleckenstein, L. Gumprecht, L. Galli, S. Bajt, M. Barthelmess, O. Yefanov, D. Oberthür, C. Gati, M. Heymann, C. Seuring, M. Metz, A. Morgan, V. Mariani, A. Tolstikova, J. Knoska, X. L. Pauraj, K. Ayyer

ASU

J. Spence, P. Fromme, U. Weierstall, B. Doak, X. Wang, I. Grotjohann, R. Fromme, N. Zatsepin, D. Wang, D. James, S. Basu, C. Kupitz, J. Coe, C. Conrad, K. Dörner, D. James, G. Nelson

MPG Med. Res.

I. Schlichting, R. Shoeman, L. Lomb, S. Kassemeyer, K. Nass, T. Barends, S. Botha

SLAC

S. Boutet, M. Liang, A. Aquila, G. Williams, C. Bostedt, J. Koglin, M. Messerschmidt, and many others

Uppsala

J. Hajdu, N. Timneanu, J. Andreasson, M. Seibert, F. Maia, M. Svenda, T. Ekeberg, J. Andreasson, A. Rocker, O. Jonsson, D. Westphal

Gotheburg

R. Neutze, L. Johansson, D. Arnlund

LLNL

S. Hau-Reige, M. Frank

U. Hamburg

C. Betzel, D. Redhers, D. Oberthür, M. Perbandt

U. Lübeck

L. Redecke

CFEL DESY Theory

R. Santra, S.-K. Son

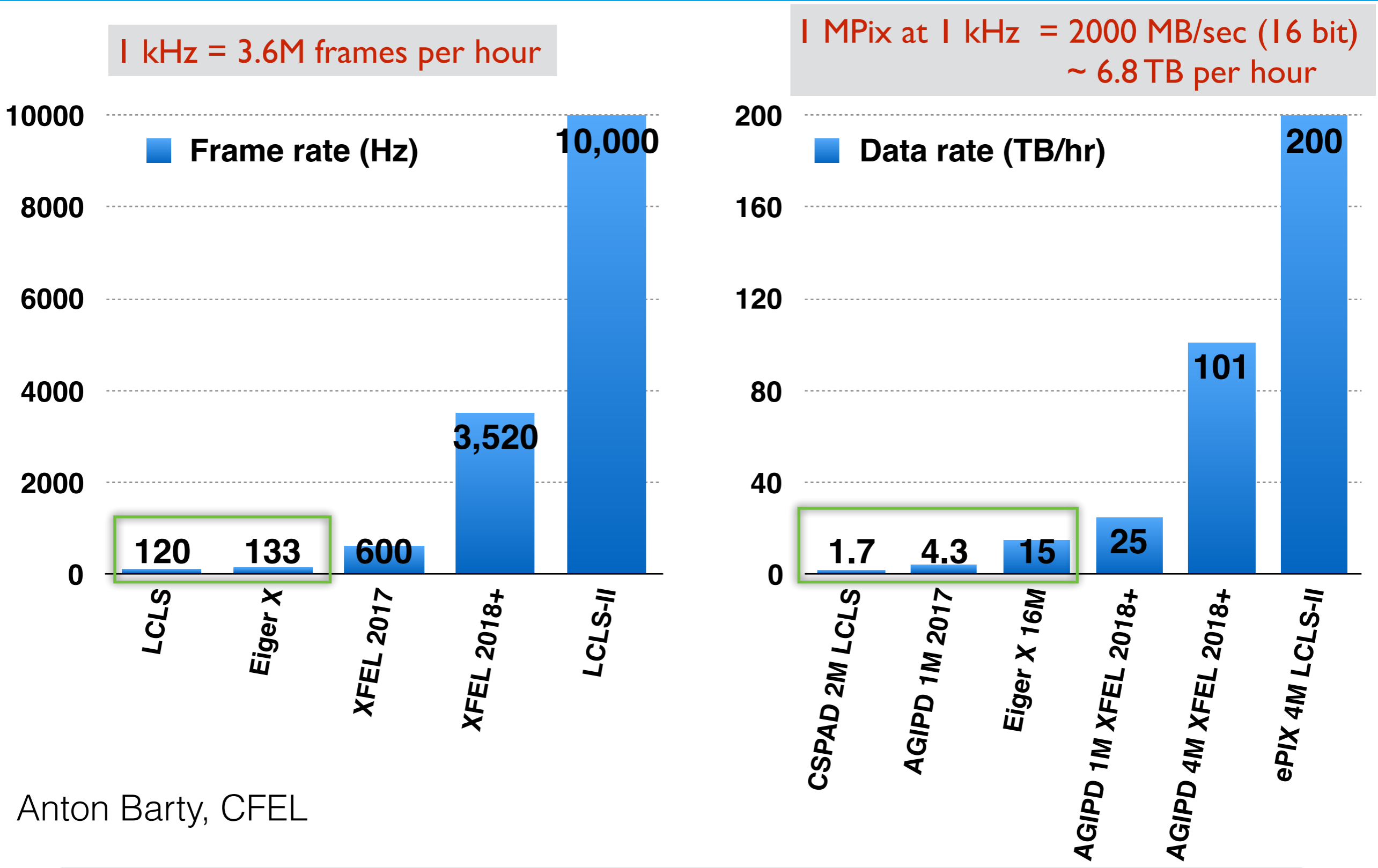
U. Milwaukee Wisconsin

M. Schmidt, J. Tenboer, K. Pande

Funding:



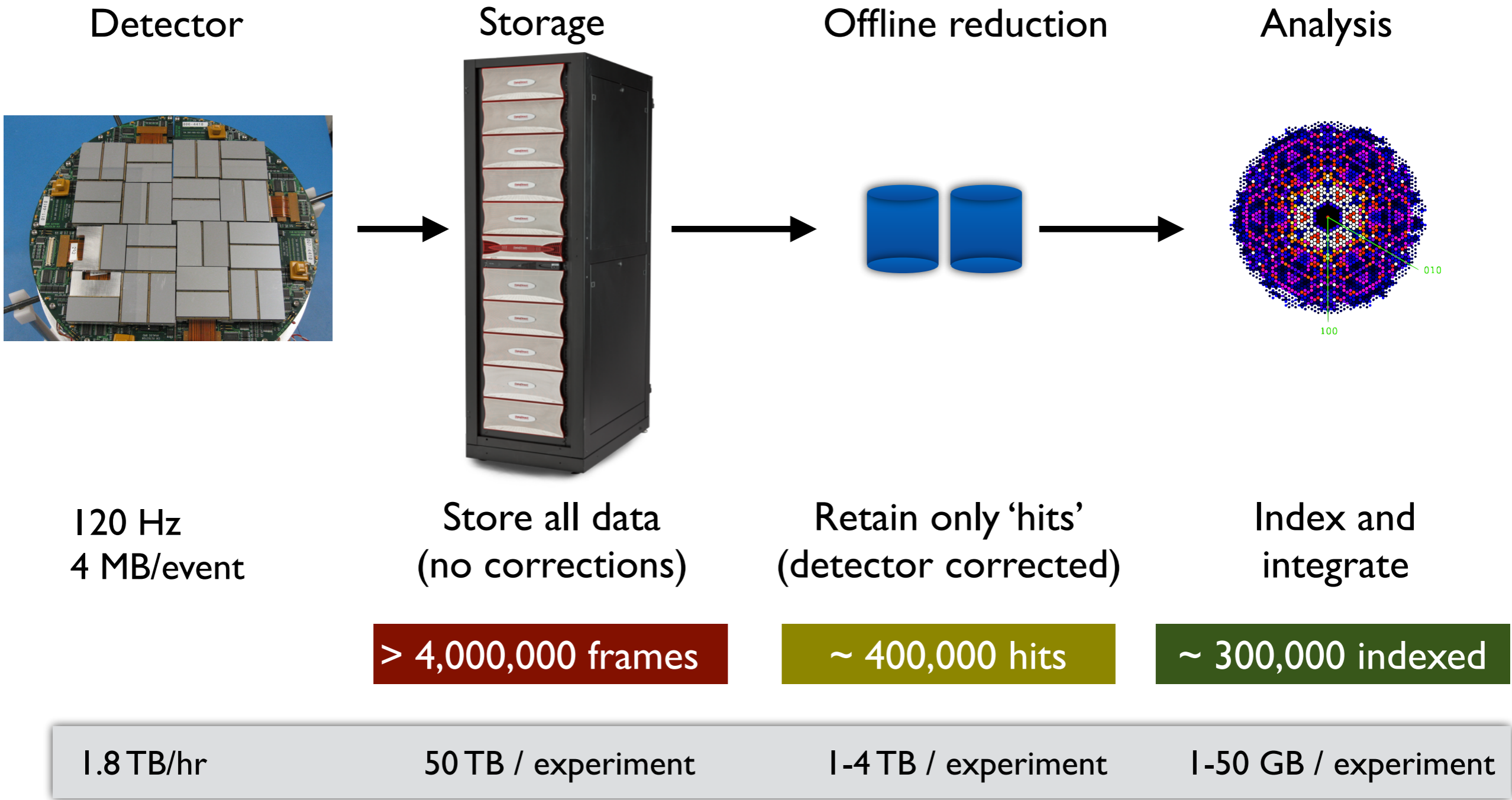
New sources and detectors are producing an explosion in experimental data volumes



Anton Barty, CFEL

LCLS-II estimates a cost of over \$250M to save all data, \$35M to save two weeks' worth

Data processing is an exercise in data management and reduction



Automated high throughput data processing is essential